Latest results on top quark properties at the CMS experiment

Giulia Negro (Purdue University)
on behalf on the CMS collaboration

LHCP2019
Puebla, 20-25 May 2019

Outline

- Introduction
- Recent measurements of top quark properties :
  - Polarizations and ttbar spin correlations (CMS-PAS-TOP-18-006)
  - Mass (Eur. Phys. J. C 79 (2019) 313, arXiv:1812.10505 - accepted for publication in Eur. Phys. J. C, arXiv:1904.05237 - submitted to Eur. Phys. J.)
  - Strong coupling strength (arXiv:1812.10505 - accepted for publication in Eur. Phys. J. C, arXiv:1904.05237 - submitted to Eur. Phys. J.)
  - PDF (arXiv:1904.05237 - submitted to Eur. Phys. J.)
  - Yukawa coupling (CMS-PAS-TOP-17-004, CMS-PAS-TOP-18-003)
  - Charge asymmetries (JHEP 02 (2019) 149)
- Summary

Other related talks @LHCP:
A. Jung's plenary on top properties @LHC
V. M. Mikuni's parallel on cross sections
P. K. Mal's parallel on EFT interpretations

Focus on a selection of recent results..
for other CMS results you can look here

Introduction

- Top quark :
  - heaviest elementary particle discovered so far
  - extremely short lifetime (10^{-25} s) → decays before it can form bound states
  - spin information preserved in the angular distribution of its decay products → **ideal candidate for spin measurements**
  - large Yukawa coupling to Higgs mass
- Studies of its properties provide crucial information:
  - to test SM
  - to search for new phenomena (BSM physics)
- Top quarks pairs at the LHC are produced mostly via gluon fusion (~90%) → allows to :
  - constrain gluon PDF
  - extract α_S, m_t

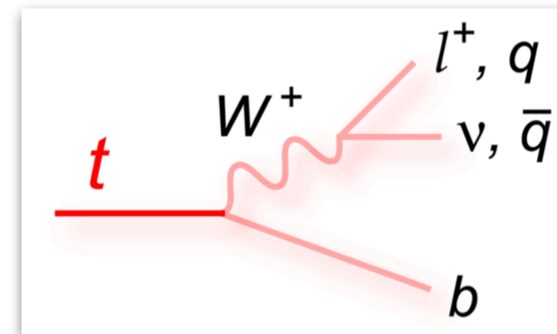

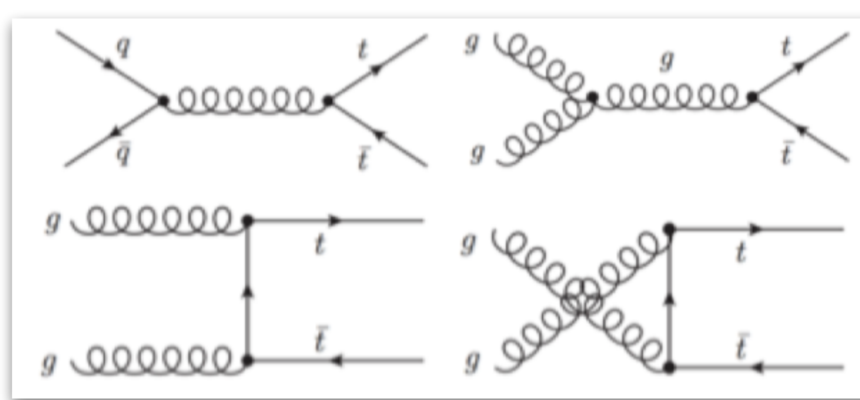

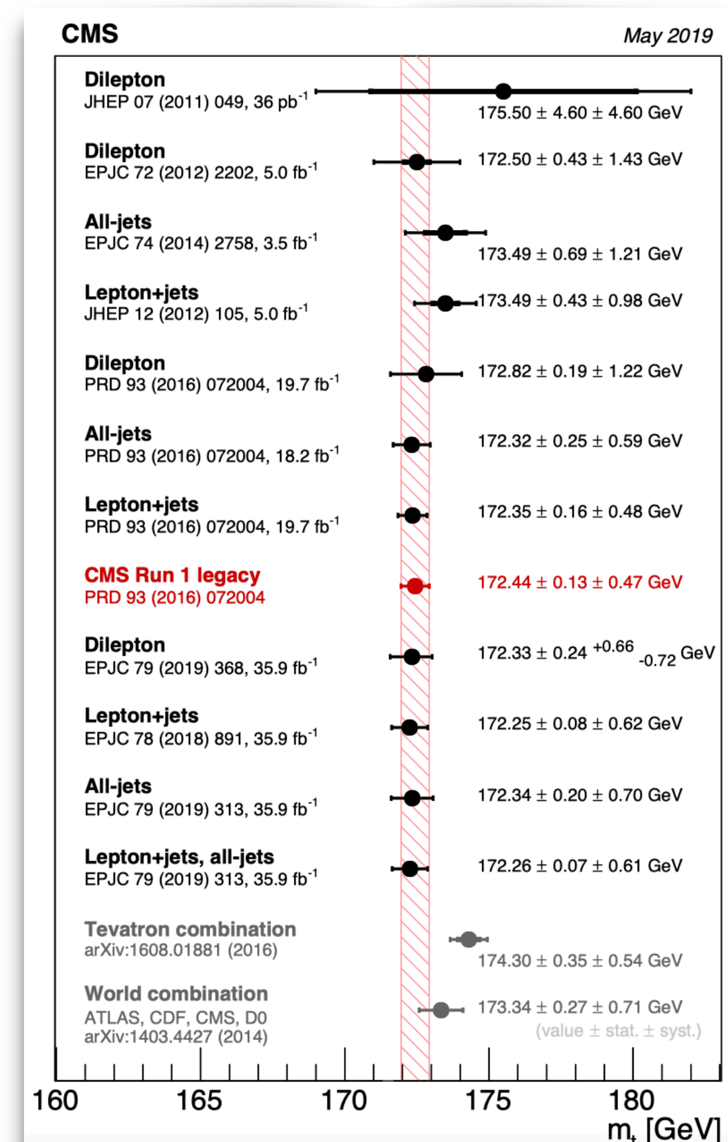

Polarization and spin correlations in dilepton channel

CMS-PAS-TOP-18-006

2016 data @13 TeV:
35.9 fb^{-1}

- **Indirect measurement** with lab-frame variables:
  - $\ell^{\pm}$ angular distributions = $(1 \pm \cos\theta)/2$
    - preferred lepton directions in the top rest frames determined by top spins
  - angle between leptons in transverse plane (lab.) = $\Delta\phi$
    - experimentally very precise for excellent resolution of lepton angles
- "Unfolding": distribution in data corrected for acceptance and migration between bins
- Tensions between data and NLO simulation:
  - reduced, but still substantial, when comparing to NNLO predictions
  - use NNLO corrections instead of NLO MC in the extrapolation to the full phase space

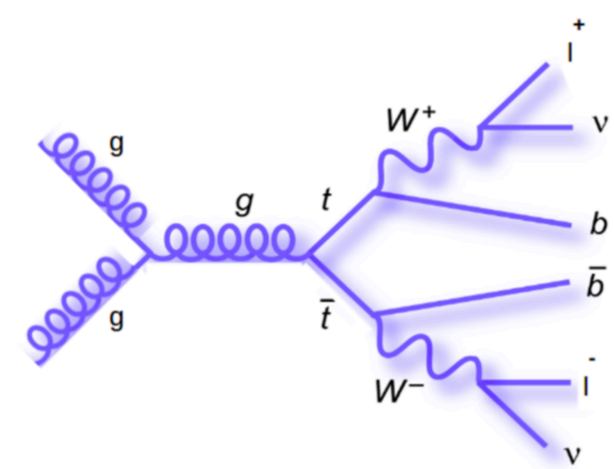

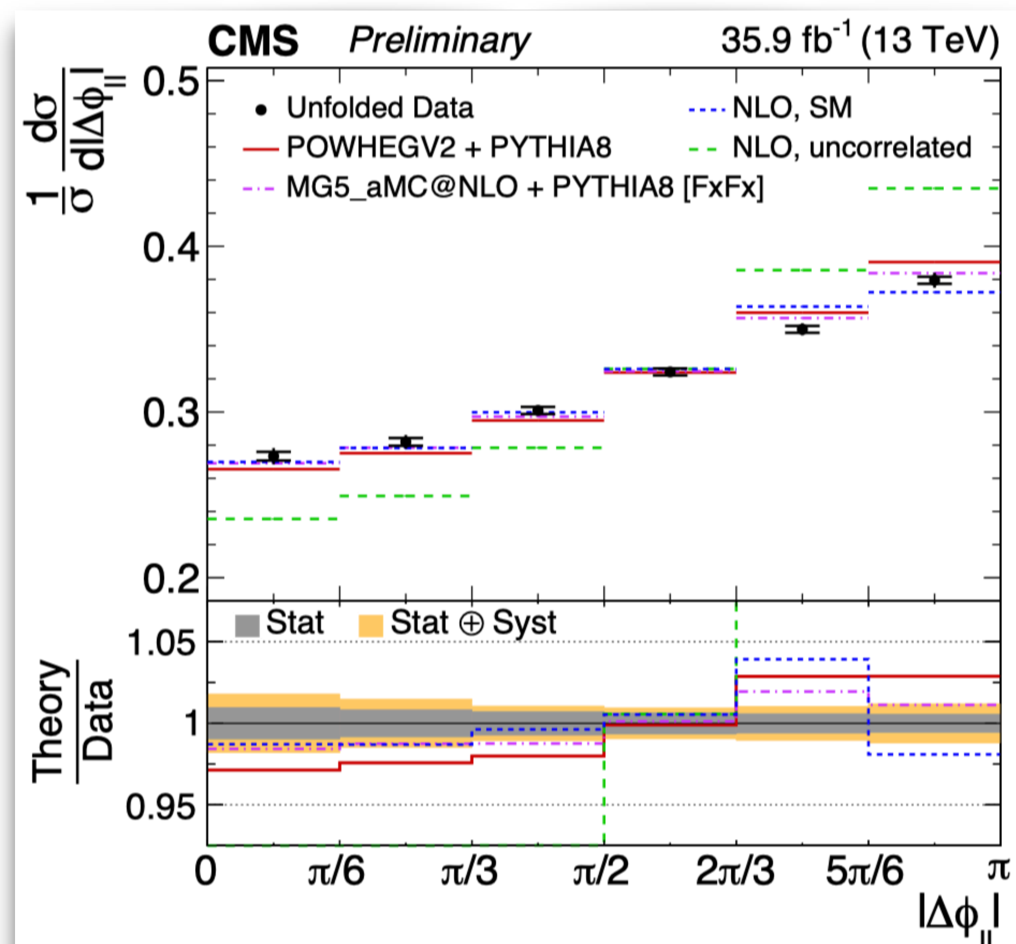

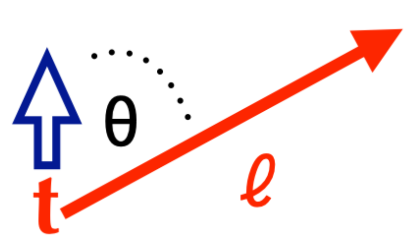

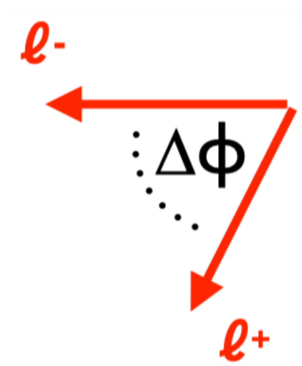

Polarization and spin correlations in dilepton channel

CMS-PAS-TOP-18-006

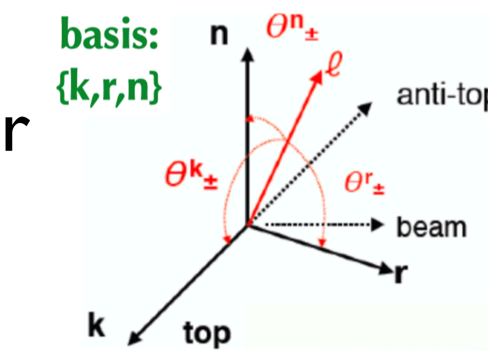

- **Direct measurement** requires full reconstruction of t and tbar
- Dilepton angular distribution probes top spin in 3 dimensions:

$$\frac{1}{\sigma}\frac{d\sigma}{d\Omega_+ d\Omega_-} = \frac{1}{(4\pi)^2}\left(1 + \mathbf{B}^+ \cdot \hat{\ell}^+ + \mathbf{B}^- \cdot \hat{\ell}^- - \hat{\ell}^+ \cdot \mathbb{C} \cdot \hat{\ell}^-\right)$$

  - 3-vectors $B^{+/-}$ = polarizations, 3x3 matrix C = spin correlations
  - spin dependence of ttbar production completely characterized by 15 coefficients, individually probed by measuring angular distribution at parton level: $\frac{1}{\sigma}\frac{d\sigma}{dx} = \frac{1}{2}(1 + [\mathbf{Coef.}]\, x)\, f(x)$ ⟶ $\frac{1}{\sigma}\frac{d\sigma}{d\cos\theta} = \frac{1}{2}(1 + B\, \cos\theta)$
- Measured top quark polarization (6 B coefficients) consistent with zero

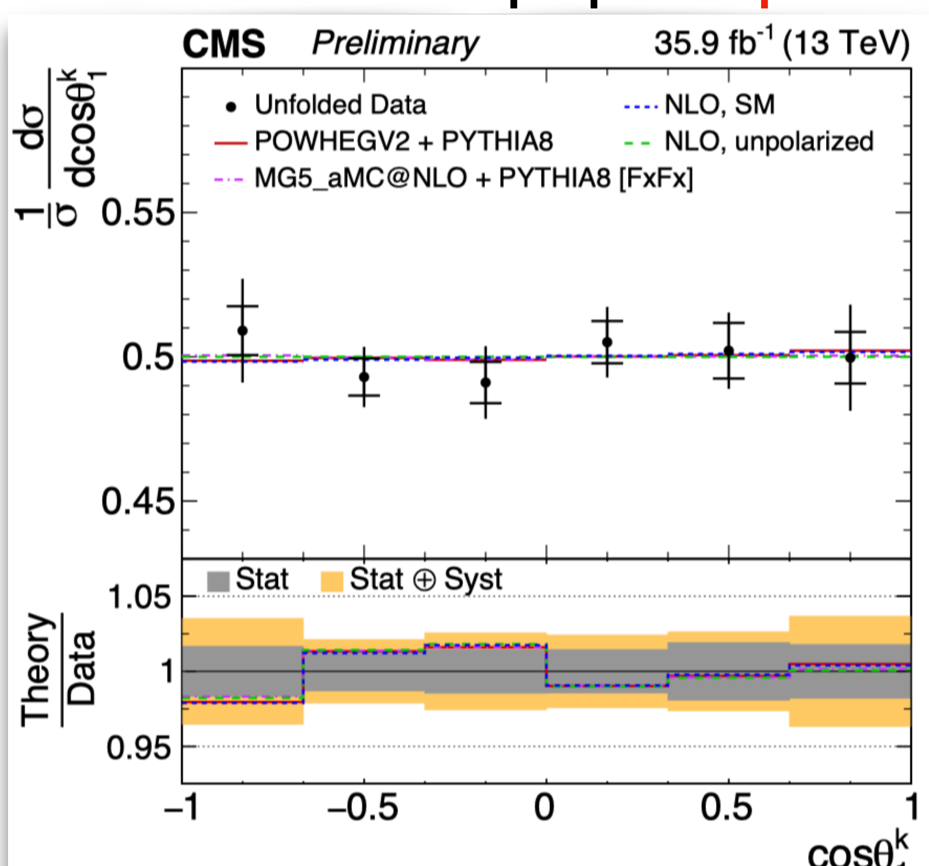

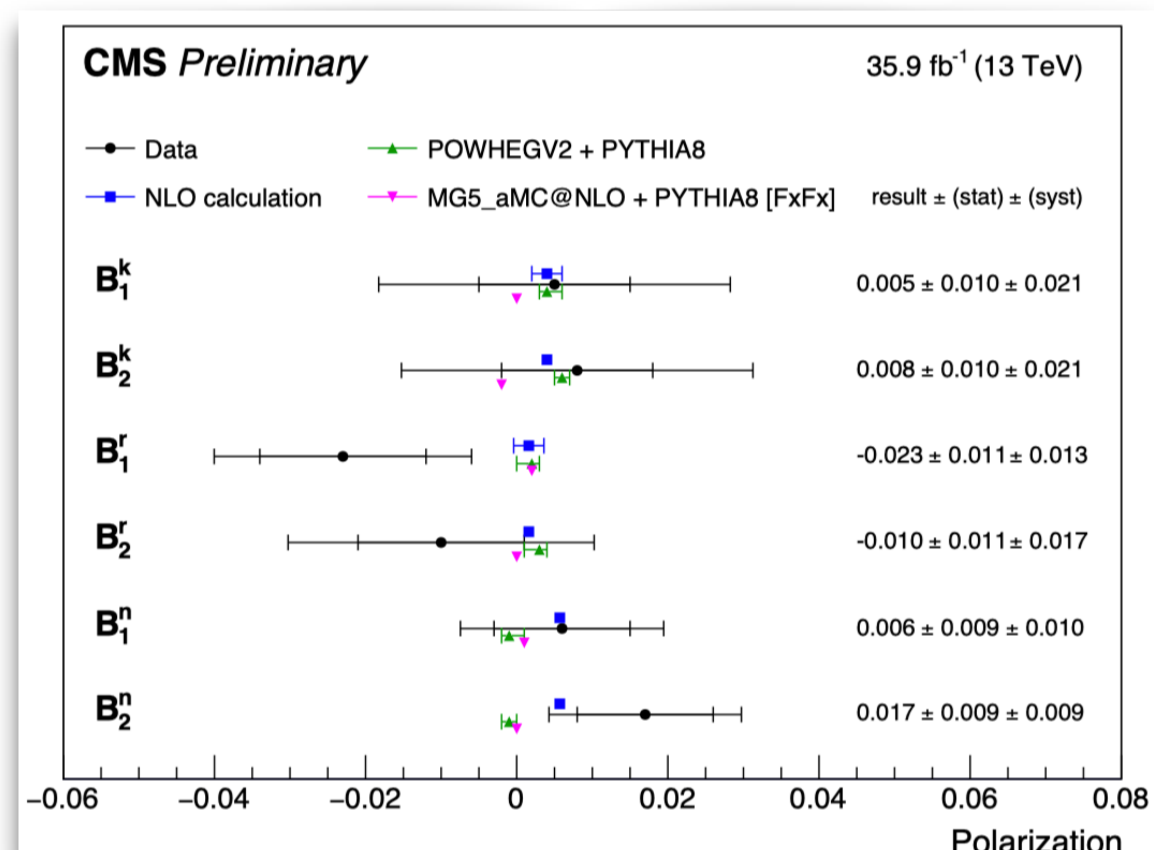

Polarization and spin correlations in dilepton channel

CMS-PAS-TOP-18-006

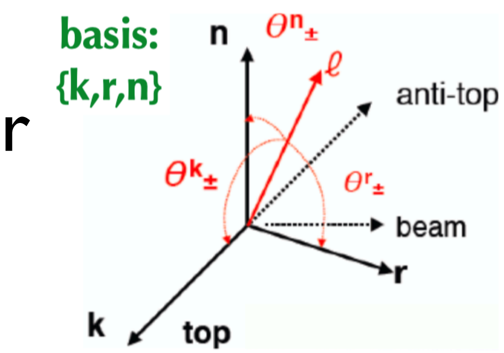

- **Direct measurement** requires full reconstruction of t and tbar
- Dilepton angular distribution probes top spin in 3 dimensions:

$$\frac{1}{\sigma}\frac{d\sigma}{d\Omega_+ d\Omega_-} = \frac{1}{(4\pi)^2}\left(1 + \mathbf{B}^+ \cdot \hat{\ell}^+ + \mathbf{B}^- \cdot \hat{\ell}^- - \hat{\ell}^+ \cdot \mathbb{C} \cdot \hat{\ell}^-\right)$$

  - 3-vectors $B^{+/-}$ = polarizations, 3x3 matrix C = spin correlations
  - spin dependence of ttbar production completely characterized by 15 coefficients, individually probed by measuring angular distribution at parton level: $\frac{1}{\sigma}\frac{d\sigma}{dx} = \frac{1}{2}(1 + [\mathbf{Coef.}]\, x)\, f(x) \longrightarrow \frac{1}{\sigma}\frac{d\sigma}{d\cos\theta_1 \cos\theta_2} = \frac{1}{2}(1 - C\, \cos\theta_1 \cos\theta_2)\log\left(\frac{1}{|\cos\theta_1 \cos\theta_2|}\right)$

- Spin correlations along each axis consistent with SM expectations

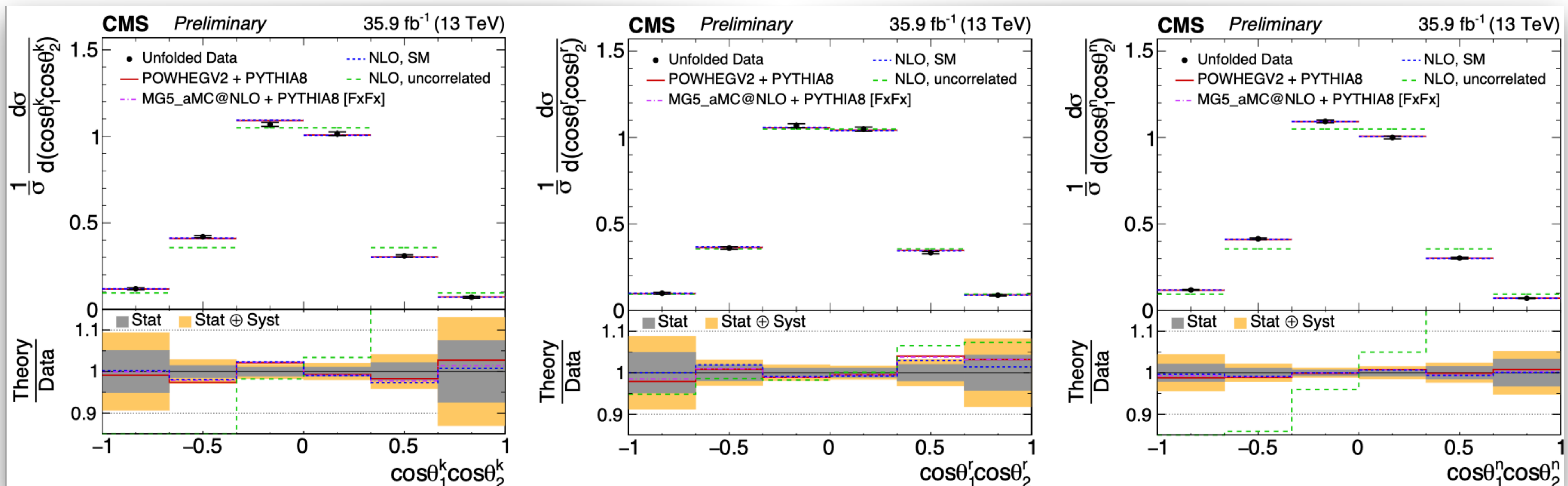

Polarization and spin correlations in dilepton channel

CMS-PAS-TOP-18-006

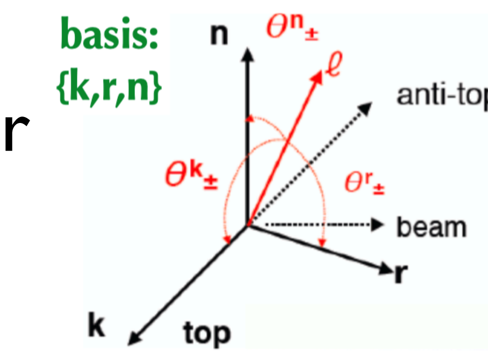

- **Direct measurement** requires full reconstruction of t and tbar
- Dilepton angular distribution probes top spin in 3 dimensions:

$$\frac{1}{\sigma}\frac{d\sigma}{d\Omega_+ d\Omega_-} = \frac{1}{(4\pi)^2}\left(1 + \mathbf{B}^+ \cdot \hat{\ell}^+ + \mathbf{B}^- \cdot \hat{\ell}^- - \hat{\ell}^+ \cdot \mathbb{C} \cdot \hat{\ell}^-\right)$$

  - 3-vectors $B^{+/-}$ = polarizations, 3x3 matrix C = spin correlations
  - spin dependence of ttbar production completely characterized by 15 coefficients, individually probed by measuring angular distribution at parton level: $\frac{1}{\sigma}\frac{d\sigma}{dx} = \frac{1}{2}(1 + [\mathbf{Coef.}]\, x)\, f(x) \longrightarrow \frac{1}{\sigma}\frac{d\sigma}{d\cos\varphi} = \frac{1}{2}(1 - D\cos\varphi)$

- cosφ = opening angle between the leptons, $D = -(C_{kk} + C_{rr} + C_{nn})/3$

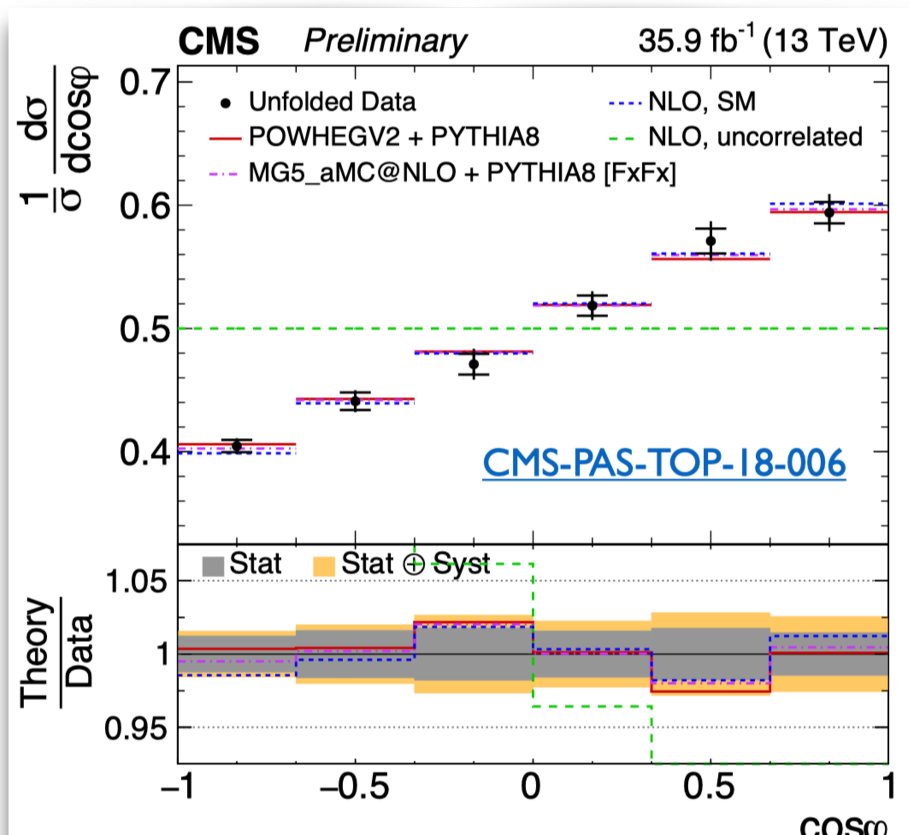

Most precise single variable

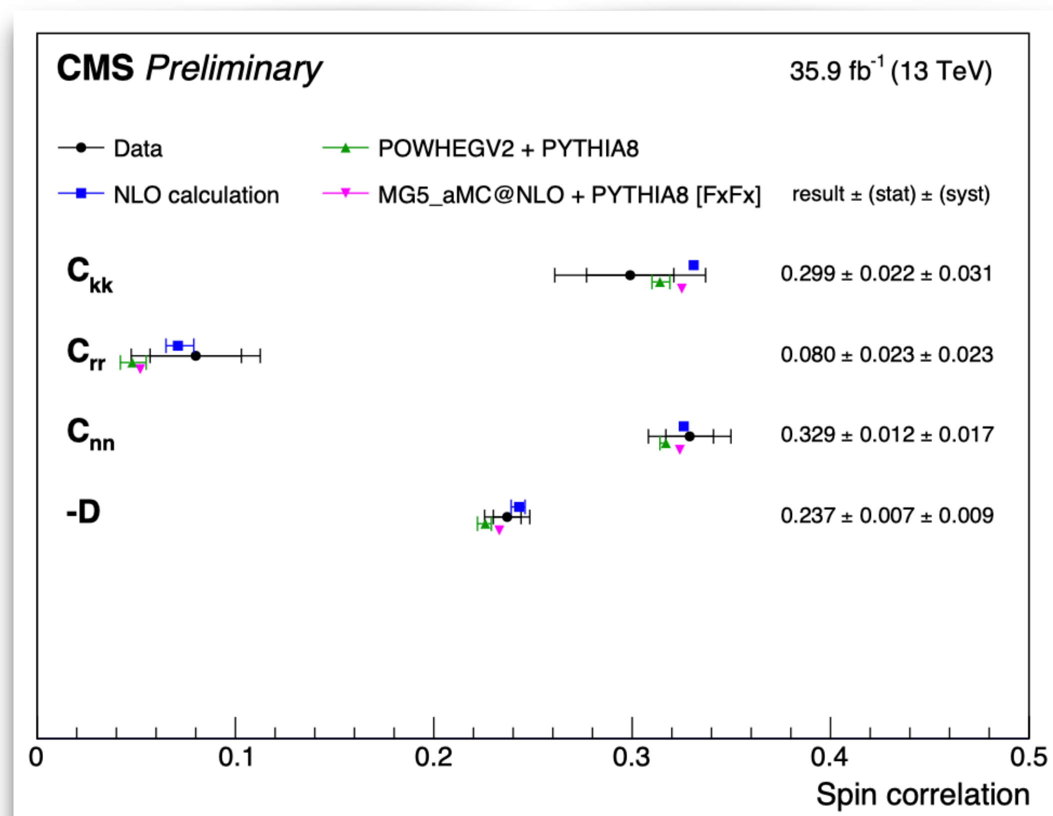

Mass in the all-jets channel and combination with lepton+jets

Eur. Phys. J. C 79 (2019) 313

2016 data @13 TeV: 35.9 fb^{-1}

- **All-jets event signature**:
  - largest BR of all ttbar decays
  - large background (multijet production) → challenging measurement
- Kinematic fit to separate signal from background events
- Ideogram method to extract m_t :
  - likelihood function simultaneously constraining m_t and additional jet energy scale factor (JSF)

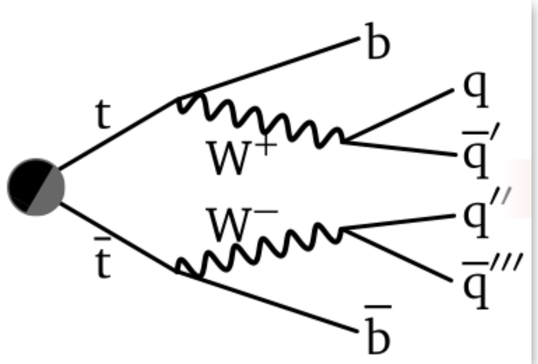

$$m_t^{\mathrm{hyb}} = 172.34 \pm 0.20\,(\mathrm{stat{+}JSF}) \pm 0.70\,(\mathrm{syst})\,\mathrm{GeV}$$
$$\mathrm{JSF}^{\mathrm{hyb}} = 0.997 \pm 0.002\,(\mathrm{stat}) \pm 0.007\,(\mathrm{syst}).$$

- **Combination with lepton+jets**:
  - 2 measurements using same mass extraction method → single likelihood
  - combined measurement has lowest total uncertainty
  - results consistent with previous measurements

$$m_t^{\mathrm{hyb}} = 172.26 \pm 0.07\,(\mathrm{stat{+}JSF}) \pm 0.61\,(\mathrm{syst})\,\mathrm{GeV}$$
$$\mathrm{JSF}^{\mathrm{hyb}} = 0.996 \pm 0.001\,(\mathrm{stat}) \pm 0.007\,(\mathrm{syst})$$

Mass in the all-jets channel and combination with lepton+jets

Eur. Phys. J. C 79 (2019) 313

2016 data @13 TeV: 35.9 fb^{-1}

- **All-jets event signature**:
  - largest BR of all ttbar decays
  - large background (multijet production) → challenging measurement
- Kinematic fit to separate signal from backgrou
- Ideogram method to extract m_t :
  - likelihood function simultaneously constraining
    additional jet energy scale factor (JSF)

$$m_t^{hyb} = 172.34 \pm 0.20\,(\text{stat+JSF}) \pm 0.70\,(\text{sy}$$
$$\text{JSF}^{hyb} = 0.997 \pm 0.002\,(\text{stat}) \pm 0.007\,(\text{syst}).$$

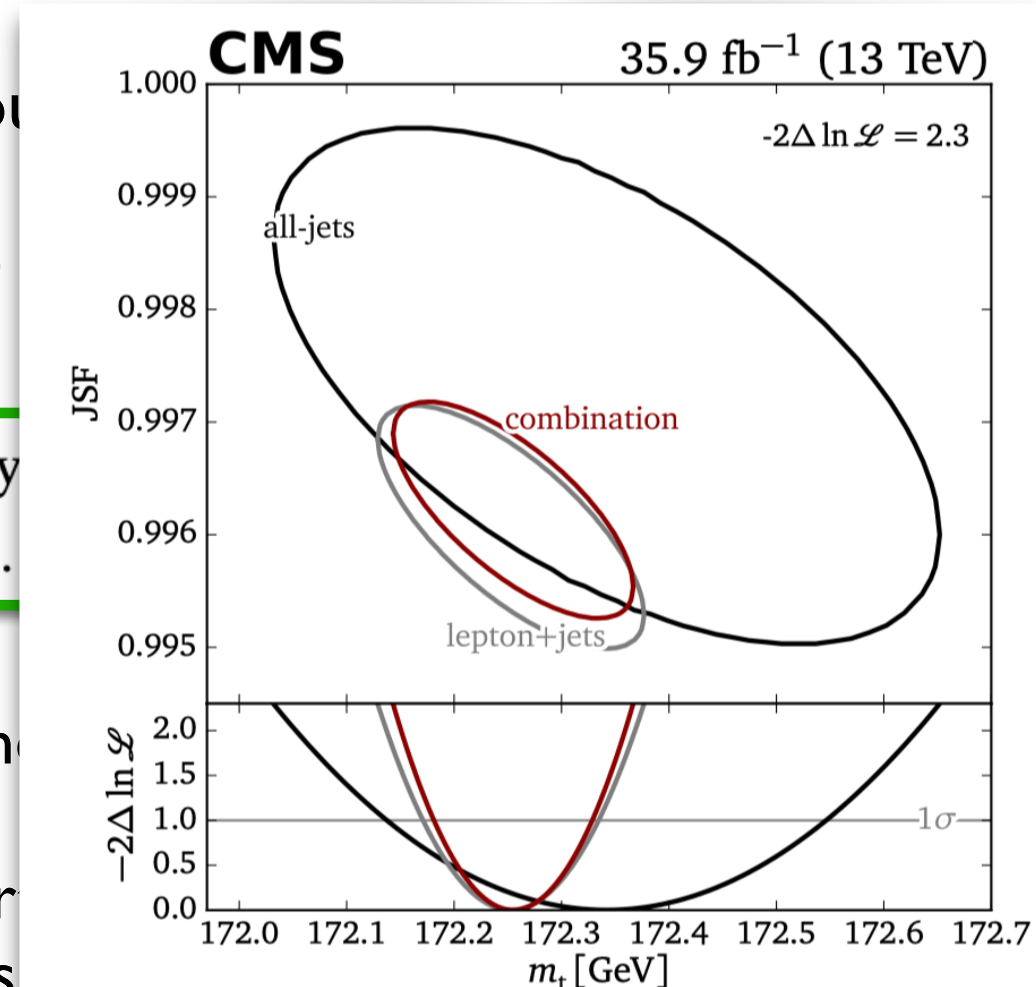

- **Combination with lepton+jets**:
  - 2 measurements using same mass extraction m
    → single likelihood
  - combined measurement has lowest total uncer
  - results consistent with previous measurements

$$m_t^{hyb} = 172.26 \pm 0.07\,(\text{stat+JSF}) \pm 0.61\,(\text{syst})\,\text{GeV}$$
$$\text{JSF}^{hyb} = 0.996 \pm 0.001\,(\text{stat}) \pm 0.007\,(\text{syst})$$

First simultaneous measurement in the combined lepton+jets and all-jets channels!

Mass: inclusive measurement

arXiv:1812.10505

2016 data @13 TeV: 35.9 fb^{-1}

- Measurement performed in $e^{\mp}\mu^{\pm}$ channel only
- Simultaneous measurement of σ_{ttbar} and m_t^{MC} from template fit to final state distributions to determine cross section at optimal mass point:

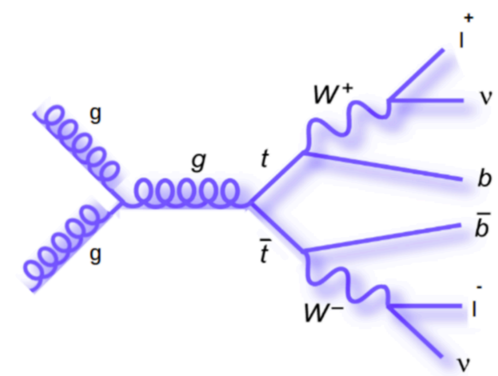

$$\sigma_{t\bar{t}} = 815 \pm 2\,(\text{stat}) \pm 29\,(\text{syst}) \pm 20\,(\text{lumi})\,\text{pb},$$
$$m_t^{MC} = 172.33 \pm 0.14\,(\text{stat})\,^{+0.66}_{-0.72}\,(\text{syst})\,\text{GeV}.$$

- Observed σ_{ttbar} compared to fixed-order theory predictions to extract top mass with different set of PDFs:
  - in the minimal subtraction renormalization scheme

PDF set	$m_t(m_t)$ [GeV]
ABMP16	$161.6 \pm 1.6\,(\text{fit} + \text{PDF} + \alpha_S)\,^{+0.1}_{-1.0}\,(\text{scale})$
NNPDF3.1	$164.5 \pm 1.6\,(\text{fit} + \text{PDF} + \alpha_S)\,^{+0.1}_{-1.0}\,(\text{scale})$
CT14	$165.0 \pm 1.8\,(\text{fit} + \text{PDF} + \alpha_S)\,^{+0.1}_{-1.0}\,(\text{scale})$
MMHT14	$164.9 \pm 1.8\,(\text{fit} + \text{PDF} + \alpha_S)\,^{+0.1}_{-1.1}\,(\text{scale})$

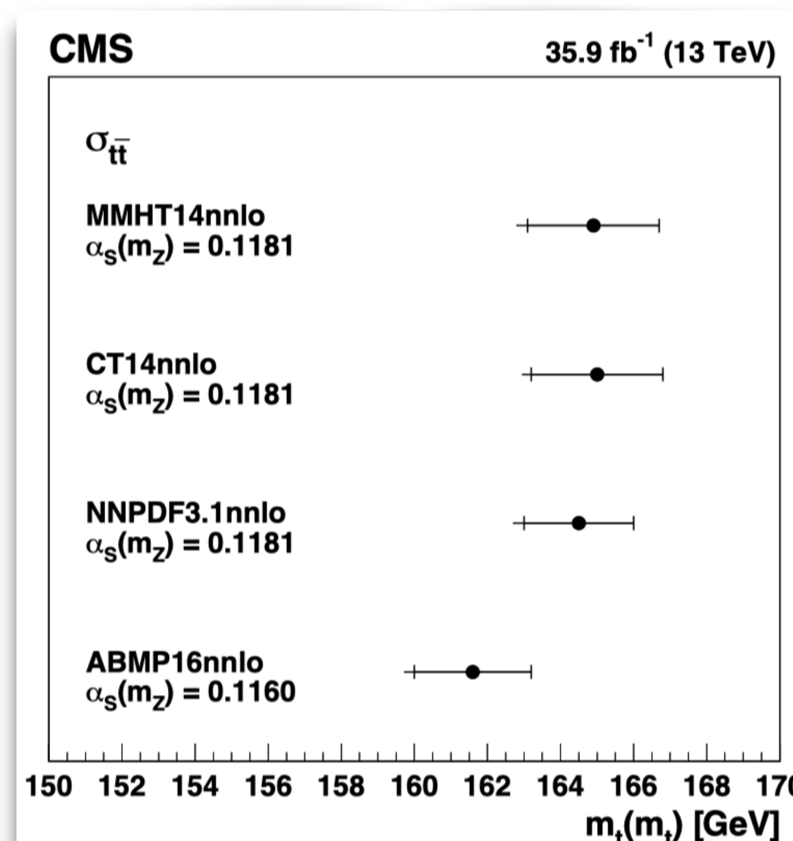

Mass:
inclusive measurement

arXiv:1812.10505

2016 data @13 TeV:
35.9 fb^{-1}

- Measurement performed in $e^{\mp}\mu^{\pm}$ channel only
- Simultaneous measurement of σ_{ttbar} and m_t^{MC} from template fit to final state distributions to determine cross section at optimal mass point:

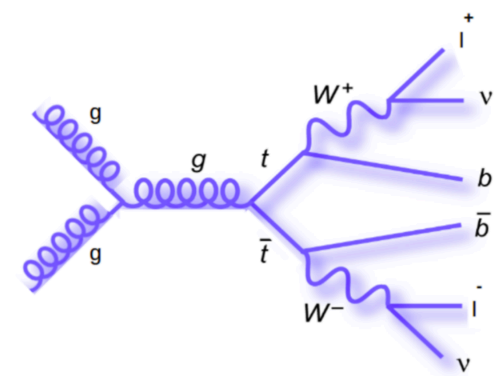

$$\sigma_{t\bar{t}} = 815 \pm 2\,(\text{stat}) \pm 29\,(\text{syst}) \pm 20\,(\text{lumi})\,\text{pb},$$
$$m_t^{\text{MC}} = 172.33 \pm 0.14\,(\text{stat})\,^{+0.66}_{-0.72}\,(\text{syst})\,\text{GeV}.$$

- Observed σ_{ttbar} compared to fixed-order theory predictions to extract top mass with different set of PDFs:
  - in the minimal subtraction renormalization scheme
  - in the pole mass scheme

PDF set	m_t^{pole} [GeV]
ABMP16	$169.9 \pm 1.8\,(\text{fit} + \text{PDF} + \alpha_S)\,^{+0.8}_{-1.2}\,(\text{scale})$
NNPDF3.1	$173.2 \pm 1.9\,(\text{fit} + \text{PDF} + \alpha_S)\,^{+0.9}_{-1.3}\,(\text{scale})$
CT14	$173.7 \pm 2.0\,(\text{fit} + \text{PDF} + \alpha_S)\,^{+0.9}_{-1.4}\,(\text{scale})$
MMHT14	$173.6 \pm 1.9\,(\text{fit} + \text{PDF} + \alpha_S)\,^{+0.9}_{-1.4}\,(\text{scale})$

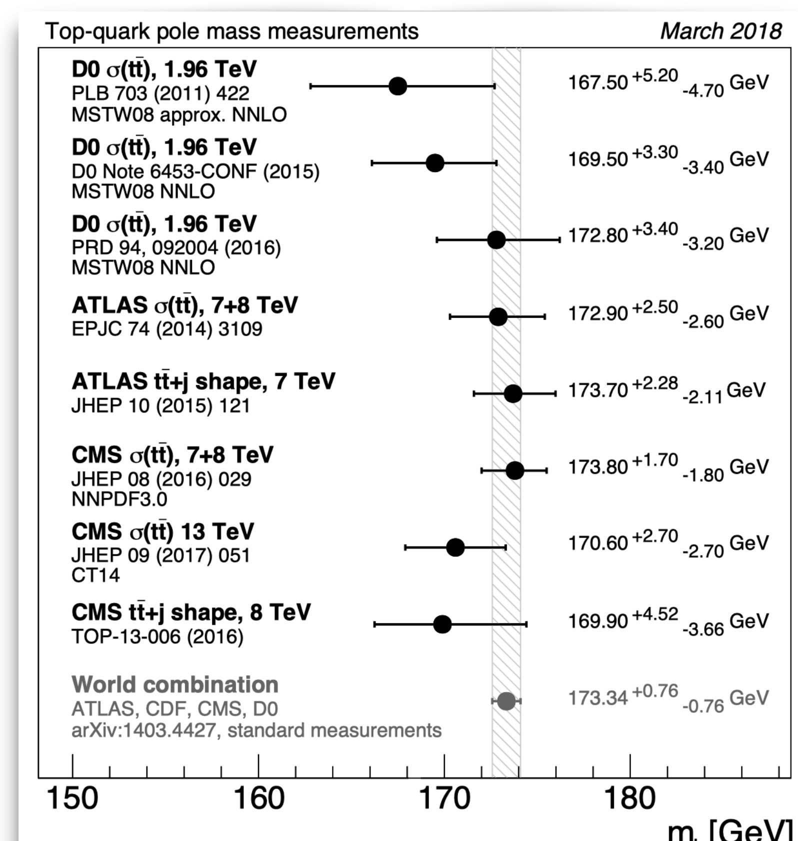

Strong coupling strength: inclusive measurement

arXiv:1812.10505

2016 data @13 TeV: 35.9 fb^{-1}

- Measurement performed in $e^{\mp}\mu^{\pm}$ channel only
- Simultaneous measurement of σ_{ttbar} and m_t^{MC} from template fit to final state distributions to determine cross section at optimal mass point:

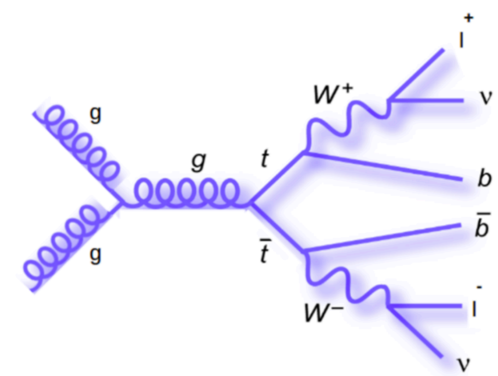

$$\sigma_{t\bar{t}} = 815 \pm 2\,(\text{stat}) \pm 29\,(\text{syst}) \pm 20\,(\text{lumi})\,\text{pb},$$
$$m_t^{MC} = 172.33 \pm 0.14\,(\text{stat})\,^{+0.66}_{-0.72}\,(\text{syst})\,\text{GeV}.$$

- Observed σ_{ttbar} compared to fixed-order theory predictions to extract $\alpha_S(M_Z)$ with different set of PDFs:
  - in the minimal subtraction renormalization scheme

PDF set	$\alpha_S(m_Z)$
ABMP16	$0.1139 \pm 0.0023\,(\text{fit}+\text{PDF})\,^{+0.0014}_{-0.0001}\,(\text{scale})$
NNPDF3.1	$0.1140 \pm 0.0033\,(\text{fit}+\text{PDF})\,^{+0.0021}_{-0.0002}\,(\text{scale})$
CT14	$0.1148 \pm 0.0032\,(\text{fit}+\text{PDF})\,^{+0.0018}_{-0.0002}\,(\text{scale})$
MMHT14	$0.1151 \pm 0.0035\,(\text{fit}+\text{PDF})\,^{+0.0020}_{-0.0002}\,(\text{scale})$

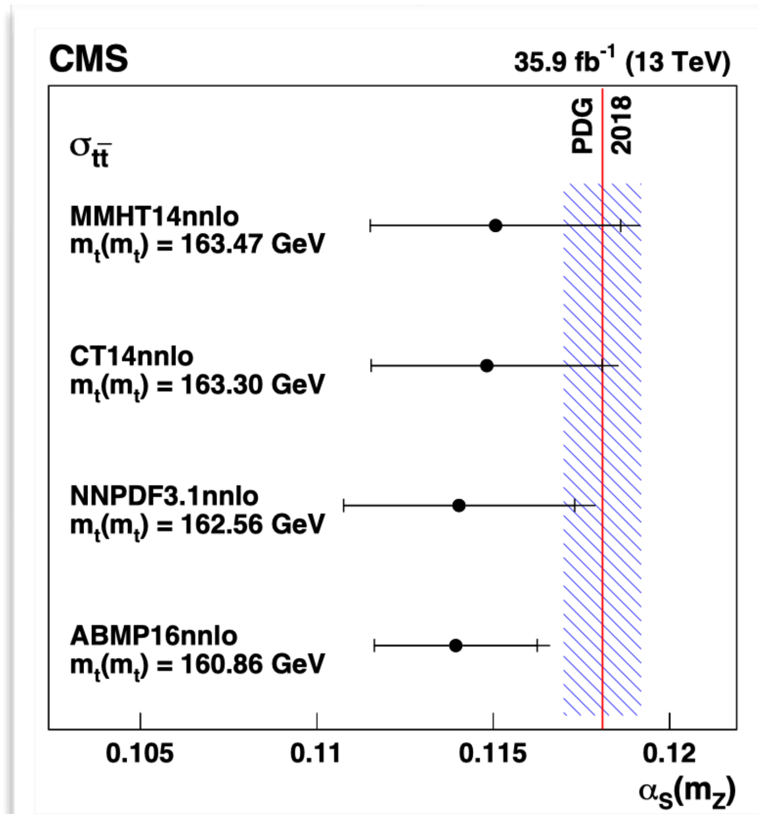

Strong coupling strength: inclusive measurement

arXiv:1812.10505

2016 data @13 TeV:
35.9 fb^{-1}

- Measurement performed in $e^{\mp}\mu^{\pm}$ channel only
- Simultaneous measurement of σ_{ttbar} and m_t^{MC} from template fit to final state distributions to determine cross section at optimal mass point:

$$\sigma_{t\bar{t}} = 815 \pm 2\,(\text{stat}) \pm 29\,(\text{syst}) \pm 20\,(\text{lumi})\,\text{pb},$$
$$m_t^{MC} = 172.33 \pm 0.14\,(\text{stat})\,^{+0.66}_{-0.72}\,(\text{syst})\,\text{GeV}.$$

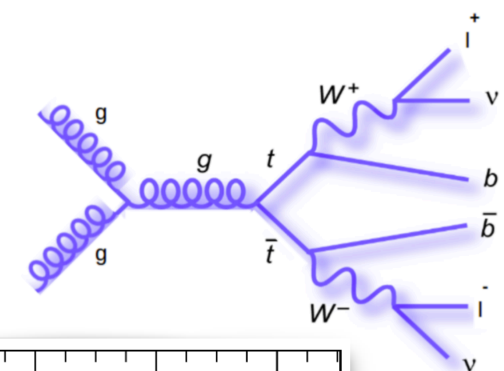

- Observed σ_{ttbar} compared to fixed-order theo
to extract $\alpha_S(M_Z)$ with different set of PDFs:
  - in the minimal subtraction renormalization

PDF set	$\alpha_S(m_Z)$
ABMP16	$0.1139 \pm 0.0023\,(\text{fit}+\text{PDF})\,^{+0.0014}_{-0.0001}\,(\text{scale})$
NNPDF3.1	$0.1140 \pm 0.0033\,(\text{fit}+\text{PDF})\,^{+0.0021}_{-0.0002}\,(\text{scale})$
CT14	$0.1148 \pm 0.0032\,(\text{fit}+\text{PDF})\,^{+0.0018}_{-0.0002}\,(\text{scale})$
MMHT14	$0.1151 \pm 0.0035\,(\text{fit}+\text{PDF})\,^{+0.0020}_{-0.0002}\,(\text{scale})$

Most precise result at a single experiment!

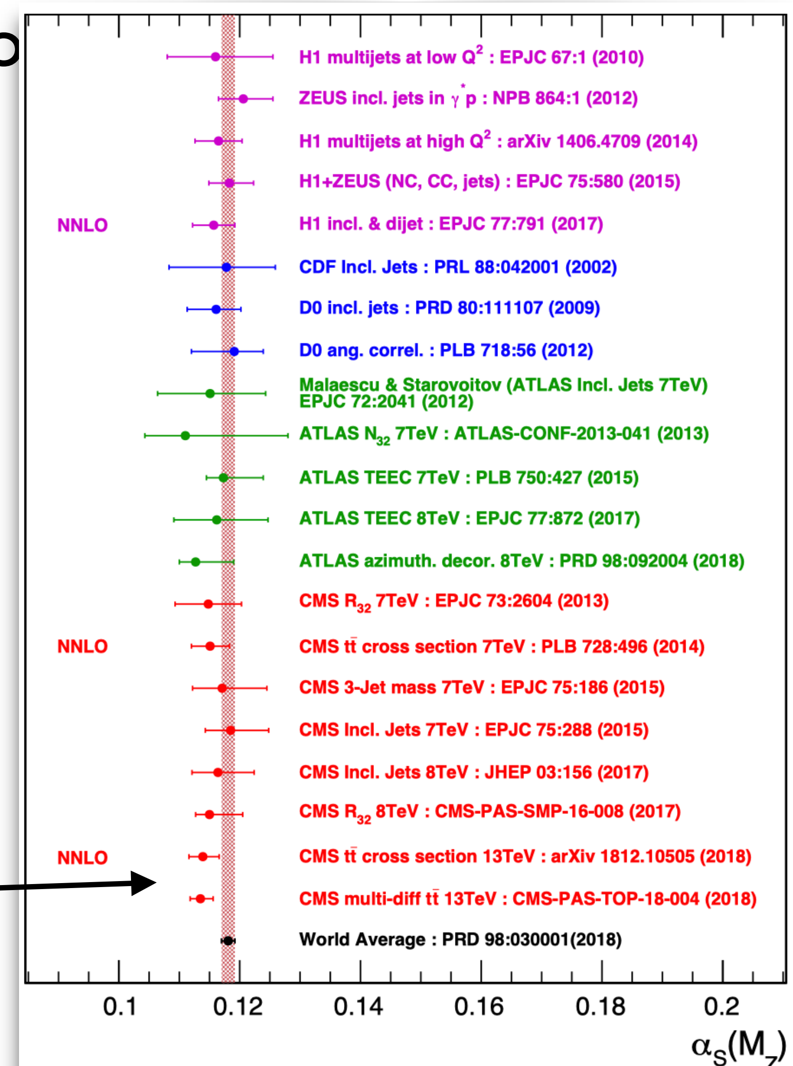

More m_t and $\alpha_S(M_Z)$: differential measurement

arXiv:1904.05237

2016 data @13 TeV:
35.9 fb^{-1}

- **Dilepton channel**: two oppositely charged leptons
- Normalized 3D cross sections vs M(ttbar), y(ttbar), N_{jet}:
  - measurement unfold to parton level
  - compared to NLO predictions with different PDFs, α_S, m_t^{pole} → extraction of α_S, m_t^{pole} :

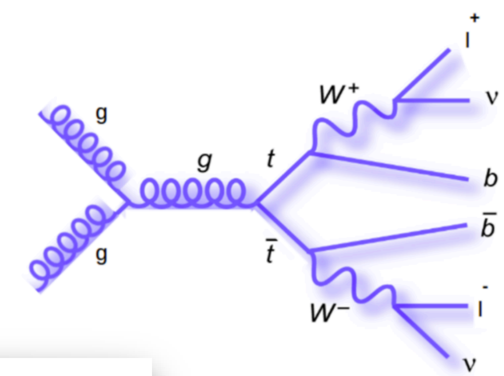

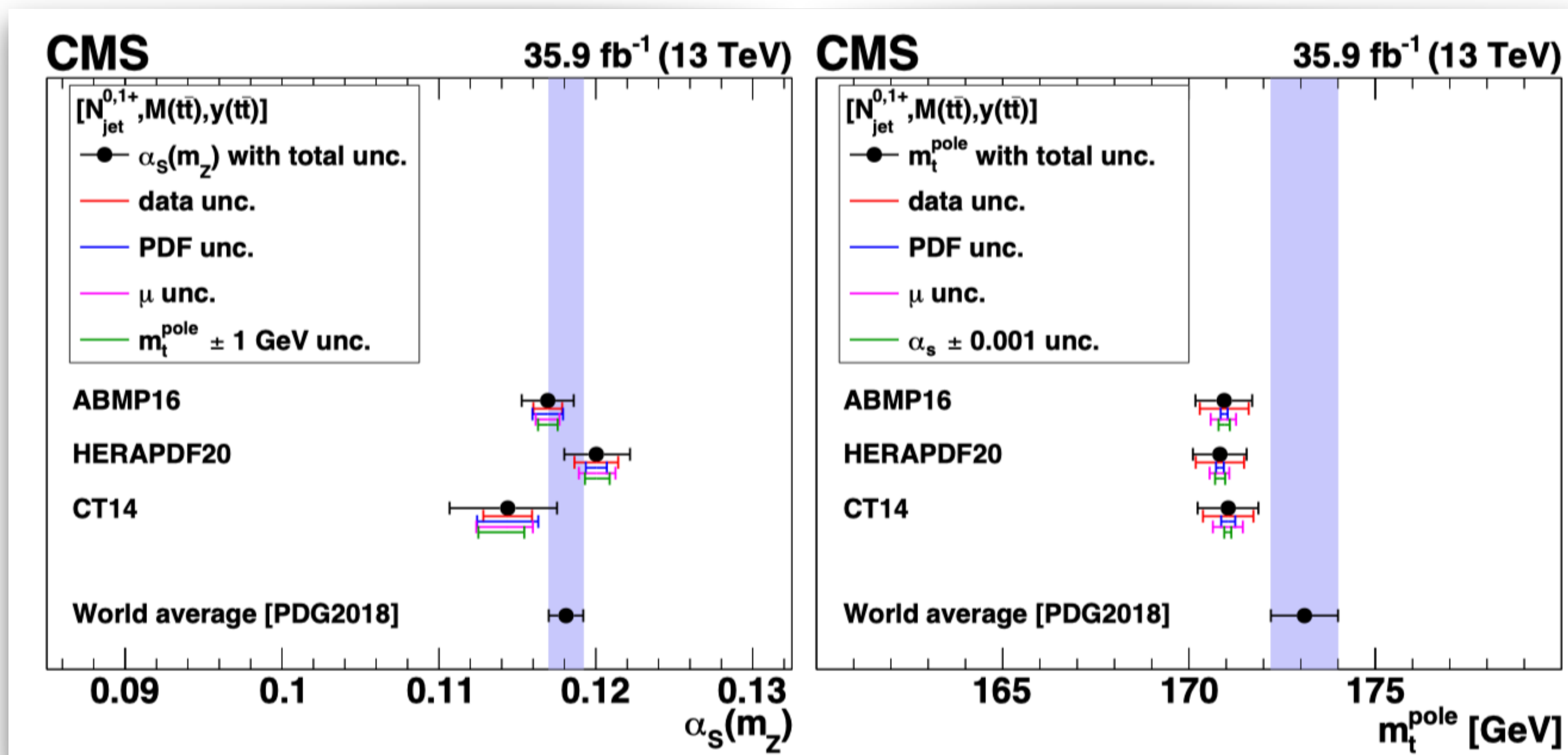

More m_t and $\alpha_S(M_Z)$: differential measurement

arXiv:1904.05237

2016 data @13 TeV: 35.9 fb^{-1}

- **Dilepton channel**: two oppositely charged leptons
- Normalized 3D cross sections vs M(ttbar), y(ttbar), N_{jet}:
  - measurement unfold to parton level
  - compared to NLO predictions with different PDFs, α_S, m_t^{pole} → extraction of α_S, m_t^{pole}
  - simultaneous fit of PDF+α_S+m_t^{pole} at NLO + HERA DIS data → extraction of α_S, m_t^{pole}:

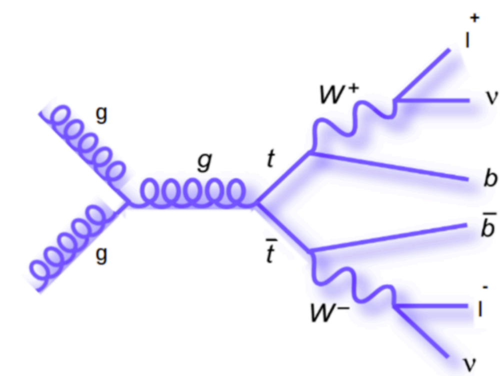

$$\alpha_S(m_Z) = 0.1135 \pm 0.0016(\text{fit})^{+0.0002}_{-0.0004}(\text{model})^{+0.0008}_{-0.0001}(\text{param})^{+0.0011}_{-0.0005}(\text{scale}) = 0.1135^{+0.0021}_{-0.0017}(\text{total}),$$

$$m_t^{\text{pole}} = 170.5 \pm 0.7(\text{fit}) \pm 0.1(\text{model})^{+0.0}_{-0.1}(\text{param}) \pm 0.3(\text{scale})\ \text{GeV} = 170.5 \pm 0.8(\text{total})\ \text{GeV}.$$

PDFs: differential measurement

arXiv:1904.05237

2016 data @13 TeV: 35.9 fb^{-1}

- **Dilepton channel**: two oppositely charged leptons
- Normalized 3D cross sections vs M(ttbar), y(ttbar), N_{jet}:
  - measurement unfold to parton level
  - compared to NLO predictions with different PDFs, α_S, m_t^{pole} → extraction of α_S, m_t^{pole}
  - simultaneous fit of PDF+α_S+m_t^{pole} at NLO + HERA DIS data → extraction of α_S, m_t^{pole}:

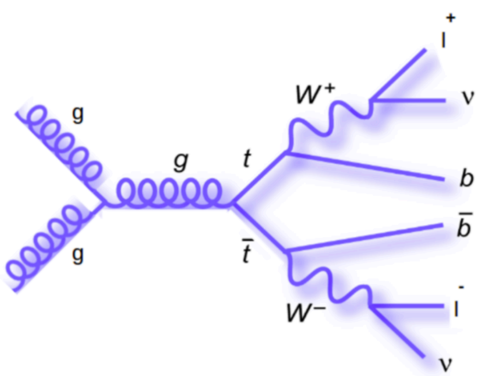

$$\alpha_S(m_Z) = 0.1135 \pm 0.0016(\text{fit})^{+0.0002}_{-0.0004}(\text{model})^{+0.0008}_{-0.0001}(\text{param})^{+0.0011}_{-0.0005}(\text{scale}) = 0.1135^{+0.0021}_{-0.0017}(\text{total}),$$
$$m_t^{\text{pole}} = 170.5 \pm 0.7(\text{fit}) \pm 0.1(\text{model})^{+0.0}_{-0.1}(\text{param}) \pm 0.3(\text{scale})\ \text{GeV} = 170.5 \pm 0.8(\text{total})\ \text{GeV}.$$

  - impact on PDFs:

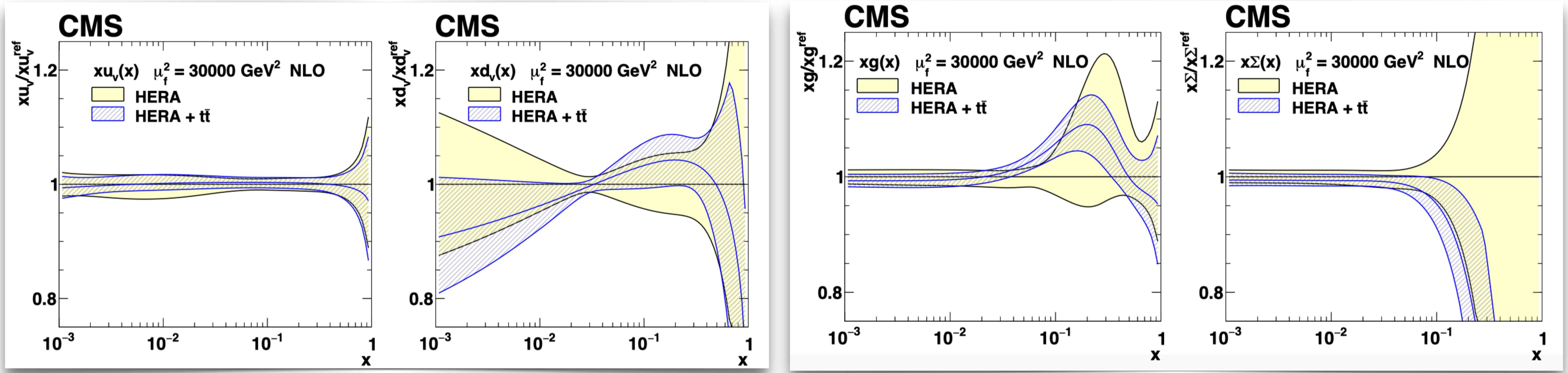

Yukawa coupling: ttbar differential measurement

CMS-PAS-TOP-17-004

2016 data @13 TeV: 35.8 fb^{-1}

- **Lepton+jets** event signature (BR = 34%, small background)
- Kinematic reconstruction of top candidates:
    - novel technique for events with 1 missing jet enhancing experimental sensitivity in the low invariant mass region
- Weak corrections:
    - due to electroweak boson exchange between the final state top quarks
    - small contribution to inclusive ttbar cross section
    - lead to large distortions of differential distributions near the production threshold region → sensitive to top-Higgs coupling Y_t
    - calculated for different value of Y_t in a given (M_{ttbar}, Δy_{ttbar})
    - applied at parton level to existing ttbar simulated samples
    - MC detector level distributions can thus be directly compared to data

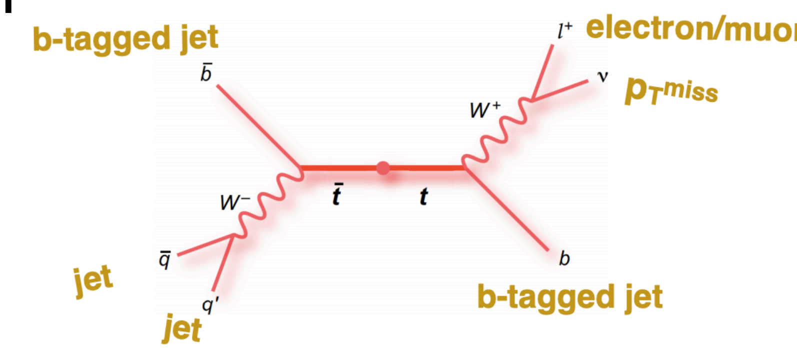

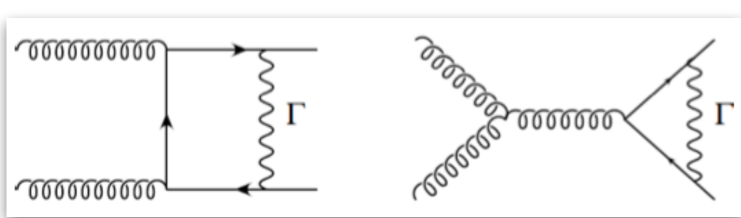

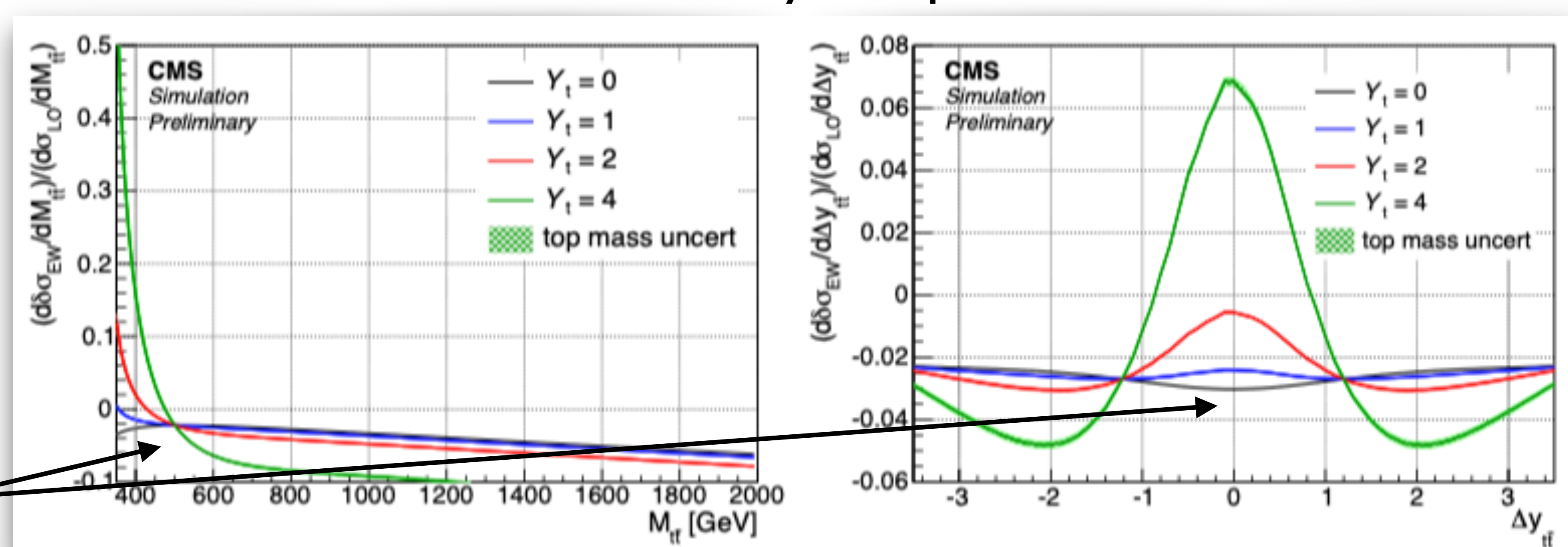

Most sensitive region

CMS-PAS-TOP-17-004

Yukawa coupling: ttbar differential measurement

2016 data @13 TeV: 35.8 fb[-1]

- 2D likelihood fit in (M_{ttbar}, Δy_{ttbar}) to constrain Y_t
- Sensitivity extracted bin-by-bin as a ratio of expected yields due to Yukawa coupling scenarios over the SM yields (no weak correction)
- Upper limit extraction on top quark Yukawa coupling:
  - limits set by scanning the likelihood with respect to Y_t
  - indirect measurement with good sensitivity, better than other measurements (tttt production indirectly constraints Y_t<1.7)

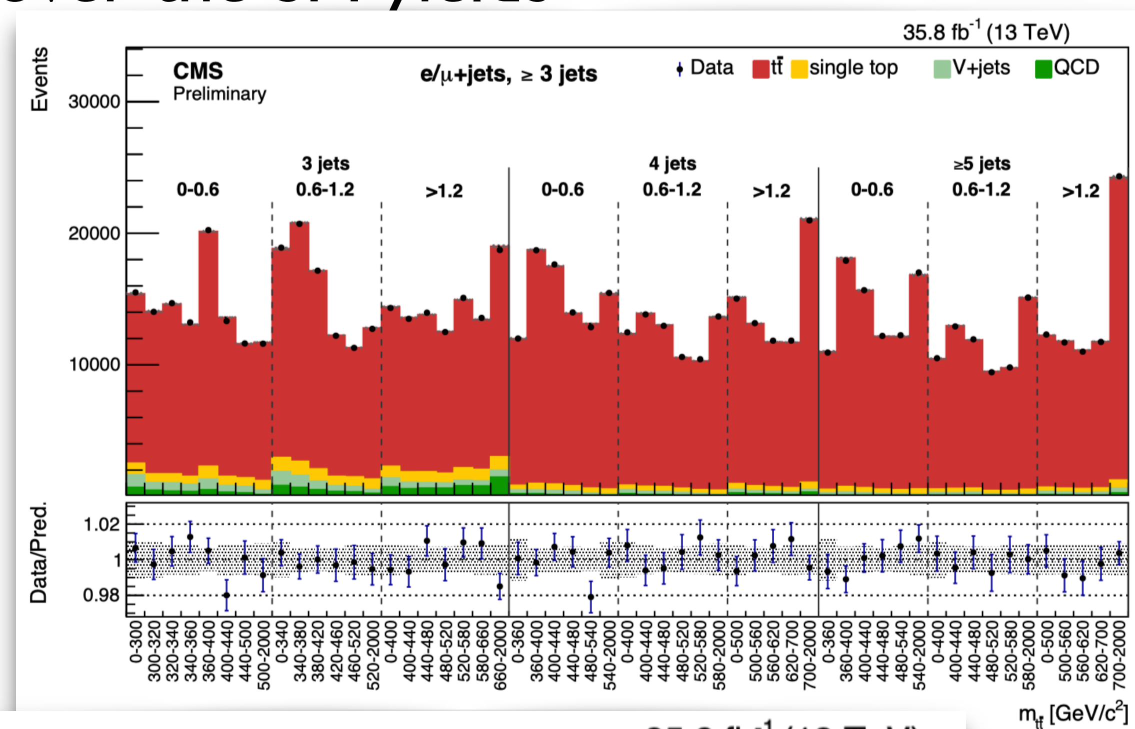

Channel	Expected 95% CL	Observed 95% CL
3 jets	$Y_t < 2.17$	$Y_t < 2.59$
4 jets	$Y_t < 1.88$	$Y_t < 1.77$
5 jets	$Y_t < 2.03$	$Y_t < 2.23$
Combined	$Y_t < 1.62$	$Y_t < 1.67$

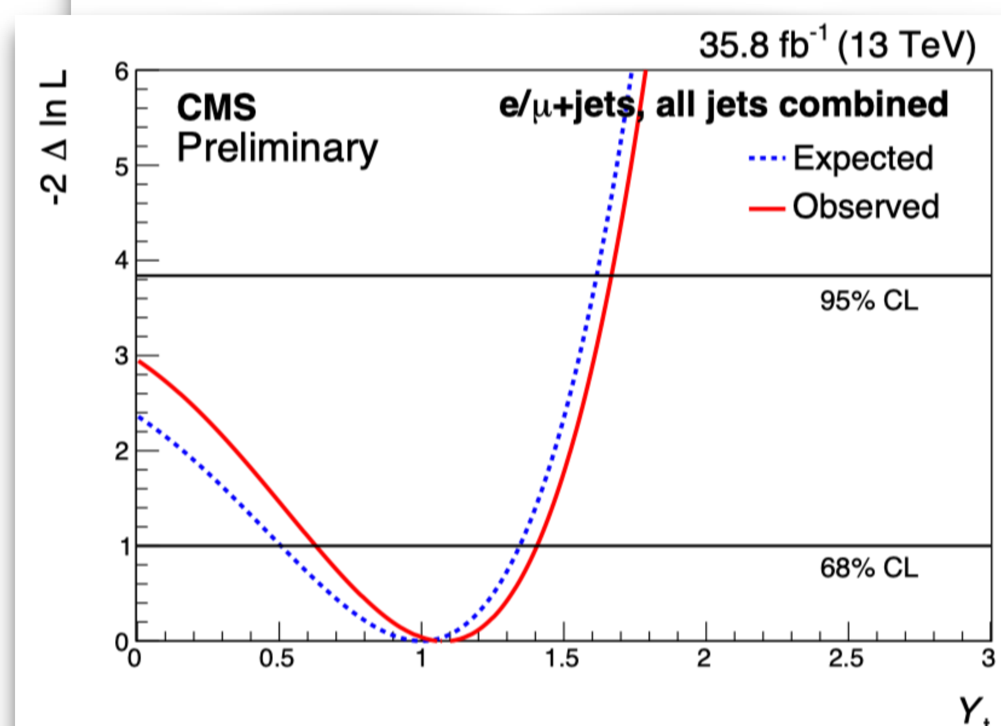

First analysis to measure Yukawa coupling with top pair production!

Yukawa coupling: 4 top quarks

CMS-PAS-TOP-18-003

Run2 data @13 TeV: 137 fb^{-1}

- **2 same-sign leptons or multi-lepton + jets** (BR ~12%):
  - low background final state → statistically-dominated
- 2 approaches used with a maximum likelihood fit to enhance signal sensitivity :
  - cut-based approach: baseline events separated into 14 bins depending on lepton and jet multiplicities
  - BDT approach: multi-variate classifier trained to separate signal from background
- Top Yukawa coupling constrained by upper limit on cross-section:
  - $|y_t / y_t^{SM}| < 1.7$ @ 95%CL

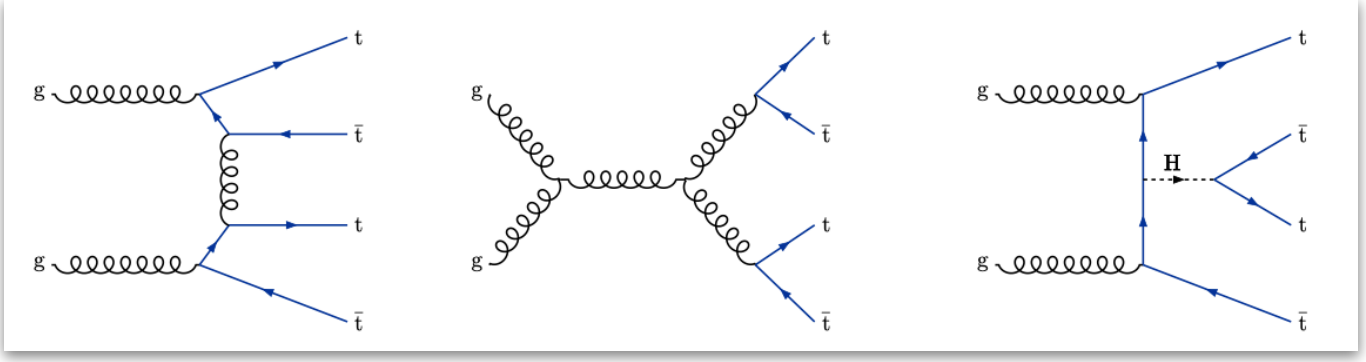

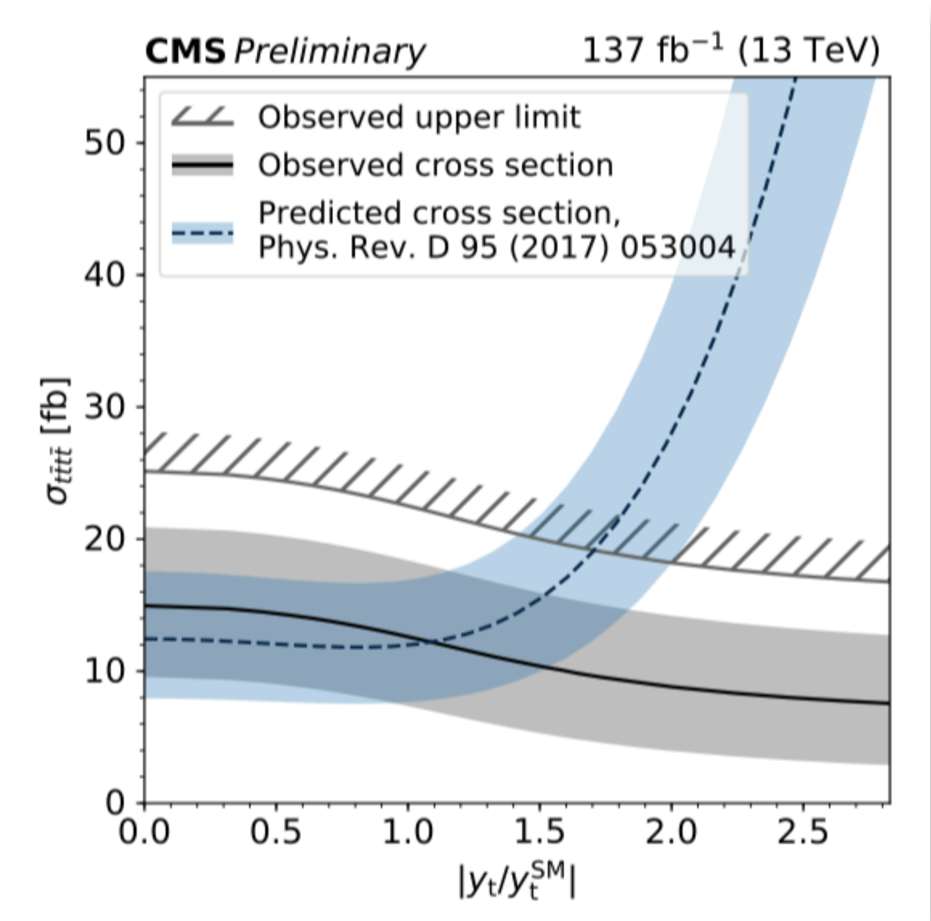

Charge asymmetries: differential measurement

JHEP 02 (2019) 149

2016 data @13 TeV: 35.9 fb^{-1}

- **Dilepton channel**: two oppositely charged leptons
- Kinematic reconstruction to define tt system
- Cut&count approach to measure differential cross sections in different bins
- Unfold to particle (fiducial) and parton (full phase space) levels
- Measurements of Δ|y|(tt) and Δ|η|(ll) allow charge asymmetries (A_C) extraction:

$$A_{c}^{t\bar{t}} = \frac{\sigma_{t\bar{t}}(\Delta|y|(t,\bar{t}) > 0) - \sigma_{t\bar{t}}(\Delta|y|(t,\bar{t}) < 0)}{\sigma_{t\bar{t}}(\Delta|y|(t,\bar{t}) > 0) + \sigma_{t\bar{t}}(\Delta|y|(t,\bar{t}) < 0)}, \quad A_{c}^{\ell\bar{\ell}} = \frac{\sigma_{t\bar{t}}(\Delta\eta(\ell,\bar{\ell}) > 0) - \sigma_{t\bar{t}}(\Delta\eta(\ell,\bar{\ell}) < 0)}{\sigma_{t\bar{t}}(\Delta\eta(\ell,\bar{\ell}) > 0) + \sigma_{t\bar{t}}(\Delta\eta(\ell,\bar{\ell}) < 0)}$$

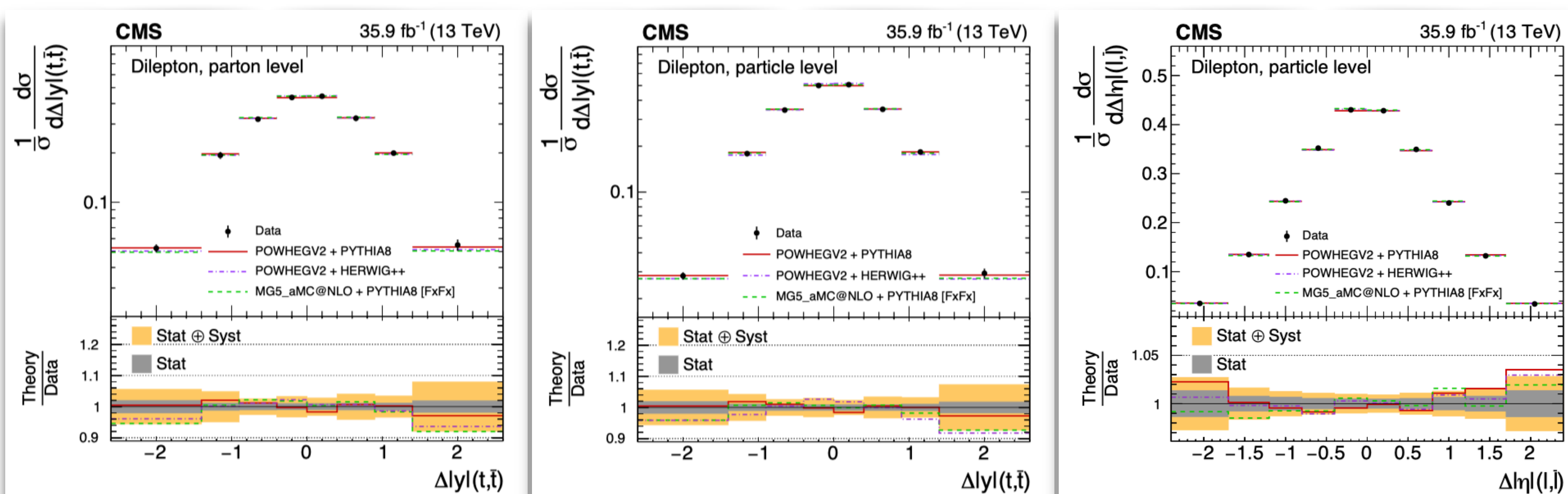

Charge asymmetries: differential measurement

JHEP 02 (2019) 149

2016 data @13 TeV: 35.9 fb^{-1}

- **Dilepton channel**: two oppositely charged leptons
- Kinematic reconstruction to define tt system
- Cut&count approach to measure differential cross sections in different bins
- Unfold to particle (fiducial) and parton (full phase space) levels
- Measurements of Δ|y|(tt) and Δ|η|(ll) allow charge asymmetries (A$_C$) extraction:

$$A_c^{t\bar{t}} = \frac{\sigma_{t\bar{t}}(\Delta|y|(t,\bar{t}) > 0) - \sigma_{t\bar{t}}(\Delta|y|(t,\bar{t}) < 0)}{\sigma_{t\bar{t}}(\Delta|y|(t,\bar{t}) > 0) + \sigma_{t\bar{t}}(\Delta|y|(t,\bar{t}) < 0)}, \quad A_c^{\ell\bar{\ell}} = \frac{\sigma_{t\bar{t}}(\Delta\eta(\ell,\bar{\ell}) > 0) - \sigma_{t\bar{t}}(\Delta\eta(\ell,\bar{\ell}) < 0)}{\sigma_{t\bar{t}}(\Delta\eta(\ell,\bar{\ell}) > 0) + \sigma_{t\bar{t}}(\Delta\eta(\ell,\bar{\ell}) < 0)}$$

- Results consistent with SM predictions:
  - NLO QCD
  - NLO QCD + EW

$$A_c^{t\bar{t}}(\text{parton level}) = 0.01 \pm 0.009,$$
$$A_c^{t\bar{t}}(\text{particle level}) = 0.008 \pm 0.009$$
$$A_c^{\ell\bar{\ell}}(\text{particle level}) = -0.005 \pm 0.004$$

First measurement @13 TeV and first time at particle level!

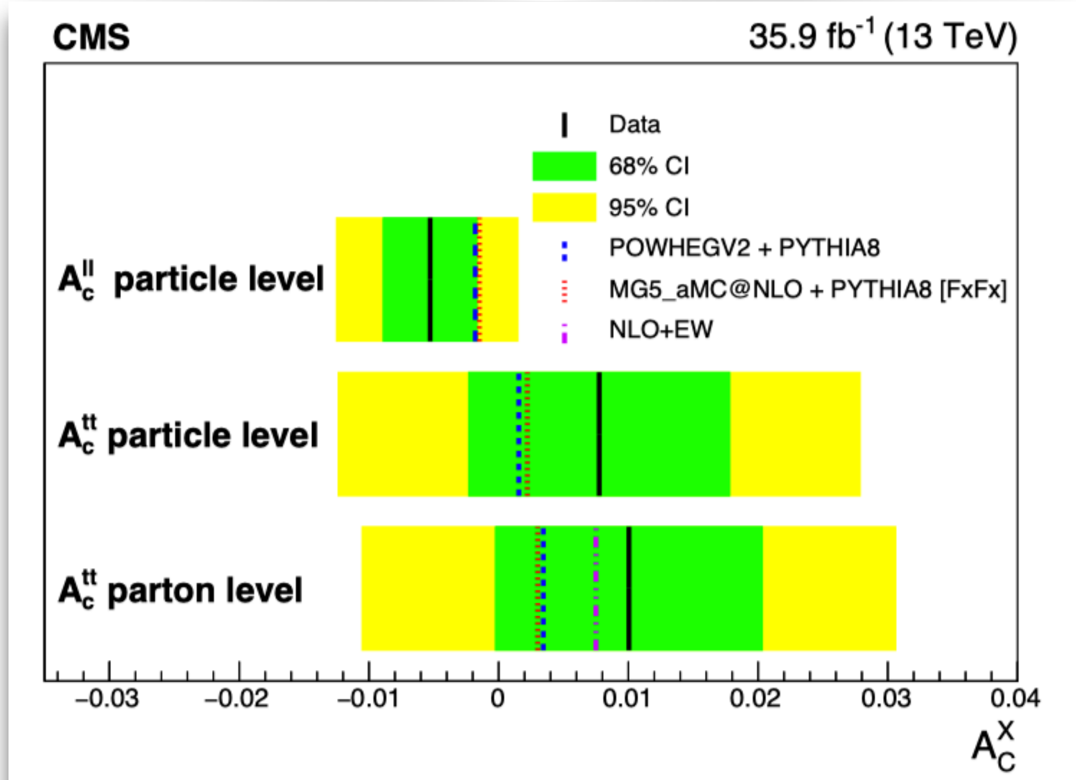

Summary

- Studies of top quark properties with **Run2 data @13 TeV**:
  - polarizations and ttbar spin correlations, mass, strong coupling strength, PDF, Yukawa coupling, charge asymmetries..
  - new precise measurements in different channels and with different approaches
  - most of them are statistically limited → will improve with higher luminosity
  - only mass limited by systematics uncertainties (usually JEC)
- New interesting results with Run2 legacy data… stay tuned!

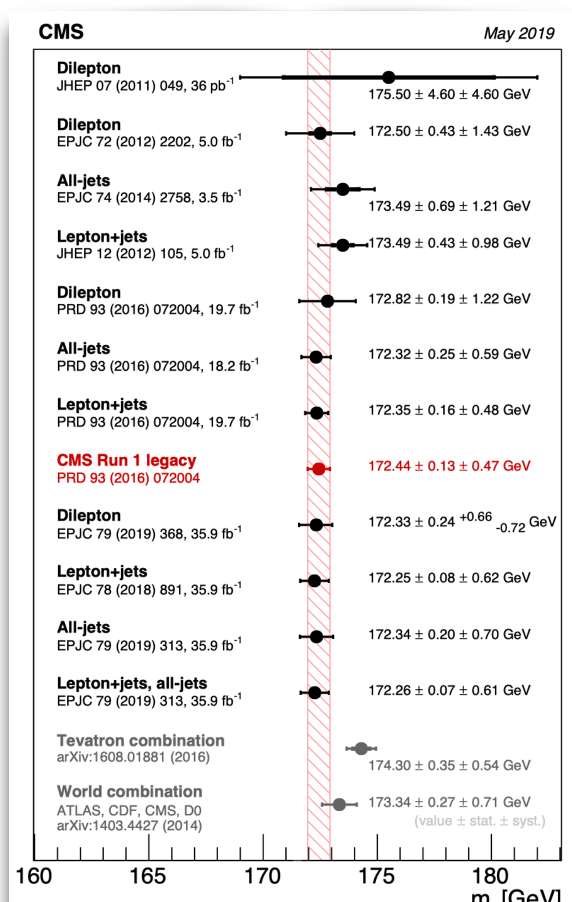

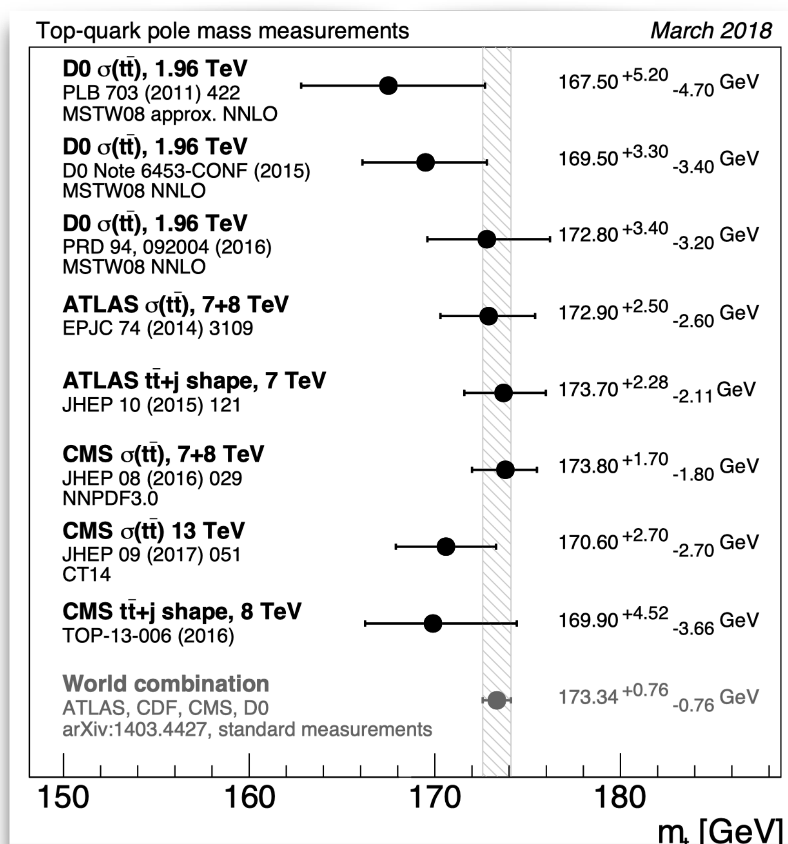

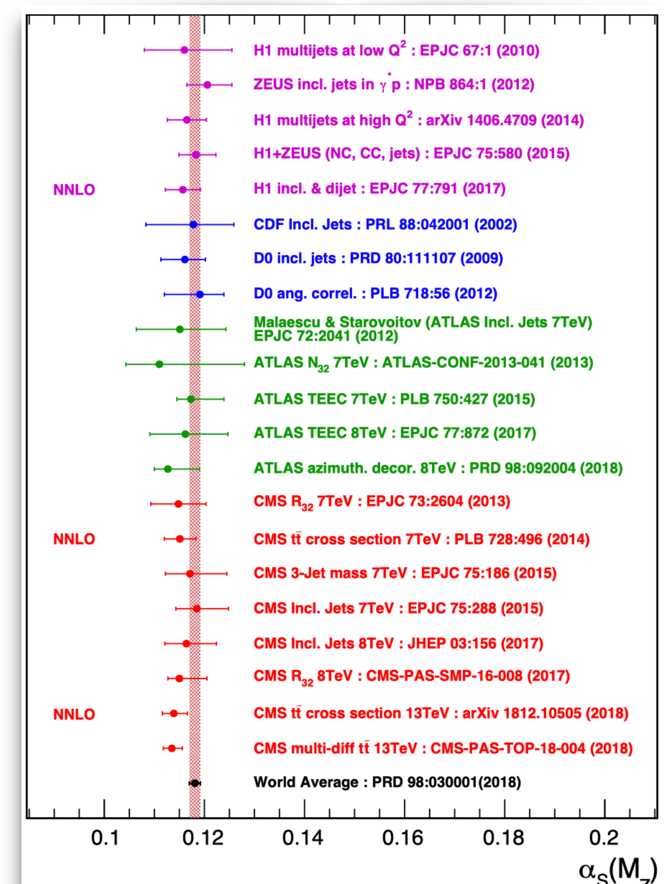

Backup

Polarization and spin correlations in dilepton channel: NNLO corrections to Δϕ

CMS-PAS-TOP-18-006

- NNLO calculations have been made both inclusively and in a fiducial region similar to that used by the experiments
- NNLO corrections are significantly larger in the fiducial phase space than in the full phase space
  - → large NNLO correction in the extrapolation to the full phase space (currently uses NLO MC)
- Calculated fiducial region not identical to those used in the analyses, but a correction of this size would account for the residual discrepancy

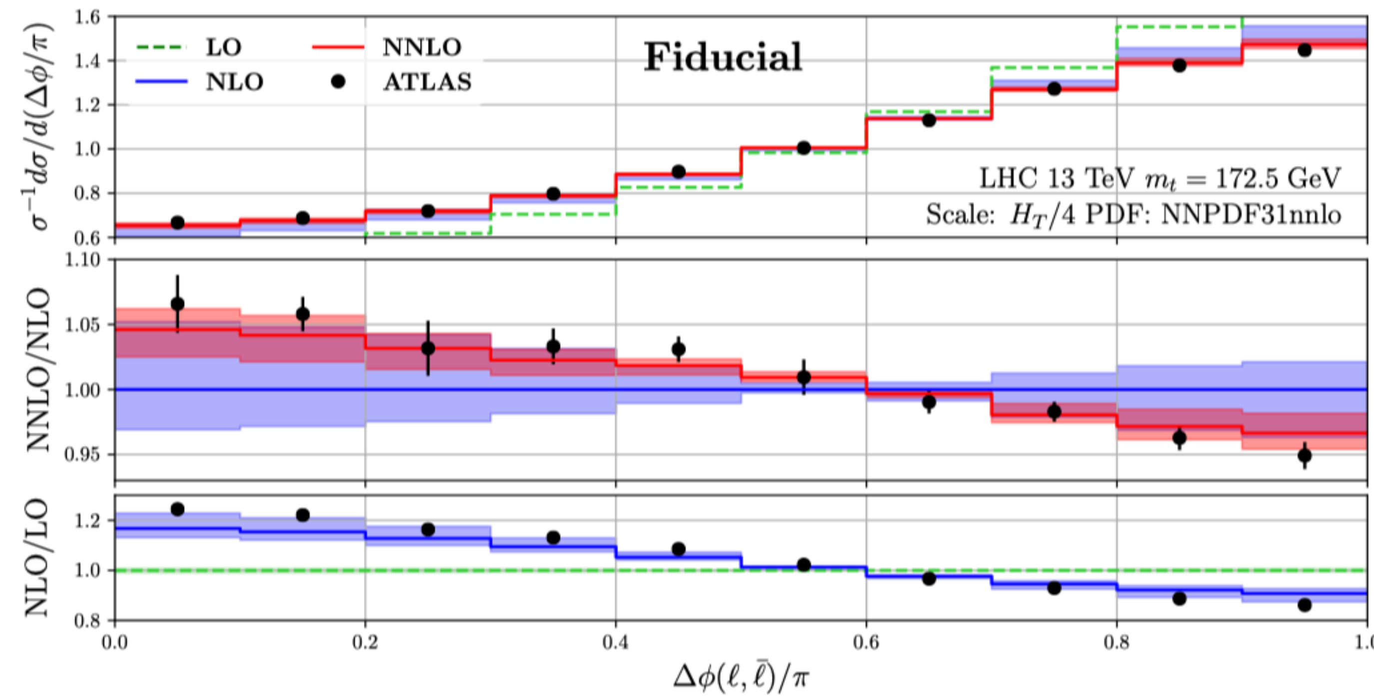

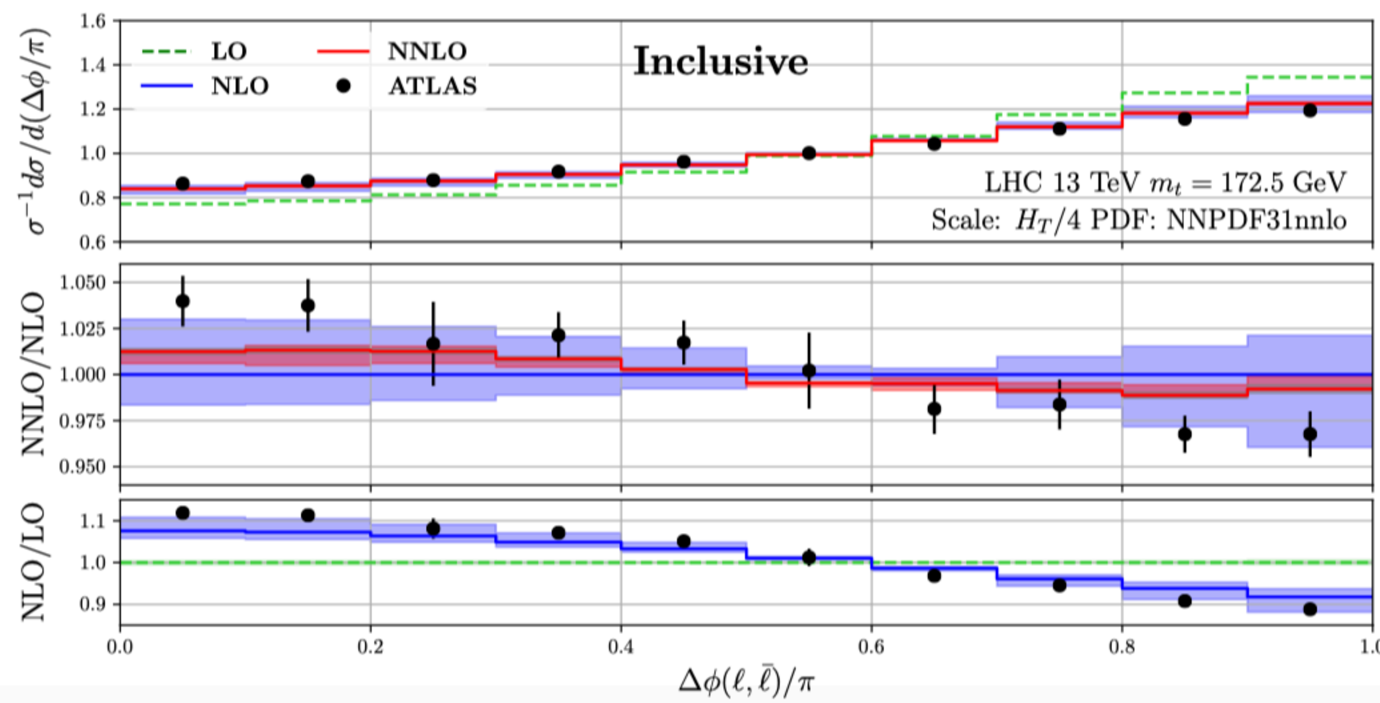

arxiv:1901.05407

Polarization and spin correlations in dilepton channel: unfolding

CMS-PAS-TOP-18-006

- Two corrections needed to compare measured distribution to theoretical calculations:
  - ”acceptance” (from fiducial region of detector with selection cuts to full phase space with no cuts)
  - ”migration” (to account for differences between true and reconstructed quantities)
- Acceptance and migration corrections parameterised by matrices that act on measured bins
  - Measured bins x related to true bins y by x= MAy
  - equation inverted with “regularisation” to suppress statistical fluctuations

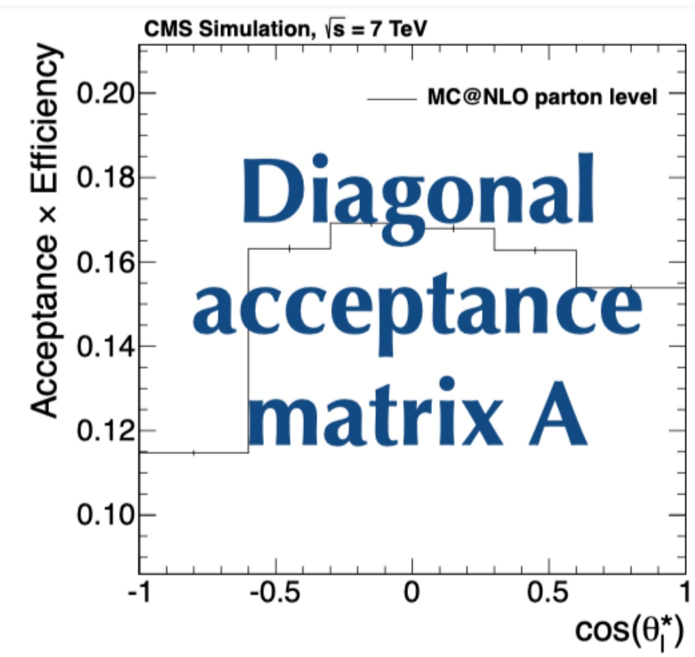

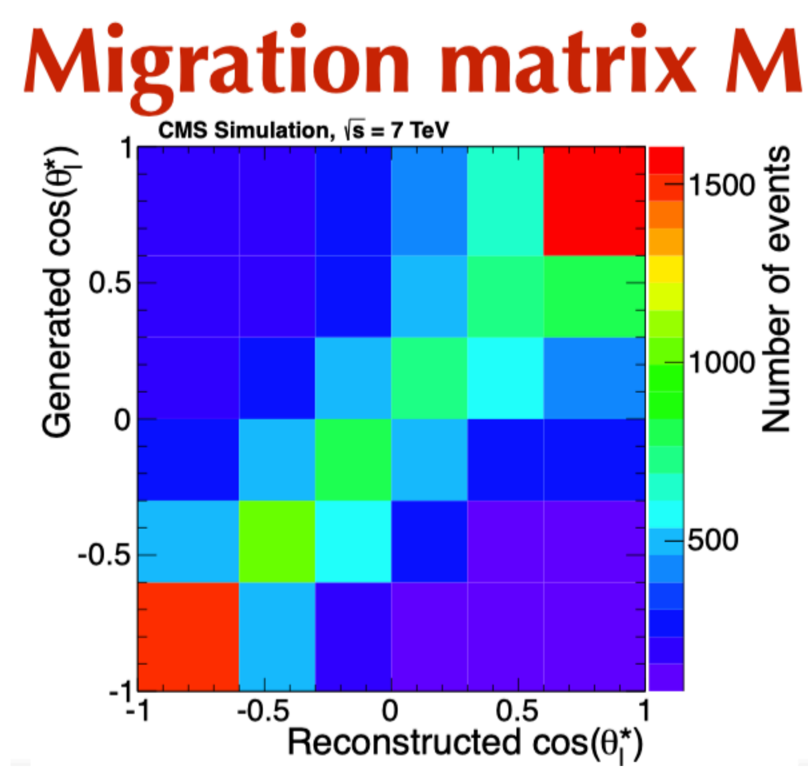

CMS-PAS-TOP-18-006

Polarization and spin correlations in dilepton channel: unfolding

- Unfolding to parton level:
  - to compare with fixed-order theoretical calculations, must correct to parton-level

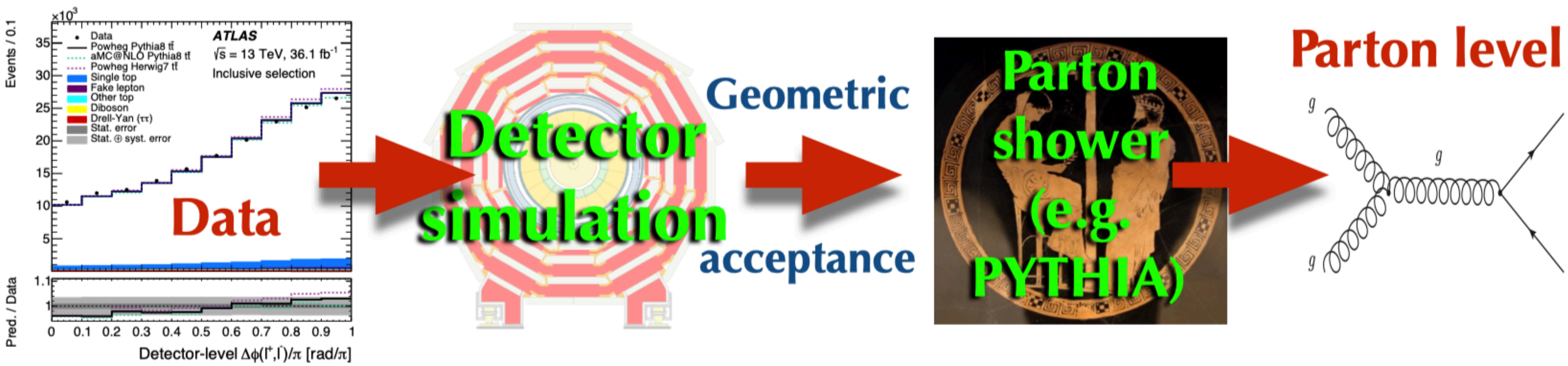

ADVANTAGES	DISADVANTAGES
Compare with fixed-order calculations	Model-dependence of parton shower
Combine with other experiments	Model-dependence of extrapolation
Can be used as part of global fit	Difficult to accurately estimate systematics

Polarization and spin correlations in dilepton channel: unfolding

CMS-PAS-TOP-18-006

- Unfolding to particle level:
    - to reduce the model-dependence, we can unfold to particle-level and minimize the acceptance extrapolation

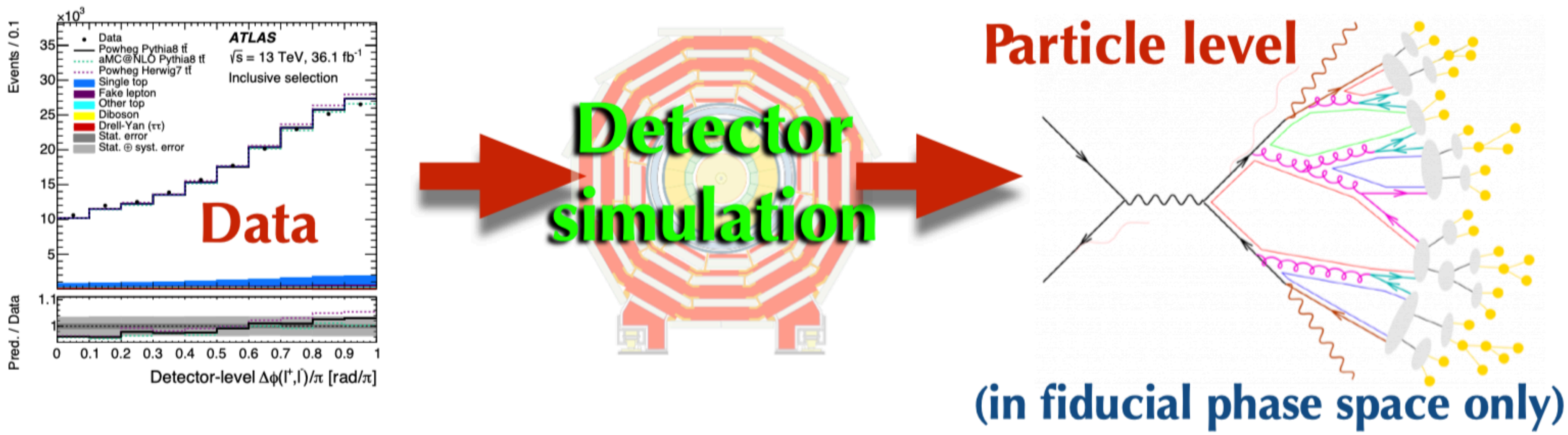

ADVANTAGES	DISADVANTAGES
Detector simulation (slow) not needed for BSM samples	Still have to produce particle-level MC
Results less dependent on model used for unfolding	No fixed-order calculations
Combinations, global fit	

Polarization and spin correlations in dilepton channel: systematic uncertainties

CMS-PAS-TOP-18-006

Table 3: Summary of the systematic uncertainties in the extracted top quark polarization coefficients.

Source	Uncertainty									
	B_1^k	B_2^k	B_1^r	B_2^r	B_1^n	B_2^n	B_1^{k*}	B_2^{k*}	B_1^{r*}	B_2^{r*}
JER	0.001	0.002	0.001	0.001	0.001	0.001	0.000	0.001	0.001	0.001
JES	0.011	0.012	0.007	0.009	0.003	0.003	0.009	0.008	0.007	0.007
Unclustered energy	0.001	0.002	0.001	0.001	0.000	0.001	0.001	0.000	0.001	0.002
Pileup	0.000	0.000	0.002	0.002	0.000	0.001	0.001	0.001	0.000	0.000
Trigger	0.001	0.001	0.001	0.001	0.000	0.000	0.001	0.001	0.002	0.002
Lepton ID/isolation	0.001	0.000	0.000	0.000	0.000	0.000	0.000	0.000	0.000	0.000
Kinematic reconstruction	0.000	0.000	0.000	0.000	0.000	0.000	0.000	0.000	0.000	0.000
b tagging	0.003	0.004	0.003	0.003	0.000	0.000	0.002	0.002	0.001	0.001
Background	0.008	0.008	0.005	0.008	0.001	0.001	0.004	0.005	0.002	0.002
Scale	0.005	0.004	0.004	0.009	0.003	0.004	0.003	0.004	0.006	0.005
B-fragmentation	0.009	0.009	0.004	0.005	0.000	0.001	0.001	0.001	0.001	0.001
B-hadron semi-lep. BF	0.001	0.001	0.000	0.000	0.000	0.000	0.000	0.000	0.000	0.000
Color reconnection	0.005	0.003	0.003	0.004	0.008	0.005	0.006	0.008	0.006	0.008
Underlying event	0.001	0.003	0.001	0.003	0.002	0.003	0.003	0.002	0.004	0.004
ME/PS matching	0.006	0.006	0.004	0.001	0.003	0.004	0.003	0.003	0.004	0.004
Top quark mass	0.006	0.007	0.000	0.001	0.001	0.002	0.002	0.001	0.002	0.002
PDF	0.002	0.002	0.000	0.000	0.000	0.000	0.004	0.004	0.002	0.002
Top quark p_T	0.003	0.003	0.001	0.001	0.000	0.000	0.001	0.001	0.000	0.000
Total systematic	0.021	0.021	0.013	0.017	0.010	0.009	0.014	0.014	0.013	0.014
Data statistics	0.009	0.008	0.009	0.009	0.007	0.008	0.010	0.010	0.010	0.009
MC statistics	0.003	0.003	0.003	0.003	0.003	0.003	0.004	0.004	0.004	0.003
Background MC statistics	0.005	0.005	0.005	0.005	0.004	0.004	0.006	0.006	0.005	0.005
Total statistical	0.010	0.010	0.011	0.011	0.009	0.009	0.012	0.012	0.012	0.011
Total	0.023	0.024	0.017	0.020	0.013	0.013	0.018	0.019	0.018	0.017

Polarization and spin correlations in dilepton channel: systematic uncertainties

CMS-PAS-TOP-18-006

Table 4: Summary of the systematic uncertainties in the extracted $t\bar{t}$ spin correlation coefficients.

Source	Uncertainty											
	C_{kk}	C_{rr}	C_{nn}	$C_{rk}+C_{kr}$	$C_{rk}-C_{kr}$	$C_{nr}+C_{rn}$	$C_{nr}-C_{rn}$	$C_{nk}+C_{kn}$	$C_{nk}-C_{kn}$	D	$A^{\text{lab}}_{\cos\varphi}$	$A_{\lvert\Delta\phi_{\ell\ell}\rvert}$
JER	0.001	0.001	0.001	0.004	0.002	0.001	0.001	0.003	0.001	0.000	0.000	0.000
JES	0.012	0.009	0.005	0.022	0.011	0.011	0.009	0.012	0.007	0.002	0.000	0.001
Unclustered energy	0.001	0.001	0.001	0.004	0.001	0.001	0.002	0.001	0.001	0.000	0.000	0.001
Pileup	0.002	0.000	0.001	0.004	0.001	0.001	0.002	0.001	0.001	0.001	0.000	0.001
Trigger	0.001	0.001	0.000	0.002	0.000	0.000	0.000	0.000	0.000	0.000	0.001	0.000
Lepton ID/isolation	0.001	0.001	0.000	0.001	0.000	0.000	0.000	0.000	0.000	0.000	0.000	0.000
Kinematic reconstruction	0.000	0.000	0.000	0.000	0.000	0.000	0.000	0.000	0.000	0.000	0.000	0.000
b tagging	0.004	0.001	0.002	0.005	0.001	0.001	0.001	0.001	0.001	0.001	0.000	0.000
Background	0.017	0.009	0.008	0.025	0.006	0.004	0.004	0.007	0.003	0.004	0.008	0.002
Scale	0.012	0.006	0.007	0.026	0.011	0.007	0.014	0.011	0.007	0.003	0.002	0.003
B-fragmentation	0.014	0.002	0.005	0.017	0.001	0.001	0.001	0.002	0.001	0.003	0.000	0.001
B-hadron semi-lep. BF	0.000	0.001	0.001	0.002	0.000	0.001	0.000	0.000	0.000	0.001	0.000	0.000
Color reconnection	0.005	0.013	0.006	0.013	0.011	0.014	0.017	0.009	0.008	0.002	0.001	0.001
Underlying event	0.008	0.002	0.002	0.004	0.010	0.007	0.005	0.007	0.002	0.003	0.001	0.001
ME/PS matching	0.004	0.003	0.001	0.009	0.016	0.011	0.001	0.012	0.009	0.002	0.002	0.004
Top quark mass	0.001	0.002	0.006	0.006	0.009	0.002	0.002	0.009	0.001	0.002	0.001	0.000
PDF	0.005	0.005	0.001	0.004	0.001	0.001	0.001	0.001	0.001	0.002	0.007	0.002
Top quark p_T	0.008	0.010	0.005	0.019	0.000	0.001	0.000	0.001	0.000	0.004	0.003	0.005
Total systematic	0.031	0.023	0.017	0.053	0.029	0.024	0.025	0.026	0.016	0.009	0.011	0.008
Data statistics	0.018	0.019	0.010	0.029	0.029	0.024	0.025	0.025	0.020	0.006	0.003	0.003
MC statistics	0.007	0.007	0.004	0.011	0.011	0.009	0.009	0.010	0.008	0.002	0.001	0.001
Background MC statistics	0.011	0.010	0.005	0.018	0.017	0.012	0.010	0.015	0.012	0.003	0.002	0.002
Total statistical	0.022	0.023	0.012	0.035	0.035	0.028	0.028	0.031	0.025	0.007	0.003	0.003
Total	0.038	0.033	0.020	0.064	0.046	0.037	0.038	0.041	0.029	0.011	0.012	0.008

Polarization and spin correlations in dilepton channel: correlation matrices

CMS-PAS-TOP-18-006

Statistical correlation matrix (all measured bins)

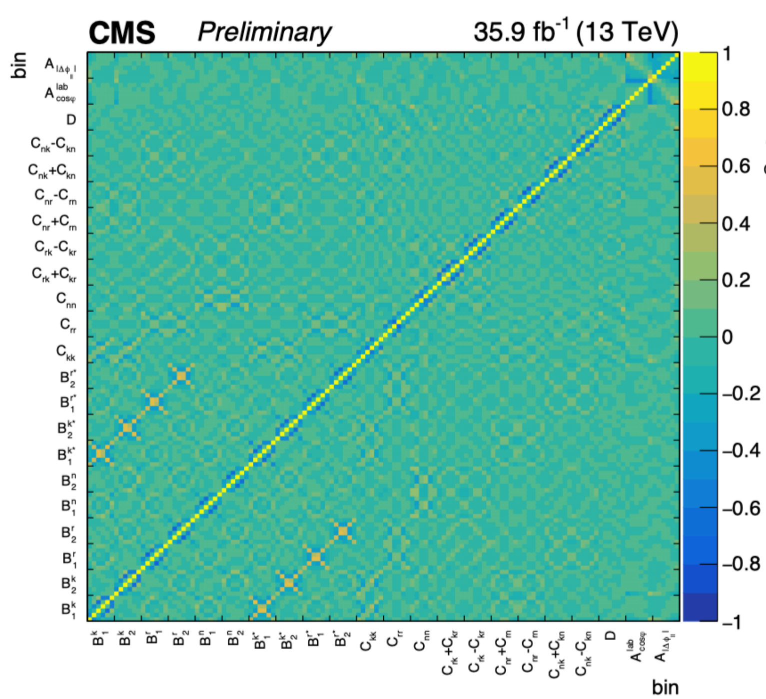

Systematic correlation matrix (all measured bins)

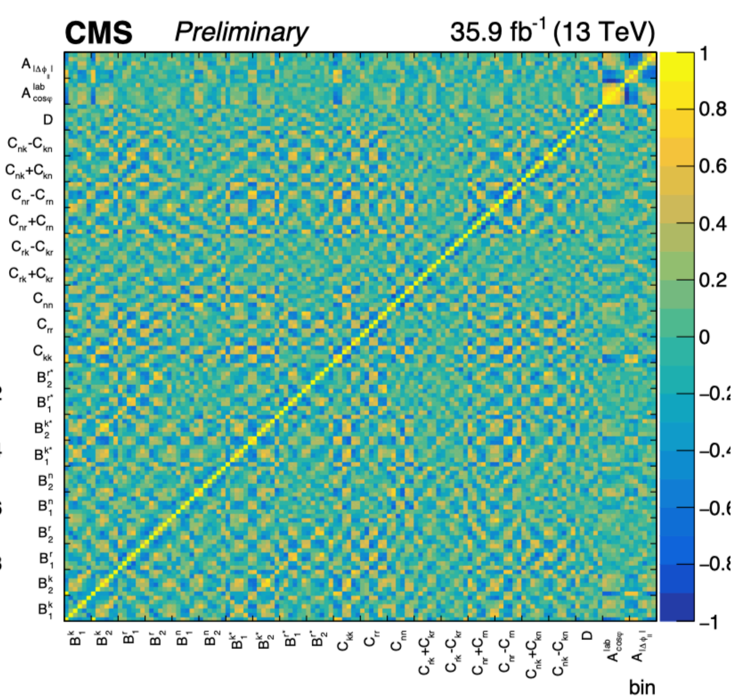

Statistical correlation matrix (all measured coefficients)

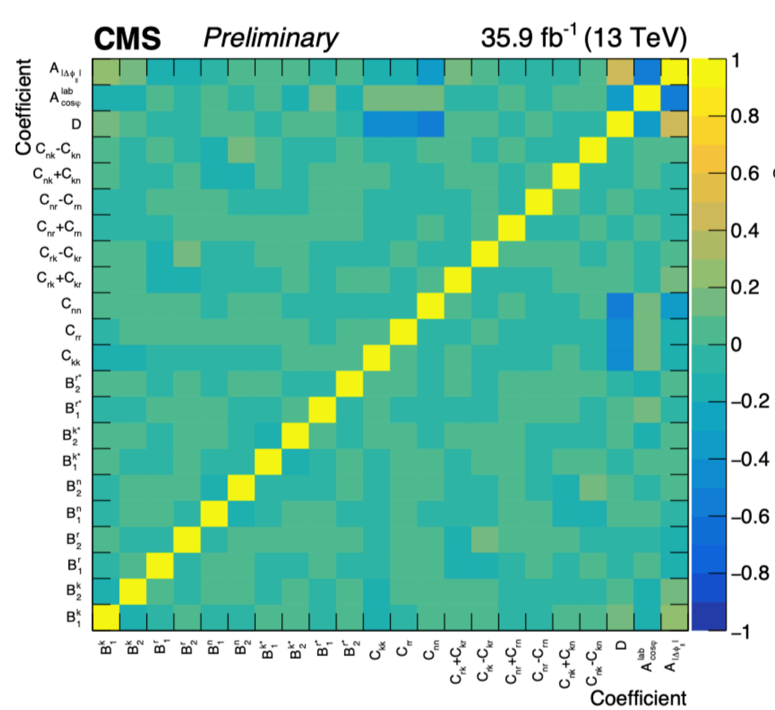

Systematic correlation matrix (all measured coefficients)

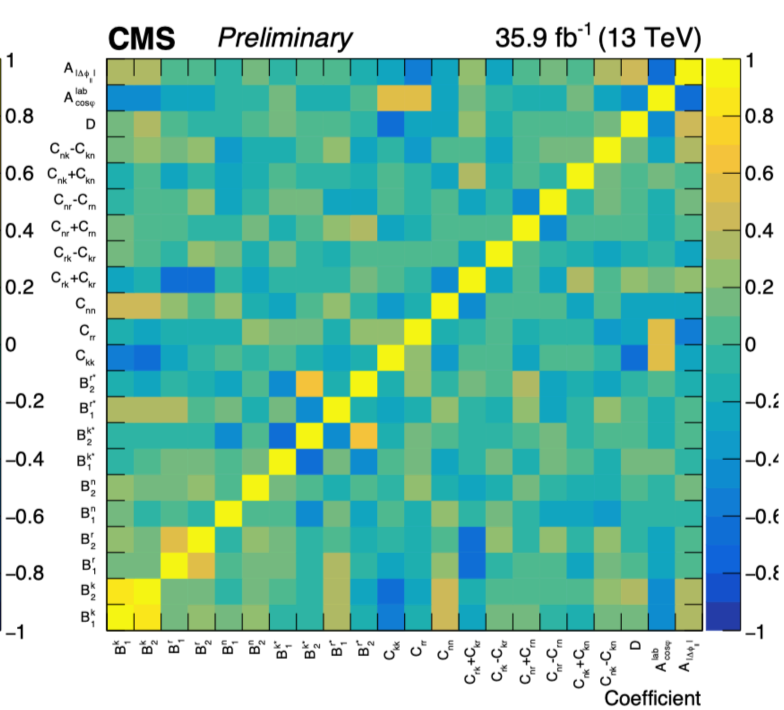

Polarization and spin correlations in dilepton channel: coefficients

CMS-PAS-TOP-18-006

Coefficient	Measured	POWHEGV2	MG5_aMC@NLO	NLO calculation
B_1^k	0.005 ± 0.023	$0.004^{+0.002}_{-0.001}$	0.000 ± 0.001	$4.0^{+1.7}_{-1.2} \times 10^{-3}$
B_2^k	0.008 ± 0.024	$0.006^{+0.001}_{-0.001}$	-0.002 ± 0.001	$4.0^{+1.7}_{-1.2} \times 10^{-3}$
B_1^r	-0.023 ± 0.017	$0.002^{+0.001}_{-0.002}$	0.002 ± 0.001	$1.6^{+1.2}_{-0.9} \times 10^{-3}$
B_2^r	-0.010 ± 0.020	$0.003^{+0.001}_{-0.002}$	0.000 ± 0.001	$1.6^{+1.2}_{-0.9} \times 10^{-3}$
B_1^n	0.006 ± 0.013	$-0.001^{+0.002}_{-0.001}$	0.001 ± 0.001	$5.7^{+0.5}_{-0.4} \times 10^{-3}$
B_2^n	0.017 ± 0.013	$-0.001^{+0.001}_{-0.001}$	0.000 ± 0.001	$5.7^{+0.5}_{-0.4} \times 10^{-3}$
B_1^{k*}	-0.016 ± 0.018	$-0.001^{+0.001}_{-0.001}$	0.000 ± 0.001	$< 10^{-3}$
B_2^{k*}	0.007 ± 0.019	$0.001^{+0.002}_{-0.003}$	0.003 ± 0.001	$< 10^{-3}$
B_1^{r*}	0.001 ± 0.018	$0.000^{+0.001}_{-0.002}$	0.000 ± 0.001	$< 10^{-3}$
B_2^{r*}	0.010 ± 0.017	$0.001^{+0.001}_{-0.002}$	0.001 ± 0.001	$< 10^{-3}$
C_{kk}	0.299 ± 0.038	$0.314^{+0.005}_{-0.004}$	0.325 ± 0.002	$0.331^{+0.002}_{-0.002}$
C_{rr}	0.080 ± 0.033	$0.048^{+0.007}_{-0.006}$	0.052 ± 0.002	$0.071^{+0.008}_{-0.006}$
C_{nn}	0.329 ± 0.020	$0.317^{+0.001}_{-0.003}$	0.324 ± 0.002	$0.326^{+0.002}_{-0.002}$
$C_{rk} + C_{kr}$	-0.193 ± 0.064	$-0.201^{+0.004}_{-0.003}$	-0.198 ± 0.002	$-0.206^{+0.002}_{-0.002}$
$C_{rk} - C_{kr}$	0.057 ± 0.046	$-0.001^{+0.005}_{-0.002}$	0.004 ± 0.002	0
$C_{nr} + C_{rn}$	-0.004 ± 0.037	$-0.003^{+0.008}_{-0.002}$	0.001 ± 0.002	$1.06^{+0.01}_{-0.01} \times 10^{-3}$
$C_{nr} - C_{rn}$	-0.001 ± 0.038	$0.002^{+0.005}_{-0.002}$	0.001 ± 0.002	0
$C_{nk} + C_{kn}$	-0.043 ± 0.041	$-0.002^{+0.005}_{-0.002}$	0.003 ± 0.002	$2.15^{+0.04}_{-0.07} \times 10^{-3}$
$C_{nk} - C_{kn}$	0.040 ± 0.029	$-0.001^{+0.003}_{-0.002}$	-0.001 ± 0.002	0
D	-0.237 ± 0.011	$-0.226^{+0.003}_{-0.004}$	-0.233 ± 0.001	$-0.243^{+0.004}_{-0.003}$
$A^{\mathrm{lab}}_{\cos\varphi}$	0.167 ± 0.012	$0.161^{+0.002}_{-0.002}$	0.174 ± 0.001	$0.181^{+0.004}_{-0.003}$
$A_{\lvert\Delta\phi_{\ell\ell}\rvert}$	0.103 ± 0.008	$0.125^{+0.004}_{-0.005}$	0.115 ± 0.001	$0.112^{+0.009}_{-0.012}$

Polarization and spin correlations in dilepton channel: spin + cross correlations

CMS-PAS-TOP-18-006

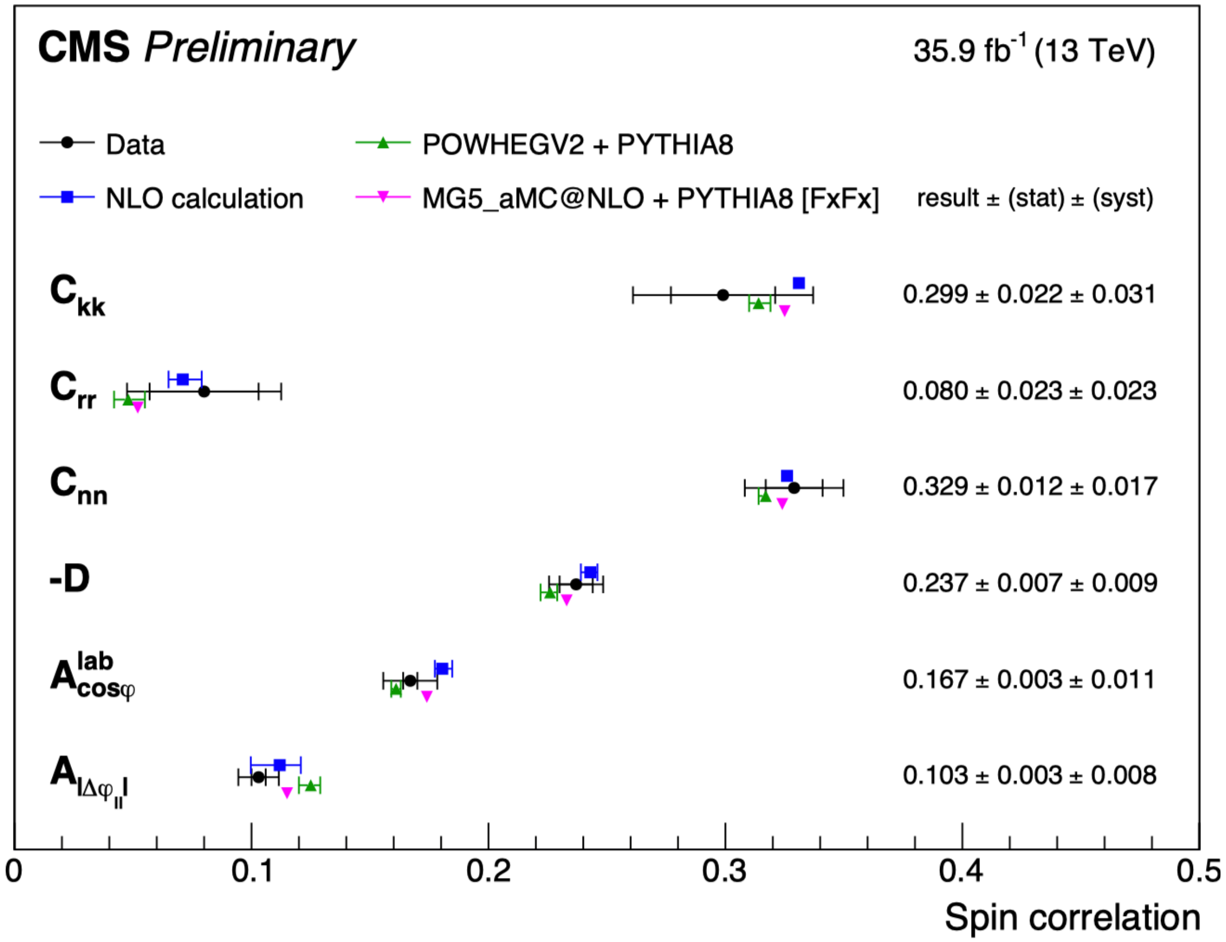

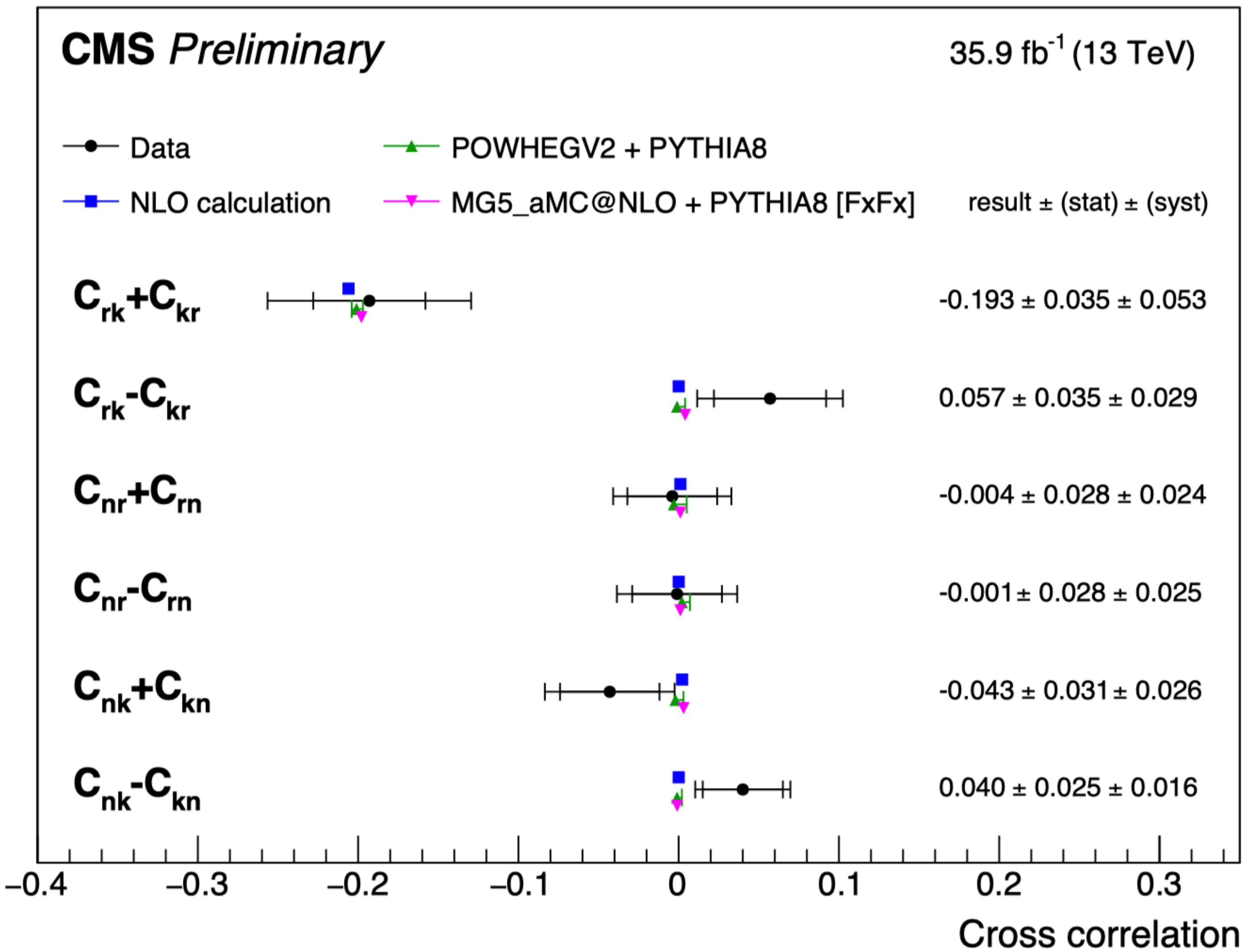

Polarization and spin correlations in dilepton channel: f_SM

CMS-PAS-TOP-18-006

Table 6: Values of f_{SM}, the strength of the measured spin correlations relative to the SM prediction for the given observable, derived from the numbers in Table 2. The uncertainties shown are statistical, systematic, and theoretical, respectively. The total uncertainty in each result, found by adding the individual uncertainties in quadrature, is shown in the last column.

Coefficient	$f_{SM} \pm$ (stat) $\pm$ (syst) $\pm$ (theor)	Total uncertainty
C_{kk}	$0.90 \pm 0.07 \pm 0.09 \pm 0.01$	± 0.12
C_{rr}	$1.13 \pm 0.32 \pm 0.33 \,^{+0.10}_{-0.13}$	$^{+0.47}_{-0.48}$
C_{nn}	$1.01 \pm 0.04 \pm 0.05 \pm 0.01$	± 0.06
$C_{rk} + C_{kr}$	$0.94 \pm 0.17 \pm 0.26 \pm 0.01$	± 0.31
D	$0.97 \pm 0.03 \pm 0.04 \,^{+0.01}_{-0.02}$	± 0.05
$A^{lab}_{\cos\varphi}$	$0.74 \pm 0.07 \pm 0.22 \,^{+0.06}_{-0.08}$	$^{+0.24}_{-0.25}$
$A_{\|\Delta\phi_{\ell\ell}\|}$	$1.10 \pm 0.04 \pm 0.09 \,^{+0.10}_{-0.14}$	$^{+0.14}_{-0.17}$

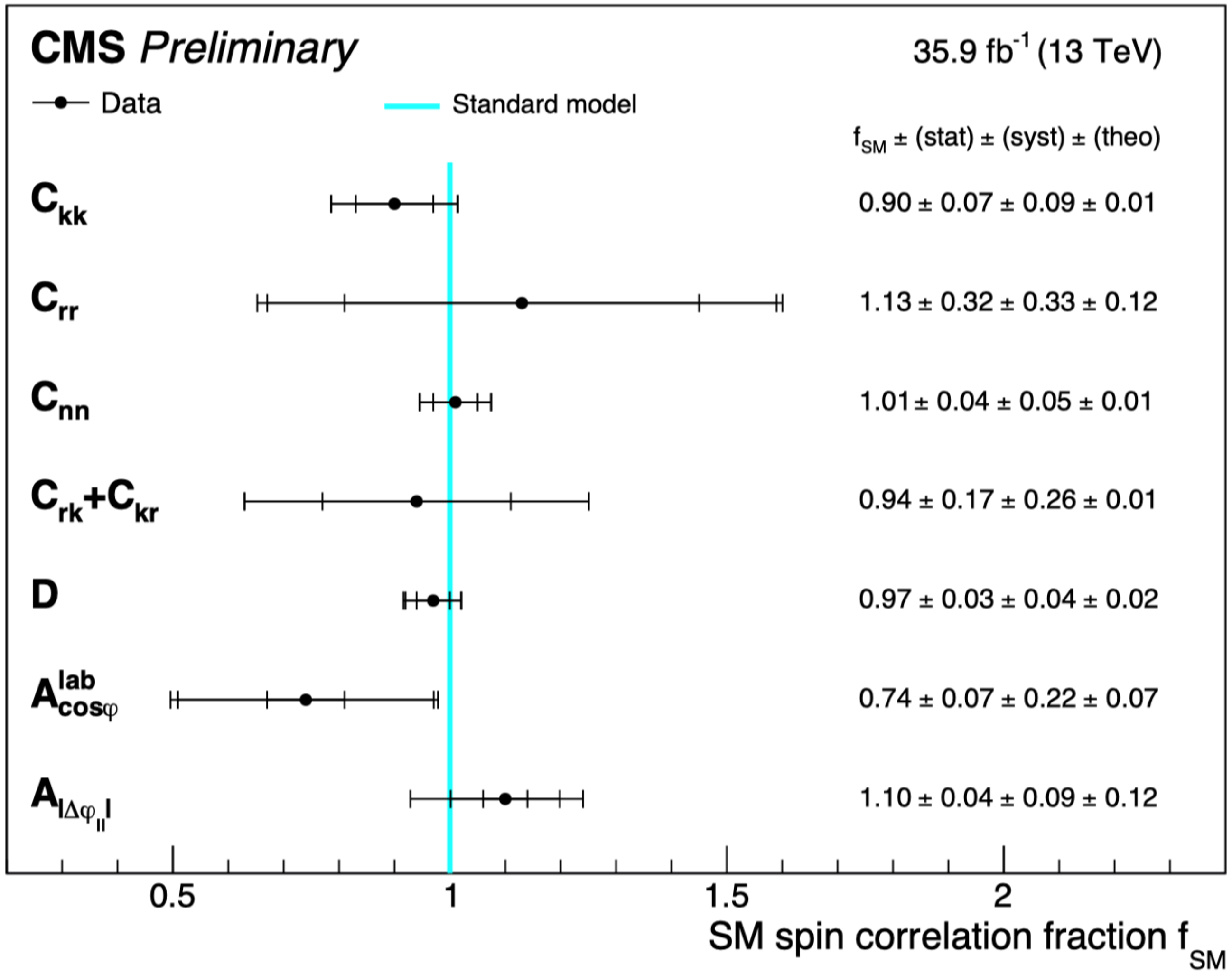

Mass in the all-jets channel: kinematic fit

Eur. Phys. J. C 79 (2019) 313

- Known decay topology:
  - pair production of heavy particle and anti-particle
  - each decaying to Wb → qq′b
- Minimize χ2 with constraints:
  - m_W+ = m_W− = 80.4GeV
  - m_t = m_tbar
  - trying all possible parton-jet assignments
  - 12 possibilities for parton-jet assignment
  - only b-tagged jets used as b candidates
  - only best (= lowest χ2) assignment used

$$\chi^2 = \sum_{j \in \text{jets}} \left[\frac{\left(p_{\mathrm{T}j}^{\text{reco}} - p_{\mathrm{T}j}^{\text{fit}}\right)^2}{\sigma^2_{p_{\mathrm{T}j}}} + \frac{\left(\eta_j^{\text{reco}} - \eta_j^{\text{fit}}\right)^2}{\sigma^2_{\eta_j}} + \frac{\left(\phi_j^{\text{reco}} - \phi_j^{\text{fit}}\right)^2}{\sigma^2_{\phi_j}} \right]$$

- The χ2 value can be used as a goodness-of-fit (gof) measure
  - for three degrees of freedom, it is translated into a p-value of

$$P_{\text{gof}} \equiv 1 - \text{erf}\left(\sqrt{\frac{\chi^2}{2}}\right) + \sqrt{\frac{2\chi^2}{\pi}} \mathrm{e}^{-\chi^2/2}.$$

- Best permutation selected by fit:
  - events are requested to fulfill Pgof > 0.1 for the best assignment

Mass in the all-jets channel: ideogram method

Eur. Phys. J. C 79 (2019) 313

- Estimate m t and additional jet scale factor (JSF)

$$P\,(m_t, \mathrm{JSF}|\mathrm{sample}) \propto P(\mathrm{JSF}) \cdot \mathcal{L}\,(\mathrm{sample}|m_t, \mathrm{JSF})$$

$$\mathcal{L}\,(\mathrm{sample}|m_t, \mathrm{JSF}) = \prod_{\mathrm{events}} \mathcal{L}\,(\mathrm{event}|m_t, \mathrm{JSF}) = \prod_{\mathrm{events}} P\left(m_t^{\mathrm{fit}}, m_W^{\mathrm{reco}} \middle| m_t, \mathrm{JSF}\right)$$

$P\left(m_W^{\mathrm{reco}}|m_t, \mathrm{JSF}\right)$
correct assignments

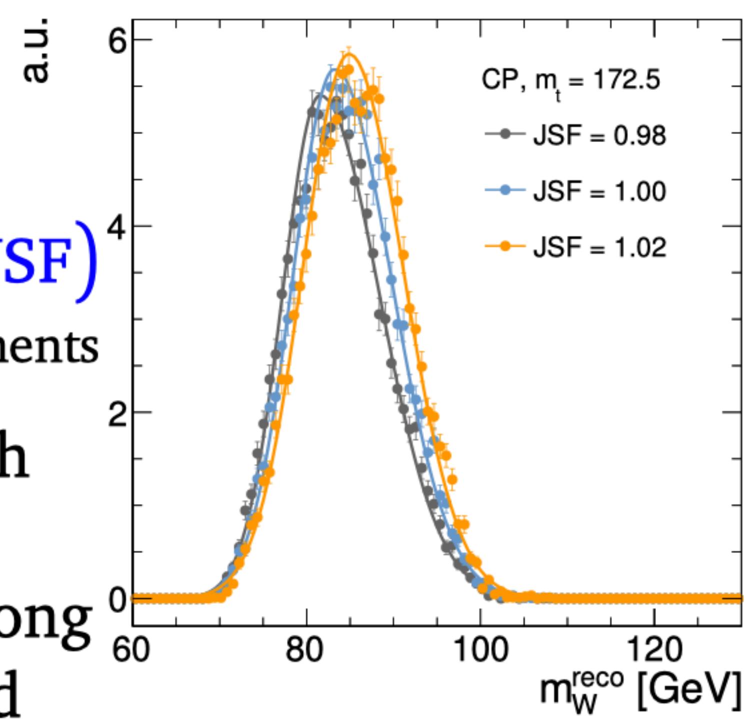

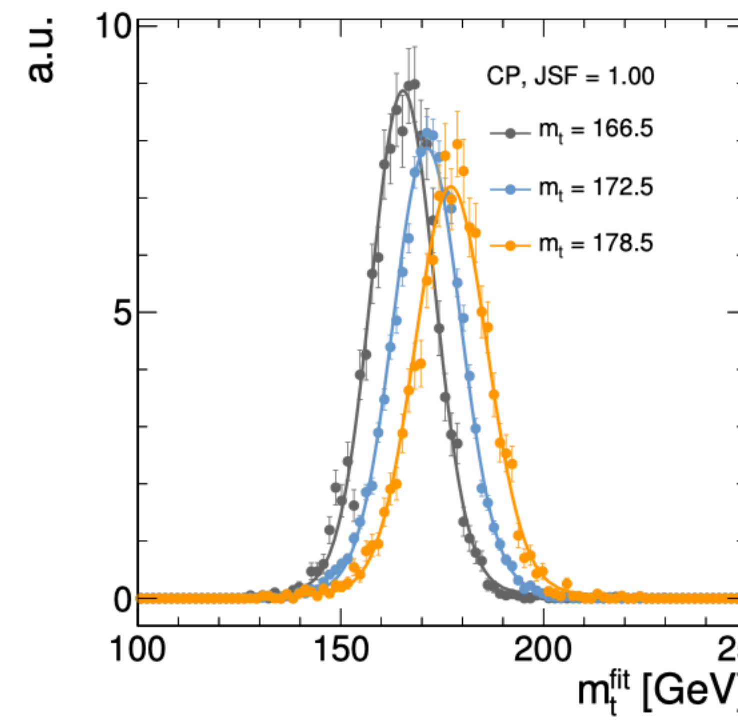

$P\left(m_t^{\mathrm{fit}}|m_t, \mathrm{JSF}\right)$
correct assignments

construct such templates for $t\bar{t}$ correct/wrong & background

- Three versions of ideogram fit:
  - only m t free (1D)
  - m t and JSF free (2D)
  - Gaussian JSF constraint (hybrid) = weighted combination of both approaches, corresponding to a measurement with a Gaussian constraint on the JSF around unity.

Mass in the all-jets channel: systematic uncertainties + results

Eur. Phys. J. C 79 (2019) 313

- Most systematic uncertainty sources are shifted by ±1 standard deviation, and the absolute value of the largest resulting shifts in m_t and JSF are quoted as systematic uncertainties for the measurement
- The hybrid measurement is the main result of this analysis, since it is constructed to provide the smallest uncertainty.

$$m_t^{2D} = 172.43 \pm 0.22\,(\text{stat+JSF}) \pm 0.88\,(\text{syst})\ \text{GeV}$$

$$\text{JSF}^{2D} = 0.996 \pm 0.002\,(\text{stat}) \pm 0.010\,(\text{syst}).$$

$$m_t^{1D} = 172.13 \pm 0.17\,(\text{stat}) \pm 1.10\,(\text{syst})\ \text{GeV},$$

- 8TeV result: 172.32 ± 0.25(stat) ± 0.59(syst)GeV:
  - the statistical uncertainty is reduced with respect result at 8 TeV because of the larger data analysis
  - larger theory uncertainty wrt. 8TeV, mainly due sophisticated color reconnection ℓ+jets)

	2D		1D	hybrid	
	δm_t^{2D} [GeV]	δJSF^{2D} [%]	δm_t^{1D} [GeV]	δm_t^{hyb} [GeV]	δJSF^{hyb} [%]
Experimental uncertainties					
Method calibration	0.06	0.2	0.06	0.06	0.2
JEC (quad. sum)	0.18	0.3	0.73	0.15	0.2
– Intercalibration	−0.04	−0.1	+0.12	−0.04	−0.1
– MPFInSitu	−0.03	0.0	+0.22	+0.08	+0.1
– Uncorrelated	−0.17	−0.3	+0.69	+0.12	+0.2
Jet energy resolution	−0.09	+0.2	+0.09	−0.04	+0.1
b tagging	0.02	0.0	0.01	0.02	0.0
Pileup	−0.06	+0.1	0.00	−0.04	+0.1
Background	0.10	0.1	0.03	0.07	0.1
Trigger	+0.04	−0.1	−0.04	+0.02	−0.1
Modeling uncertainties					
JEC flavor (linear sum)	−0.35	+0.1	−0.31	−0.34	0.0
– light quarks (uds)	+0.10	−0.1	−0.01	+0.07	−0.1
– charm	+0.03	0.0	−0.01	+0.02	0.0
– bottom	−0.29	0.0	−0.29	−0.29	0.0
– gluon	−0.19	+0.2	+0.03	−0.13	+0.2
b jet modeling (quad. sum)	0.09	0.0	0.09	0.09	0.0
– b frag. Bowler–Lund	−0.07	0.0	−0.07	−0.07	0.0
– b frag. Peterson	−0.05	0.0	−0.04	−0.05	0.0
– semileptonic b hadron decays	−0.03	0.0	−0.03	−0.03	0.0
PDF	0.01	0.0	0.01	0.01	0.0
Ren. and fact. scales	0.05	0.0	0.04	0.04	0.0
ME/PS matching	+0.32 ± 0.20	−0.3	−0.05 ± 0.14	+0.24 ± 0.18	−0.2
ISR PS scale	+0.17 ± 0.17	−0.2	+0.13 ± 0.12	+0.12 ± 0.14	−0.1
FSR PS scale	+0.22 ± 0.12	−0.2	+0.11 ± 0.08	+0.18 ± 0.11	−0.1
Top quark p_T	+0.03	0.0	+0.02	+0.03	0.0
Underlying event	+0.16 ± 0.19	−0.3	−0.07 ± 0.14	+0.10 ± 0.17	−0.2
Early resonance decays	+0.02 ± 0.28	+0.4	+0.38 ± 0.19	+0.13 ± 0.24	+0.3
CR modeling (max. shift)	+0.41 ± 0.29	−0.4	−0.43 ± 0.20	−0.36 ± 0.25	−0.3
– "gluon move" (ERD on)	+0.41 ± 0.29	−0.4	+0.10 ± 0.20	+0.32 ± 0.25	−0.3
– "QCD inspired" (ERD on)	−0.32 ± 0.29	−0.1	−0.43 ± 0.20	−0.36 ± 0.25	−0.1
Total systematic	0.81	0.9	1.03	0.70	0.7
Statistical (expected)	0.21	0.2	0.16	0.20	0.1
Total (expected)	0.83	0.9	1.04	0.72	0.7

Mass in the all-jets channel and combination with lepton+jets: systematics + results

Eur. Phys. J. C 79 (2019) 313

- ℓ+jets result: 172.25 ± 0.08(stat+JSF) ± 0.62(syst)GeV
  - the uncertainties for the combination are smaller than those for the all-jets channel and are close to the lepton+jets uncertainties, as expected because the combination is dominated by this channel.
  - combined measurement has lowest total uncertainty
  - first m t measurement in the combined ℓ+jets and all-jets channels
- Combined results:

$$m_t^{2D} = 172.39 \pm 0.08\,(\text{stat+JSF}) \pm 0.68\,(\text{syst})\ \text{GeV}$$

$$\text{JSF}^{2D} = 0.995 \pm 0.001\,(\text{stat}) \pm 0.010\,(\text{syst})$$

$$m_t^{1D} = 171.94 \pm 0.05\,(\text{stat}) \pm 1.07\,(\text{syst})\ \text{GeV},$$

	2D		1D	hybrid	
	δm_t^{2D} [GeV]	δJSF^{2D} [%]	δm_t^{1D} [GeV]	δm_t^{hyb} [GeV]	δJSF^{hyb} [%]
Experimental uncertainties					
Method calibration	0.03	0.0	0.03	0.03	0.0
JEC (quad. sum)	0.12	0.2	0.82	0.17	0.3
– Intercalibration	−0.01	0.0	+0.16	+0.04	+0.1
– MPFInSitu	−0.01	0.0	+0.23	+0.07	+0.1
– Uncorrelated	−0.12	−0.2	+0.77	+0.15	+0.3
Jet energy resolution	−0.18	+0.3	+0.09	−0.10	+0.2
b tagging	0.03	0.0	0.01	0.02	0.0
Pileup	−0.07	+0.1	+0.02	−0.05	+0.1
All-jets background	0.01	0.0	0.00	0.01	0.0
All-jets trigger	+0.01	0.0	0.00	+0.01	0.0
ℓ+jets Background	−0.02	0.0	+0.01	−0.01	0.0
ℓ+jets Trigger	0.00	0.0	0.00	0.00	0.0
Lepton isolation	0.00	0.0	0.00	0.00	0.0
Lepton identification	0.00	0.0	0.00	0.00	0.0
Modeling uncertainties					
JEC flavor (linear sum)	−0.39	+0.1	−0.31	−0.37	+0.1
– light quarks (uds)	+0.11	−0.1	−0.01	+0.07	−0.1
– charm	+0.03	0.0	−0.01	+0.02	0.0
– bottom	−0.31	0.0	−0.31	−0.31	0.0
– gluon	−0.22	+0.3	+0.02	−0.15	+0.2
b jet modeling (quad. sum)	0.08	0.1	0.04	0.06	0.1
– b frag. Bowler–Lund	−0.06	+0.1	−0.01	−0.05	0.0
– b frag. Peterson	−0.03	0.0	0.00	−0.02	0.0
– semileptonic b hadron decays	−0.04	0.0	−0.04	−0.04	0.0
PDF	0.01	0.0	0.01	0.01	0.0
Ren. and fact. scales	0.01	0.0	0.02	0.01	0.0
ME/PS matching	−0.10 ± 0.08	+0.1	+0.02 ± 0.05	+0.07 ± 0.07	+0.1
ME generator	+0.16 ± 0.21	+0.2	+0.32 ± 0.13	+0.21 ± 0.18	+0.1
ISR PS scale	+0.07 ± 0.08	+0.1	+0.10 ± 0.05	+0.07 ± 0.07	0.1
FSR PS scale	+0.23 ± 0.07	−0.4	−0.19 ± 0.04	+0.12 ± 0.06	−0.3
Top quark p_T	+0.01	−0.1	−0.06	−0.01	−0.1
Underlying event	−0.06 ± 0.07	+0.1	+0.00 ± 0.05	−0.04 ± 0.06	+0.1
Early resonance decays	−0.20 ± 0.08	+0.7	+0.42 ± 0.05	−0.01 ± 0.07	+0.5
CR modeling (max. shift)	+0.37 ± 0.09	−0.2	+0.22 ± 0.06	+0.33 ± 0.07	−0.1
– "gluon move" (ERD on)	+0.37 ± 0.09	−0.2	+0.22 ± 0.06	+0.33 ± 0.07	−0.1
– "QCD inspired" (ERD on)	−0.11 ± 0.09	−0.1	−0.21 ± 0.06	−0.14 ± 0.07	−0.1
Total systematic	0.71	1.0	1.07	0.61	0.7
Statistical (expected)	0.08	0.1	0.05	0.07	0.1
Total (expected)	0.72	1.0	1.08	0.61	0.7

Mass in the all-jets channel and combination with lepton+jets: comparison of results

Eur. Phys. J. C 79 (2019) 313

- Comparison to ℓ+jets result:

- Comparison to RunI results:

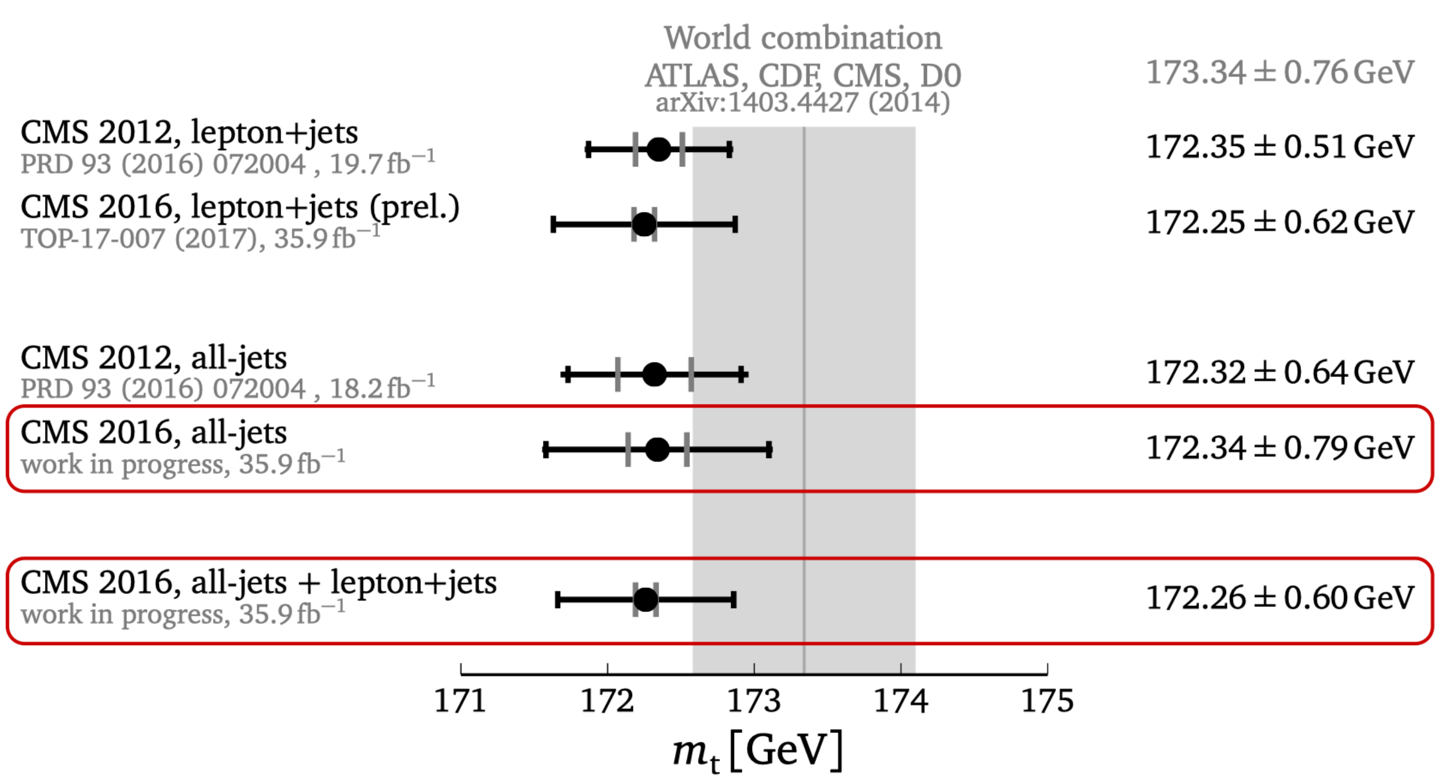

	δm_t^{hyb} [GeV]		
	all-jets	ℓ+jets	combination
Experimental uncertainties			
Method calibration	0.06	0.05	0.03
JEC (quad. sum)	0.15	0.18	0.17
– Intercalibration	−0.04	+0.04	+0.04
– MPFInSitu	+0.08	+0.07	+0.07
– Uncorrelated	+0.12	+0.16	+0.15
Jet energy resolution	−0.04	−0.12	−0.10
b tagging	0.02	0.03	0.02
Pileup	−0.04	−0.05	−0.05
All-jets background	0.07	–	0.01
All-jets trigger	+0.02	–	+0.01
ℓ+jets background	–	+0.02	−0.01
Modeling uncertainties			
JEC flavor (linear sum)	−0.34	−0.39	−0.37
– light quarks (uds)	+0.07	+0.06	+0.07
– charm	+0.02	+0.01	+0.02
– bottom	−0.29	−0.32	−0.31
– gluon	−0.13	−0.15	−0.15
b jet modeling (quad. sum)	0.09	0.12	0.06
– b frag. Bowler–Lund	−0.07	−0.05	−0.05
– b frag. Peterson	−0.05	+0.04	−0.02
– semileptonic b hadron decays	−0.03	+0.10	−0.04
PDF	0.01	0.02	0.01
Ren. and fact. scales	0.04	0.01	0.01
ME/PS matching	+0.24	−0.07	+0.07
ME generator	–	+0.20	+0.21
ISR PS scale	+0.14	+0.07	+0.07
FSR PS scale	+0.18	+0.13	+0.12
Top quark p_T	+0.03	−0.01	−0.01
Underlying event	+0.17	−0.07	−0.06
Early resonance decays	+0.24	−0.07	−0.07
CR modeling (max. shift)	−0.36	+0.31	+0.33
– "gluon move" (ERD on)	+0.32	+0.31	+0.33
– "QCD inspired" (ERD on)	−0.36	−0.13	−0.14
Total systematic	0.70	0.62	0.61
Statistical (expected)	0.20	0.08	0.07
Total (expected)	0.72	0.63	0.61

Mass from inclusive measurement: fit strategy

arXiv:1812.10505

- template fit to distributions of final state observables
  - systematic uncertainties treated as nuisance parameters and constrained in situ (with exception of luminosity)
  - events categorized in bins of jet and b-tag multiplicity in order to constrain modelling systematics and b-tagging efficiency
  - jet p T spectra are used to constrained JEC uncertainties

- binned Likelihood based on Poisson statistics :

$$L = \prod_i \frac{e^{-\nu_i} \nu_i^{n_i}}{n_i!} \prod_j \pi(\lambda_j)$$

$$\nu_i = s_i(\sigma_{t\bar{t}}^{vis}, \vec{\lambda}) + \sum_k b_{k,i}^{MC}(\vec{\lambda})$$

  - i denotes the bin of the respective final-state distribution
  - ν i and n i are the expected and observed number of events in bin I
    - s i denotes the expected number of tt signal events in bin i and the quantity b k,i represents the prediction of the number of background events in bin i from source k
  - λ is a set of nuisance parameters
  - π(λm) parametrizes the prior knowledge of m_th parameter
- MINUIT minimizes −2 ln (L) and MINOS estimates the uncertainties

Mass from inclusive measurement: systematic uncertainties

arXiv:1812.10505

ttbar xsec: template fit

Source	Uncertainty [%]
Trigger	0.3
Lepton ident./isolation	2.0
Muon momentum scale	0.1
Electron momentum scale	0.1
Jet energy scale	0.4
Jet energy resolution	0.4
b tagging	0.4
Pileup	0.1
$t\bar{t}$ ME scale	0.2
tW ME scale	0.2
DY ME scale	0.1
PDF	1.1
Top quark p_T	0.5
ME/PS matching	0.2
UE tune	0.3
$t\bar{t}$ ISR scale	0.4
tW ISR scale	0.1
$t\bar{t}$ FSR scale	0.8
tW FSR scale	0.1
b quark fragmentation	0.7
b hadron BF	0.1
Colour reconnection	0.3
DY background	0.9
tW background	1.1
Diboson background	0.2
W+jets background	0.2
$t\bar{t}$ background	0.2
Statistical	0.2
Integrated luminosity	2.5
MC statistical	1.1
Total $\sigma_{t\bar{t}}^{vis}$ uncertainty	3.8
Extrapolation uncertainties	
$t\bar{t}$ ME scale	$\mp^{0.3}_{0.1}$
PDF	$\pm^{0.8}_{0.6}$
Top quark p_T	$\mp^{0.5}_{<0.1}$
$t\bar{t}$ ISR scale	$\mp^{0.1}_{<0.1}$
$t\bar{t}$ FSR scale	$\pm^{0.1}_{<0.1}$
UE tune	<0.1
Total $\sigma_{t\bar{t}}$ uncertainty	4.0

Simultaneous fit

Source	Uncertainty [%]
Trigger	0.4
Lepton ident./isolation	2.2
Muon momentum scale	0.2
Electron momentum scale	0.2
Jet energy scale	0.7
Jet energy resolution	0.5
b tagging	0.3
Pileup	0.3
$t\bar{t}$ ME scale	0.5
tW ME scale	0.7
DY ME scale	0.2
NLO generator	1.2
PDF	1.1
m_t^{MC}	0.4
Top quark p_T	0.5
ME/PS matching	0.2
UE tune	0.3
$t\bar{t}$ ISR scale	0.4
tW ISR scale	0.4
$t\bar{t}$ FSR scale	1.1
tW FSR scale	0.2
b quark fragmentation	1.0
b hadron BF	0.2
Colour reconnection	0.4
DY background	0.8
tW background	1.1
Diboson background	0.3
W+jets background	0.3
$t\bar{t}$ background	0.2
Statistical	0.2
Integrated luminosity	2.5
MC statistical	1.2
Total $\sigma_{t\bar{t}}^{vis}$ uncertainty	4.2
Extrapolation uncertainties	
$t\bar{t}$ ME scale	$\mp^{0.4}_{<0.1}$
PDF	$\pm^{0.8}_{0.6}$
Top quark p_T	$\pm^{0.2}_{0.3}$
$t\bar{t}$ ISR scale	$\mp^{0.2}_{<0.1}$
$t\bar{t}$ FSR scale	± 0.1
UE tune	<0.1
m_t^{MC}	$\mp^{0.2}_{0.3}$

absolute uncertainties in mtMC and their sources from the simultaneous fit

Source	Uncertainty [GeV]
Trigger	0.02
Lepton ident./isolation	0.02
Muon momentum scale	0.03
Electron momentum scale	0.10
Jet energy scale	0.57
Jet energy resolution	0.09
b tagging	0.12
Pileup	0.09
$t\bar{t}$ ME scale	0.18
tW ME scale	0.02
DY ME scale	0.06
NLO generator	0.14
PDF	0.05
$\sigma_{t\bar{t}}$	0.09
Top quark p_T	0.04
ME/PS matching	0.16
UE tune	0.03
$t\bar{t}$ ISR scale	0.16
tW ISR scale	0.02
$t\bar{t}$ FSR scale	0.07
tW FSR scale	0.02
b quark fragmentation	0.11
b hadron BF	0.07
Colour reconnection	0.17
DY background	0.24
tW background	0.13
Diboson background	0.02
W+jets background	0.04
$t\bar{t}$ background	0.02
Statistical	0.14
MC statistical	0.36
Total m_t^{MC} uncertainty	$^{+0.68}_{-0.73}$

Mass from inclusive measurement: extraction of $\alpha_S(M_Z)$

arXiv:1812.10505

- To extract the value of α S (m Z) from σ tt , the measured cross section is compared to the theoretical prediction, and for each α S (m Z) member of each PDF set, the χ 2 is evaluated.
- The optimal value of α S (m Z) is subsequently determined from a parabolic fit to the χ 2 (α S) values of the form:

$$\chi^2(\alpha_S) = \chi^2_{\min} + \left(\frac{\alpha_S - \alpha_S^{\min}}{\delta(\alpha_S^{\min})}\right)^2$$

  - χ min 2 is the χ 2 value at α S = α min
  - δ(α min) is the fitted experimental uncertainty in α min S , which also accounts for the PDF uncertainty
- χ 2 (α S) scan for the PDF sets used, demonstrating a clear parabolic behaviour.
  - χ 2 versus α S obtained from the comparison of the measured σ tt value to the NNLO prediction in the MS scheme using different PDFs (symbols of different styles).

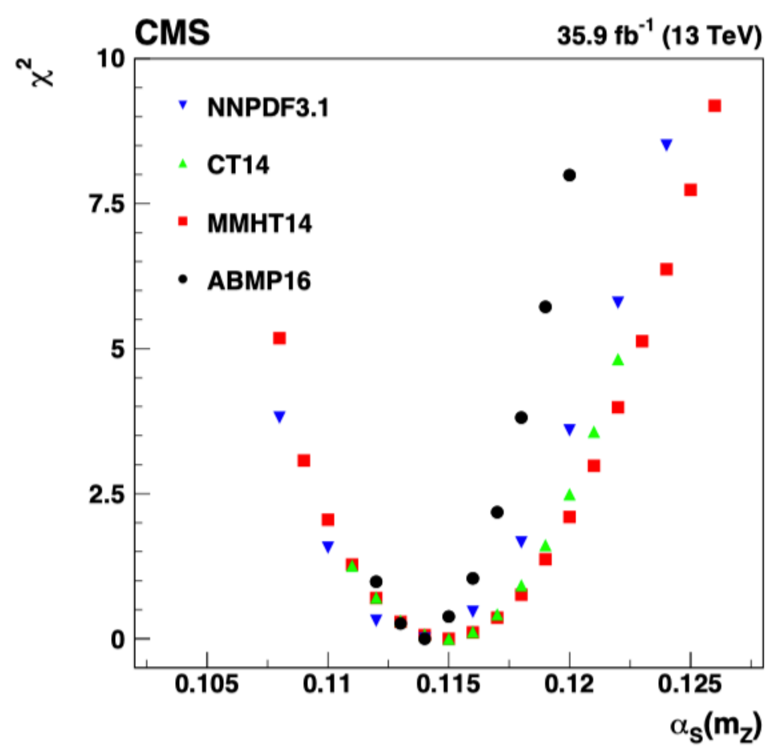

Mass from inclusive measurement: dependence of $\alpha_S(M_Z)$ from mt

arXiv:1812.10505

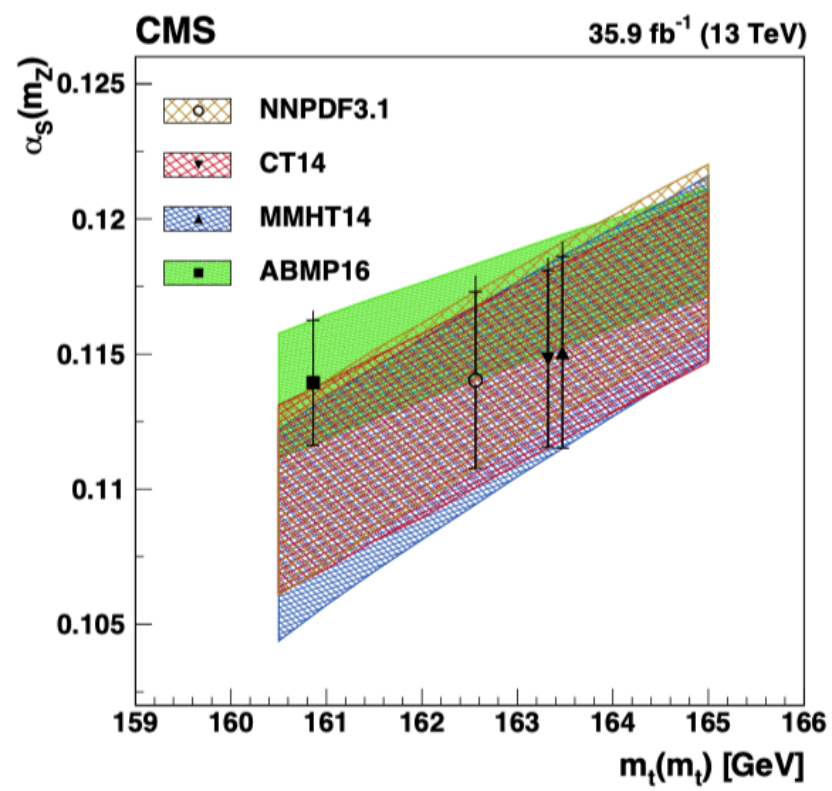

Figure 13: Values of $\alpha_S(m_Z)$ obtained in the comparison of the $\sigma_{t\bar{t}}$ measurement to the NNLO prediction using different PDFs, as a function of the $m_t(m_t)$ value used in the theoretical calculation. The results from using the different PDFs are shown by the bands with different shadings, with the band width corresponding to the quadratic sum of the experimental and PDF uncertainties in $\alpha_S(m_Z)$. The resulting measured values of $\alpha_S(m_Z)$ are shown by the different style points at the $m_t(m_t)$ values used for each PDF. The inner vertical bars on the points represent the quadratic sum of the experimental and PDF uncertainties in $\alpha_S(m_Z)$, while the outer vertical bars show the total uncertainties.

More m_t and $\alpha_S(M_Z)$ from differential measurement: systematic uncertainties

arXiv:1904.05237

- Experimental uncertainties arising from imperfect modelling of the detector response,
- Theoretical uncertainties arising from the modelling of the signal and background processes.
- Each source of systematic uncertainty is assessed by changing in the simulation the corresponding efficiency, resolution, or scale by its uncertainty:
    - for each change made, the cross section determination is repeated, and the difference with respect to the nominal result in each bin is taken as the systematic uncertainty.
- The total systematic uncertainty in each measurement bin is estimated by adding all the contributions described above in quadrature, separately for positive and negative cross section variations. If a systematic uncertainty results in two cross section variations of the same sign, the largest one is taken, while the opposite variation is set to zero.
- the total uncertainties for all measured cross sections are about 510%, but exceed 20% in some regions of phase space, such as the last N jet range of the [N jet 0,1,2+ , M (tt), y(tt)] distribution.
- The largest experimental systematic uncertainty is associated with the JES.

More m_t and $\alpha_S(M_Z)$ from differential measurement: extraction of α_S, m_t^{pole}

arXiv:1904.05237

- The values of α S (m Z) and m t are extracted by calculating a χ 2 between data and NLO predictions as a function of the input α S (m Z) or m t value, and approximating the dependence pole with a parabola. The minimum of the parabola is taken as the extracted α S (m Z) or m t value, while its uncertainty is estimated from the Δχ 2 = 1 variation. This extraction is performed separately using different PDF sets, as well as different scale values.
- α S (m Z) and m t scans for different PDF sets

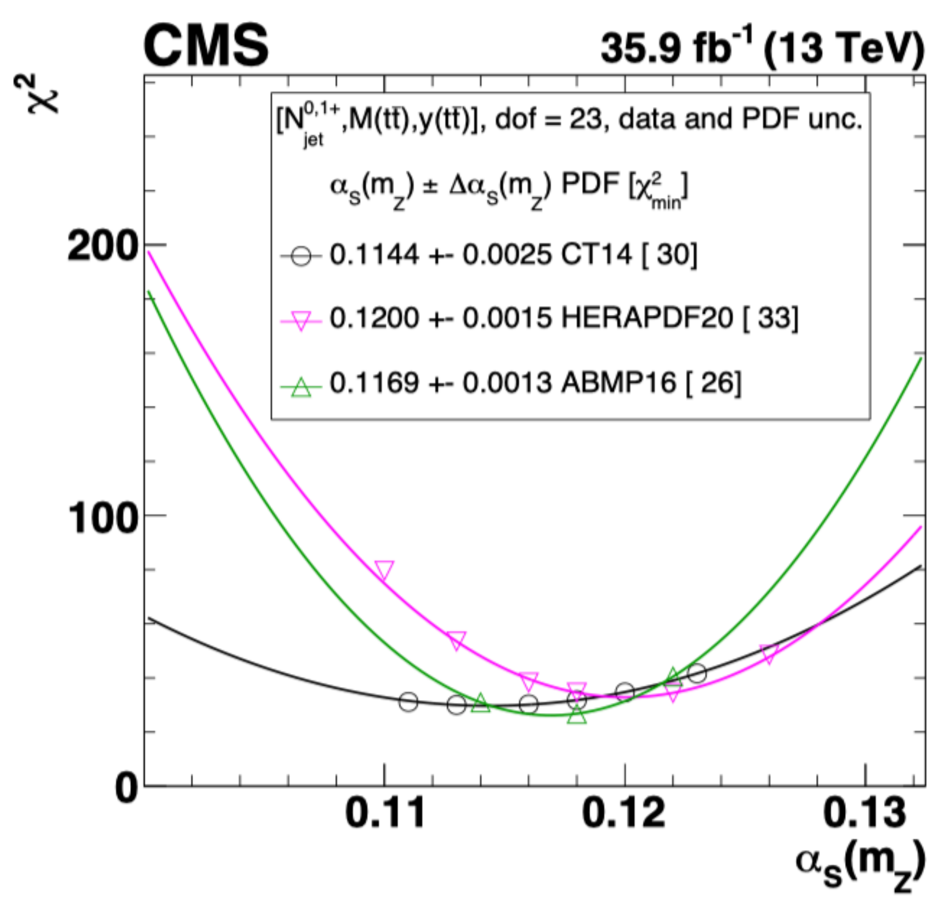

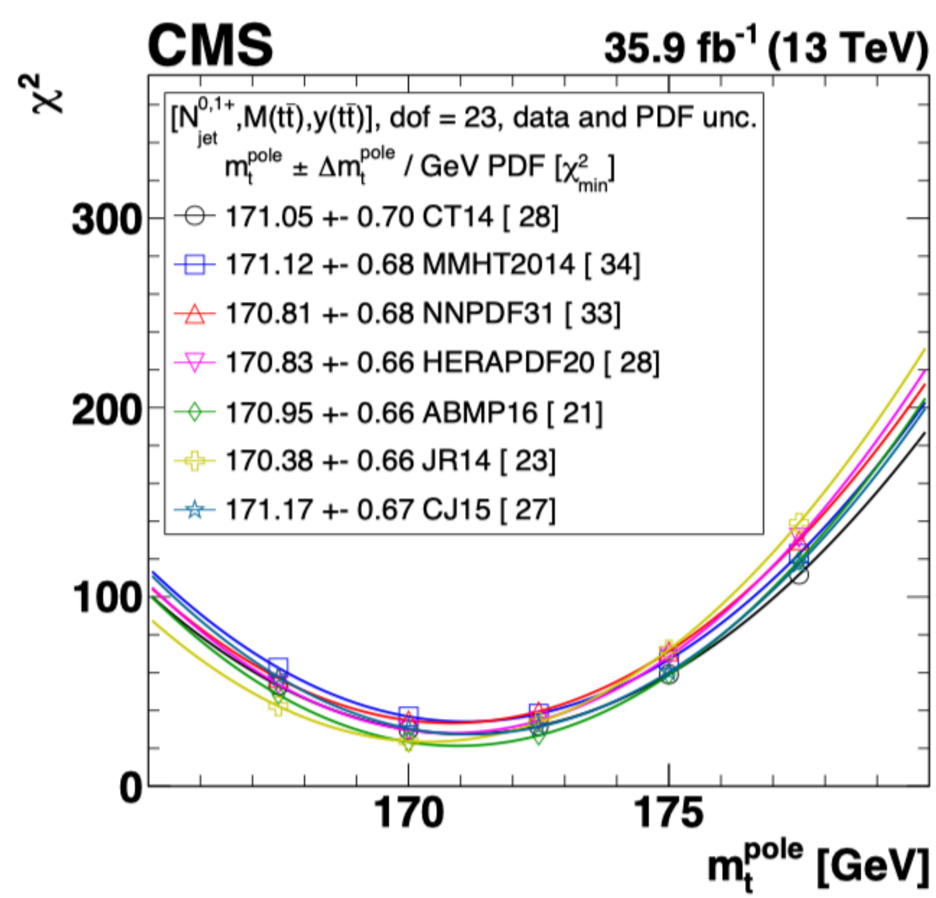

More m_t and $\alpha_S(M_Z)$ from differential measurement: extraction of $\alpha_{S,}$ m_t^{pole}

arXiv:1904.05237

- Correlation between α s and gluon:
  - A shallow χ 2 dependence on α S (m Z) is present when using only the HERA DIS data
  - Once the tt data are included in the fit, a distinctly sharper minimum in χ 2 is observed which coincides with the one found in the simultaneous PDF and α S (m Z) fit

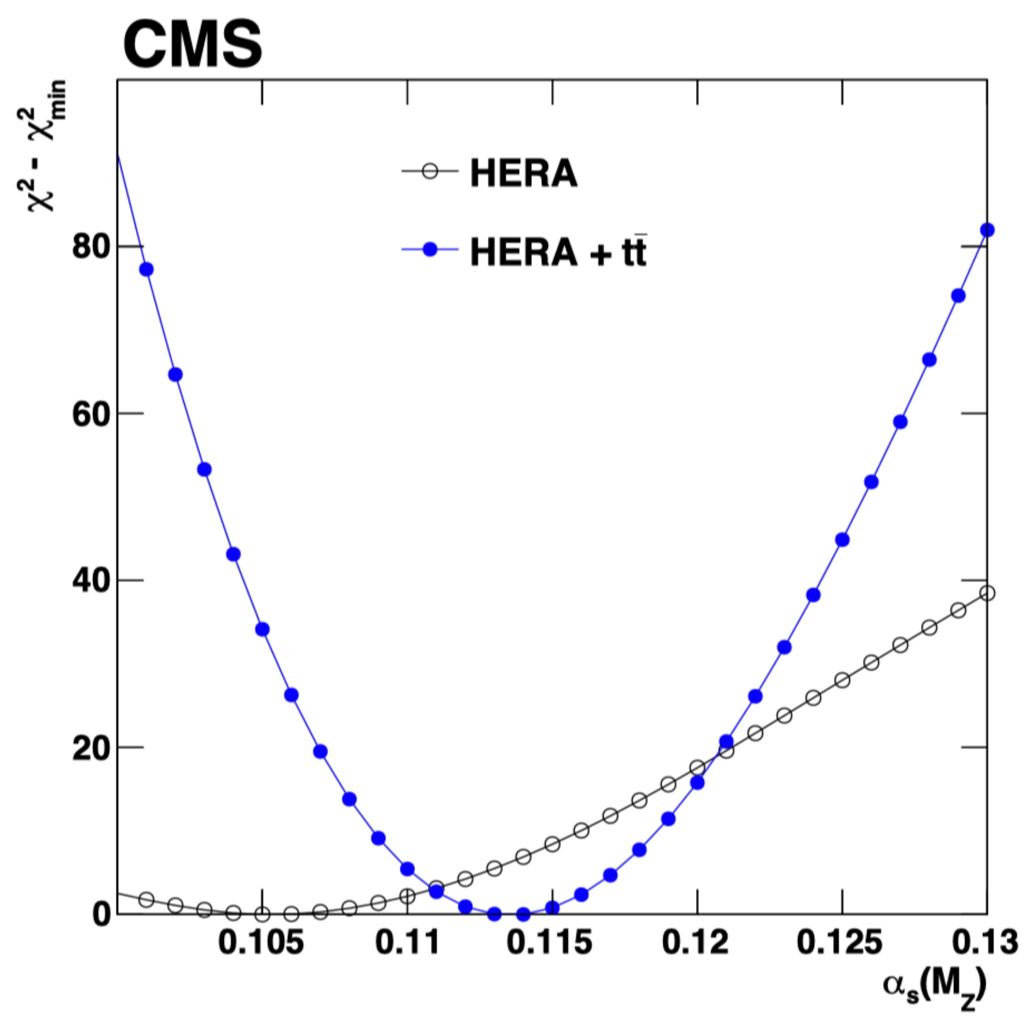

Figure 21: $\Delta\chi^2 = \chi^2 - \chi^2_{min}$ as a function of $\alpha_S(m_Z)$ in the QCD analysis using the HERA DIS data only, or HERA and $t\bar{t}$ data.

More m_t and $\alpha_S(M_Z)$ from differential measurement: PDFs

arXiv:1904.05237

- A reduction of uncertainties is observed for the gluon distribution, especially at x ~ 0.1 where the included tt data are expected to provide constraints, while the improvement at x . 0.1 originates mainly from the reduced correlation between α S (m Z) and the gluon PDF. α S (m Z) fit

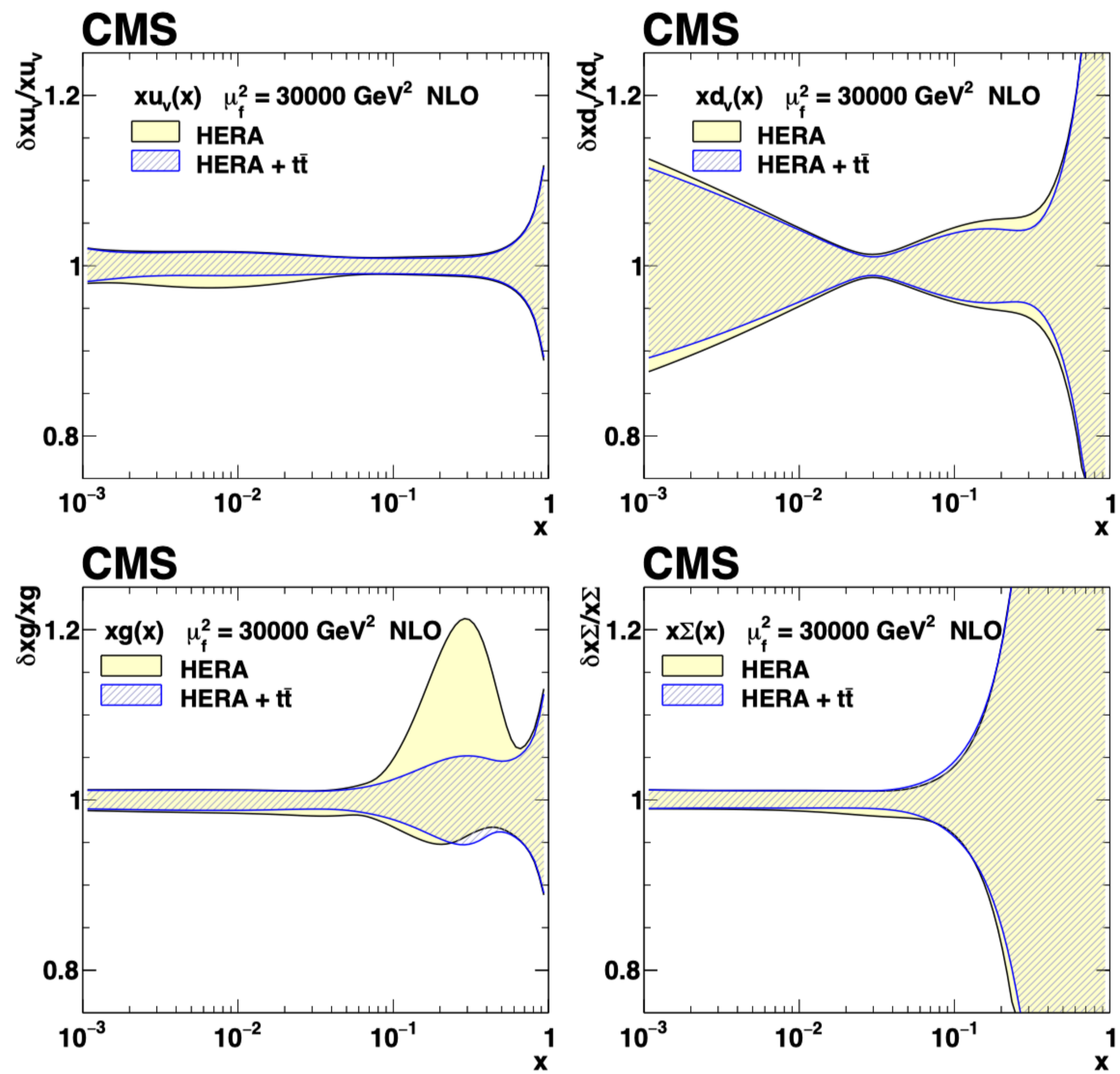

Figure 23: The relative total PDF uncertainties in the fit using the HERA DIS data only, and the HERA DIS and tt̄ data.

More m_t and $\alpha_S(M_Z)$ from differential measurement: correlations for and mtpole

arXiv:1904.05237

- When using only the HERA DIS data, the largest dependence on α S (m Z) is observed for the gluon distribution. The tt data reduce this dependence, because they provide constraints on both the gluon distribution and α S , reducing their correlation.

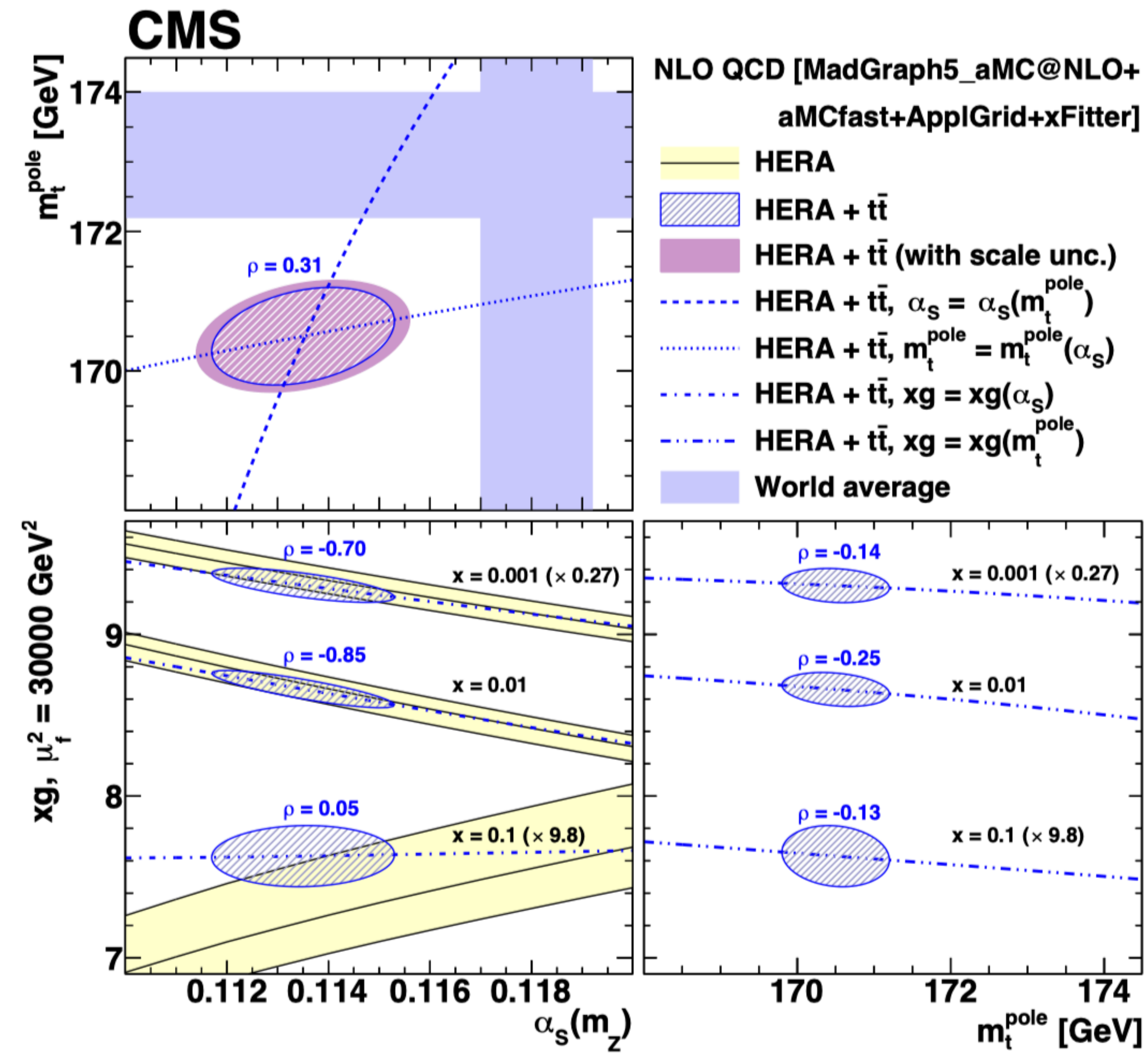

Figure 24: The extracted values and their correlations for α_S and m_t^{pole} (upper left), α_S and gluon PDF (lower left), and m_t^{pole} and gluon PDF (lower, right). The gluon PDF is shown at the scale $\mu_f^2 = 30\,000\,\text{GeV}^2$ for several values of x. For the extracted α_S and m_t^{pole} values, also shown are the additional uncertainties arising from the dependence on scale variations (see Eq. (8) and Table 2). The correlation coefficients ρ are also displayed. Furthermore, values of α_S (m_t^{pole}, gluon PDF) extracted using fixed values of m_t^{pole} (α_S) are displayed as dashed, dotted, or dash-dotted lines. The world average values $\alpha_S(m_Z) = 0.1181 \pm 0.0011$ and $m_t^{\text{pole}} = 173.1 \pm 0.9\,\text{GeV}$ from Ref. [94] are shown for reference.

Yukawa couplings in ttbar differential measurement: reconstruction of ttbar

CMS-PAS-TOP-17-004

- Neutrino momentum reconstruction:
  - W boson and top quark mass constraints applied on leptonically decaying top (solution represented by an ellipse)
  - pz-component of neutrino momentum that distinguish the leptonic b-jet given by the minimum distance Dnu,min between the ellipse projection onto the transverse plan (px, py) and the measured ptmiss

$$(p_\nu + p_\ell)^2 = m_{\mathrm{W}}^2$$

$$(p_\nu + p_\ell + p_{\mathrm{b}_\ell})^2 = m_{\mathrm{t}}^2$$

- Likelihood discriminant:
  - built to minimize Dnu,min and ensure the W boson and top quark mass constraints applied on hadronically decaying top:

$$-\ln(\lambda_4) = -\ln(P_{\mathrm{m}}(m_2, m_3)) - \ln(P_\nu(D_{\nu,\mathrm{min}}))$$

    - Pm = 2D probability distribution to correctly reconstruct W boson and top quark invariant mass
    - Pnu = Dnu,min distribution for a correctly selected bl
  - the highest value of the discriminant between each jet-quark assignment is used to correctly match jets to quarks:
    - Jets with Dnu,min>150 are rejected

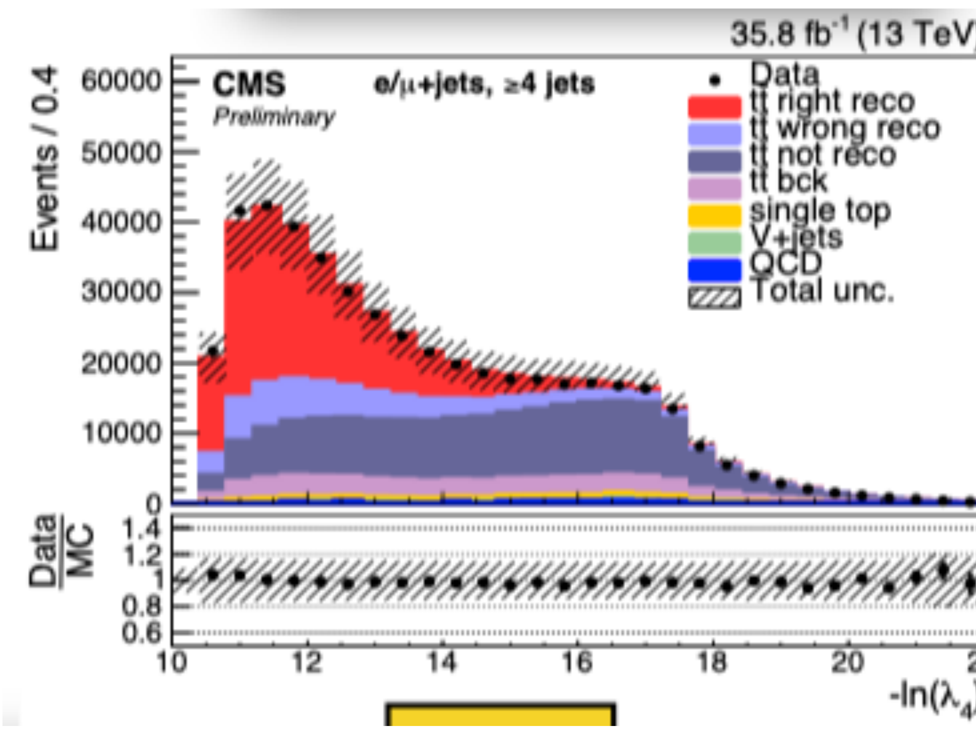

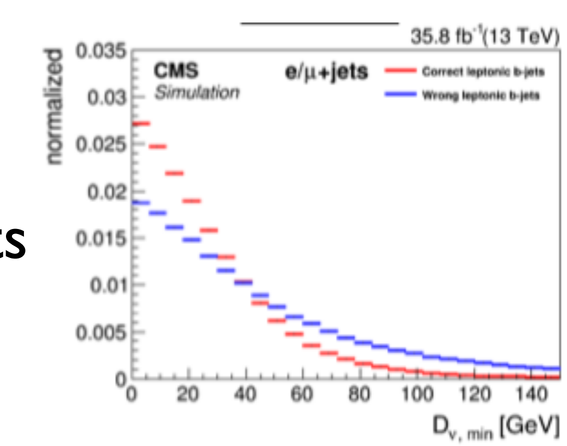

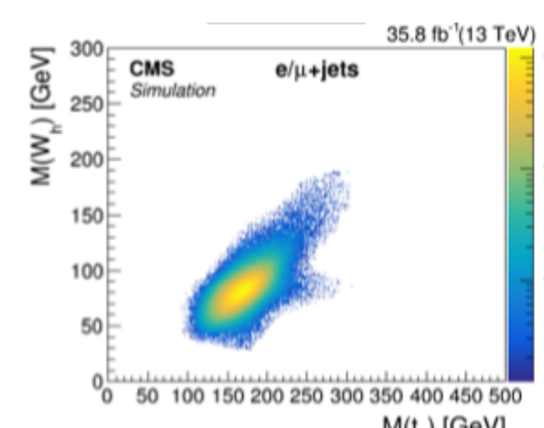

Yukawa coupling in ttbar differential measurement: reconstruction of 3jets events

CMS-PAS-TOP-17-004

- Reconstruction algorithm for events with 1 missing jet developed to mitigate low efficiency in threshold region where one jet is likely out of the acceptance (p T and η event selections):
  - assuming that the two highest b-tagged jets are associated with b-quarks from tt decays, the missing jet is mostly the softer p T jet from W decays
  - the only ambiguity is in the assignment of the b-tagged jets (coming from leptonically or hadronically decaying top)
  - a likelihood discriminant is built with the minimum distance Dnu,min and the invariant mass mth of the 2jets coming from the hadronically decaying top:

$$-\ln(\lambda_3) = -\ln(P_{m_{t_h}}) - \ln(P_{\nu}(D_{\nu,\mathrm{min}})).$$

  - to identify the best jet-to-parton assignment the lowest value of the discriminant is taken:
    - Jets with -ln(lambda3)>13 are discarded to improve signal/bkg
    - b-jets correctly identified in 80% of events

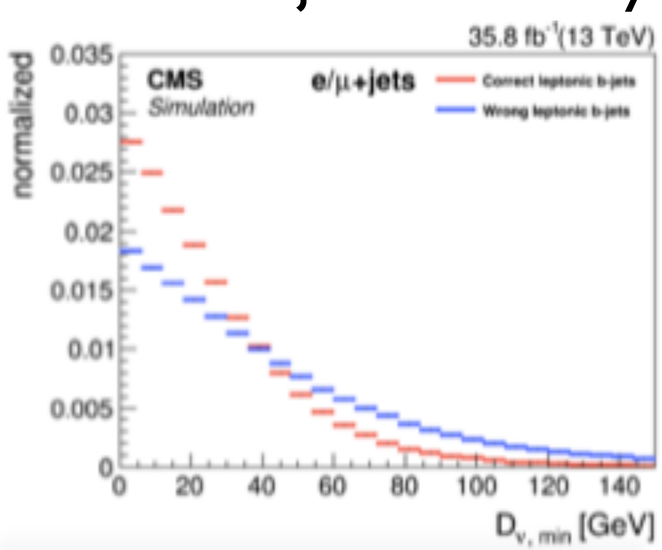

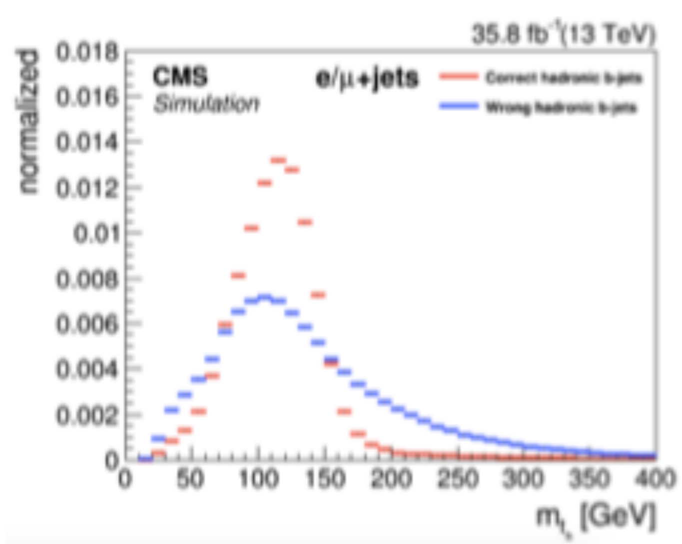

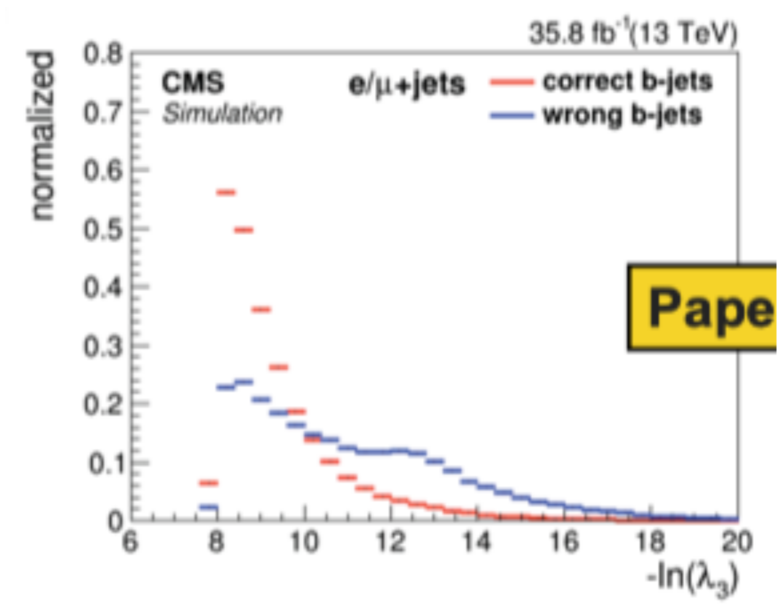

Yukawa coupling in ttbar differential measurement: reconstruction of 3jets events

CMS-PAS-TOP-17-004

- Reconstruction algorithm for 3jets events competitive with the one used in the 4jet category:
  - similar resolution for the ttbar invariant mass and the difference in rapidity
- It allows to :
  - increase the yields in the sensitive low Mtt region
  - gain a category with compatible sensitivity compared to all other categories (see table event yields)
  - reduce the systematic uncertainty due to sources that cause migration between jet multiplicity bins (JEC variation and hadronization model)

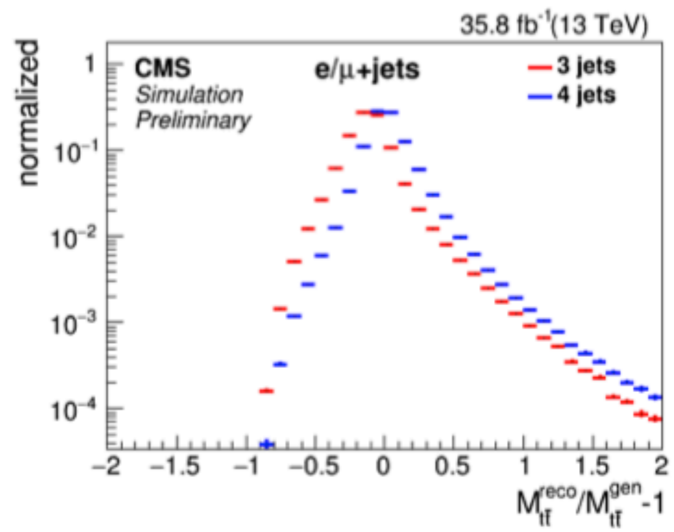

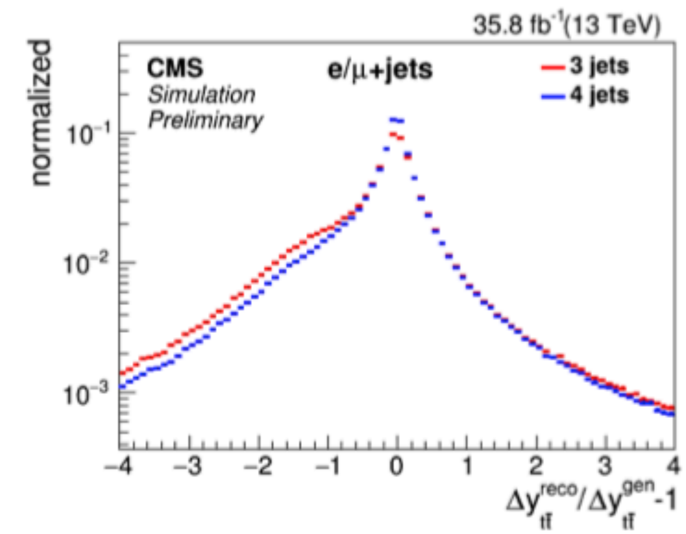

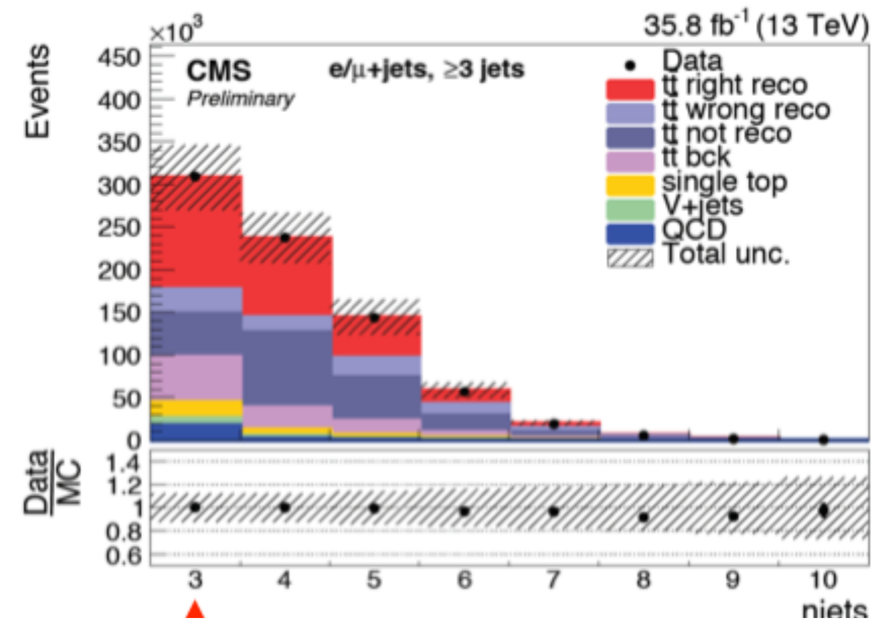

Source	3 jets	4 jets	≥5 jets
$t\bar{t}$ right	130523.1 ± 153.8	92895.1 ± 129.5	71642.6 ± 114.1
$t\bar{t}$ wrong	29297.9 ± 73.1	17355.6 ± 56.6	43073.0 ± 89.3
$t\bar{t}$ semi	50695.4 ± 96.2	88762.8 ± 127.1	80960.1 ± 122.1
$t\bar{t}$ background	53464.6 ± 99.0	26084.5 ± 69.1	25043.6 ± 68.1
single t	17847.8 ± 40.0	6922.3 ± 27.1	6294.3 ± 25.9
V+jets	8989.7 ± 100.3	2823.7 ± 51.6	2477.6 ± 48.9
QCD multijet	19834.8 ± 6247.0	2100.4 ± 603.2	1082.9 ± 209.6
MC sum	310653.4 ± 253.8	236944.5 ± 211.9	230574.0 ± 211.0
Data	308932.0 ± 555.8	237491.0 ± 487.3	226788.0 ± 476.2

Yukawa coupling in ttbar differential measurement: likelihood model

CMS-PAS-TOP-17-004

- Likelihood model constructed as a product of Poisson likelihoods for the observed number of events in each mtt, deltaY bin :

$$\mathcal{L} = \prod_{\text{bin} \in (M_{t\bar{t}}, \Delta y_t)} \mathcal{L}_{\text{bin}} = \prod_{\text{bin}} \text{Pois}(n^{\text{bin}}_{\text{obs}} | s^{\text{bin}}(\theta) \times R^{\text{bin}}(Y_t) + b^{\text{bin}}(\theta)) \times \rho(\theta|\tilde{\theta})$$

  - s bin is MC prediction of the tt production
  - b bin includes MC prediction from single top, QCD, and V+jets
  - R bin (Y t) encodes the effects of different Y t coupling scenarios, formulated as quadratic equations in each bin
  - *ρ* encodes pdfs for systematic uncertainties θ
- Sensitivity formulated as a quadratic equation for each bin in the likelihood model: Rbin(Y t) = s bin (Y t)/s bin (SM) -> represents the strength of the EW correction over the uncorrected POWHEG yields. The strength R(Y t) = 1 corresponds to the SM top Yukawa coupling prediction.
- Systematic uncertainties treated as nuisance parameters and constraint in situ

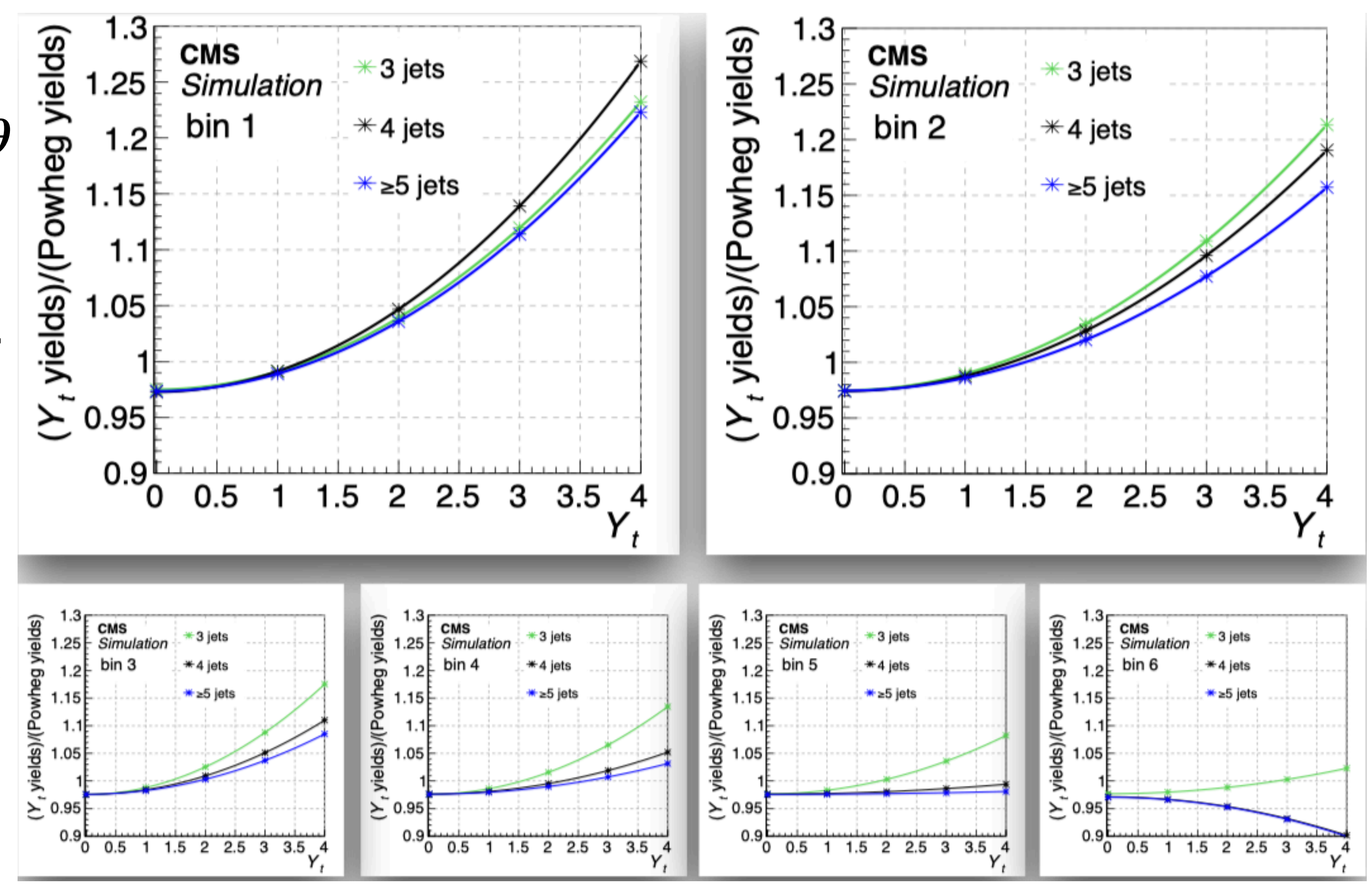

Yukawa coupling in ttbar differential measurement: experimental uncertainties

CMS-PAS-TOP-17-004

- Normalization uncertainties for background cross sections
- lepton IDs and triggers, JEC/JER, b-tagging and mis-tagged efficiencies, pile-up, lumi
  - MET negligible
  - JEC split into 19 independent sources → dominant experimental uncertainty
- QCD shape uncertainty derived by b-tagging inversion → larger and higher impact uncertainties for 3 jets channel

Uncertainty	$t\bar{t}$	single t	V+jets	QCD
Luminosity	2.5%	2.5%	2.5%	2.5%
Pile-up	shape	shape	-	-
JEC (19 independent variations)	shape	shape	-	-
JER	shape	-	-	-
Lepton ID/trigger	shape	shape	shape	-
b tagging scale factor	shape	shape	shape	-
b mis-tagging scale factor	shape	shape	shape	-
Background normalization	-	15%	30%	30%
CSV invertsion on QCD template	-	-	-	shape

Yukawa coupling in ttbar differential measurement: modeling uncertainties

CMS-PAS-TOP-17-004

- Renormalization&Factorization scale uncertainty described by 4 nuisances includes the shapes both for total correlation and total anti-correlation
- PDF uncertainty described by 8 nuisances derived by grouping 100 replicas (NNPDF) with similar variations on the analysis bins
- Top mass systematic derived by ±1GeV MC samples
- Parton shower (6 nuisances) :
  - NLO Matrix element shower matching: dedicated MC samples with h damp variation
  - ISR/FSR scale: dedicated MC samples with variations (FSR shape)
  - Underlying events: dedicated MC samples with tune variations (negligible)
  - b-jet fragmentation: fragmentation and uncertainties change in MC by reweighing (shape)
  - B meson decaying Br: change leptonic branching fraction in MC by reweighing (shape)
  - Color reconnection: dedicate MC sample including color reconnection of resonant decays
- Uncertainty due to weak correction estimated by bin-by-bin (scale variation due to due to fact.&reno. scale up/down)x(weak correction) → tiny systematic variation and low impact, dependent from Yt

Uncertainty	$t\bar{t}$	single t	V+jets	QCD
Fact. & reno. scale	shape	shape	shape	-
PDF	shape	shape	-	-
$\alpha_s(M_Z)$ in PDFs	shape	shape	-	-
Top mass	shape	-	-	-
Parton Shower				
-NLO shower matching	shape	-	-	-
-Color reconnection	shape	-	-	-
-ISR	2%/2%/3%	-	-	-
-FSR	shape	shape	-	-
-b-jet fragmentation	shape	shape	-	-
-B hadron decaying Br.	shape	shape	-	-
Weak correction $\delta_{QCD}\delta_{EW}$	shape	-	-	-

4 top quarks: strategy

CMS-PAS-TOP-18-003

- Cut-based approach:
  - Baseline events are separated into 14 bins depending on lepton and (b-tagged) jet multiplicities along with 2 high statistics regions enriched in ttW and ttZ (inverting the Z-veto) for normalization constraints
- BDT approach:
  - a multi-variate classifier is also trained tight to separate signal from background
  - Baseline events are passed through the classifier and the discriminator output is sliced into 17 bins
  - The ttZ-enriched control region from the cut-based procedure is also included as another bin

4 top quarks: systematic uncertainties

CMS-PAS-TOP-18-003

- Experimental uncertainties are treated as:
  - fully correlated among signal regions for all signal and background processes
  - fully uncorrelated across years
- Systematic uncertainties in the data-driven estimates and theoretical uncertainties on the normalization of each background process are treated as uncorrelated between processes but fully correlated among signal regions and across the three years.
- Scale and PDF uncertainties, as well as uncertainties on N jets ISR/FSR and on the number of additional b quarks, are correlated between processes, signal regions, and years.
- Statistical uncertainties due to the limited number of simulated events or control region events are considered uncorrelated.

Source	Uncertainty (%)	Impact on the $t\bar{t}t\bar{t}$ cross section (%)
Integrated luminosity	2.3–2.5	3
Pileup	0–5	1
Trigger efficiency	2–7	2
Lepton selection	2–10	2
Jet energy scale	1–15	9
Jet energy resolution	1–10	6
b tagging	1–15	6
Size of simulated sample	1–25	<1
Scale and PDF variations †	10–15	2
ISR/FSR (signal) †	5–15	2
$t\bar{t}H$ (normalization) †	25	5
Rare, $X\gamma$, $t\bar{t}VV$ (norm.) †	11-20	<1
$t\bar{t}Z$, $t\bar{t}W$ (norm.) †	40	3-4
Charge misidentification †	20	<1
Nonprompt leptons †	30–60	3
$N_{\text{jets}}^{\text{ISR/FSR}}$ †	1-30	2
$\sigma(t\bar{t}b\bar{b})/\sigma(t\bar{t}jj)$ †	35	11

Charge asymmetries from differential measurement: systematic uncertainties

JHEP 02 (2019) 149

- each uncertainty propagated through analysis chain individually:
  - sys. uncertainty in bin = difference of the changed result wrt nominal
  - determined individually for each bin through variation of sys. source
  - applying b-tagging efficiency dependent correction for systematic uncertainty estimation due to theory related sources, JES, and JER
  - following recommendations in all cases
- 39 observables:
  - The total uncertainty in each bin of each measurement is determined by summing the experimental and theoretical uncertainties in quadrature and ranges from 4–25%, depending on the observable and the bin. In Section 7, figures showing the contribution of each systematic uncertainty, the statistical uncertainty, and the total uncertainty in each bin for selected normalised parton-level differential cross sections as a function of top-quark-related kinematic observables are provided.
  - For most bins in a majority of these distributions, the JES is the dominant systematic uncertainty

Charge asymmetries from differential measurement: systematic uncertainties

JHEP 02 (2019) 149

- experimental uncertainties considered in this analysis:
  - trigger eff., lepton ID/Iso, kin. reco. eff.: vary accordingly to uncertainties
  - JES (individual sources), JER, b-tagging: prescription by POGs
  - b-tagging: additional variations depending on jet kinematics
  - unclustered MET variations
  - pile-up reweighting: : +/- 4.6% on min-bias cross section
  - lumi: 2.5% variation
  - background normalisations: 30% variations
- modeling uncertainties
  - u f u R –
    - ME-level: u f u R varied coherently and separately
    - PS-level: vary scale of ISR/FSR alpha s (FSR variation rescaled)
  - m t : alternative +/- 3 GeV samples rescaled to +/- 1 GeV
  - ME-PS matching: hdamp variation samples
  - UE-tune: varied CUETP8T2M4 parameters
  - PDF: replica variations + alpha S
  - b-fragmentation: gen-level reweighting
  - colour reconnection: model comparisons via samples
  - b-semi-lep BR: varied according to PDG
  - dileptonic branching ratio: +/-1.5% (PDG) (absolute results in full phase space only)